From: <JAFPR343@entergy.com>
To: "nbl@nrc.gov " <nbl@nrc.gov>
Date: 2/20/2007 10:59:56 AM
Subject: Scan from a Xerox WorkCentre Pro

Please open the attached document. It was scanned and sent to you using a Xerox WorkCentre Pro.

Sent by: Guest [JAFPR343@ENTERGY.COM]
Number of Images: 129
Attachment File Type: PDF

WorkCentre Pro Location: ASG
Device Name: JAFPR343

For more information on Xerox products and solutions, please visit http://www.xerox.com

Mail Envelope Properties (45DB1AE2.0DD : 1 : 57565)

Subject:	Scan from a Xerox WorkCentre Pro
Creation Date	2/20/2007 11:43:18 AM
From:	<JAFPR343@entergy.com>
Created By:	JAFPR343@entergy.com

Recipients
nrc.gov
TWGWPO01.HQGWDO01
NBL (Ngoc Le)

Post Office	**Route**
TWGWPO01.HQGWDO01	nrc.gov

Files	**Size**	**Date & Time**
MESSAGE	329	2/20/2007 11:43:18 AM
Scan001.PDF	5518175	
Mime.822	7589553	

Options

Expiration Date:	None
Priority:	Standard
ReplyRequested:	No
Return Notification:	None
Concealed Subject:	No
Security:	Standard

Junk Mail Handling Evaluation Results
Message is eligible for Junk Mail handling
This message was not classified as Junk Mail

Junk Mail settings when this message was delivered
Junk Mail handling disabled by User
Junk Mail handling disabled by Administrator
Junk List is not enabled
Junk Mail using personal address books is not enabled
Block List is not enabled

GE Nuclear Energy

Technical Services Business
General Electric Company
175 Curtner Avenue, San Jose, CA 95125

GE-NE-B1100732-01, Revision 1
Final Report
Class II
February 1998

PLANT FITZPATRICK RPV SURVEILLANCE MATERIALS TESTING AND ANALYSIS OF 120° CAPSULE AT 13.4 EFPY

Prepared by: Timothy J. Griesbach
T. J. Griesbach, Director
ATI Consulting

Verified by: R. G. Carey
R. G. Carey, Engineer
Structural Mechanics and Materials

Approved by: B. J. Branlund
B. J. Branlund, Project Manager
Structural Mechanics and Materials

Pagano, Terry

From: Porter, Anne
Sent: Thursday, November 10, 2005 10:33 AM
To: Pagano, Terry
Subject: FW: Fitz Doc

Terry – can you get this please

From: LOYD, LELAND
Sent: Thursday, November 10, 2005 10:21 AM
To: Porter, Anne
Cc: Harrison, Douglas; Herrmann, Terry; BARTON, SANDRA
Subject: Fitz Doc

Good Morning Anne
I need GE-NE-B1100732-01 (JAF RPV surveillance materials testing & analysis of 120 degree capsule at 13.4 EFPY (effective full power years) – including BJB-9907 and attachment to BJB-9907).

If you send it hard copy send to Sandy

ENTERGY CORPORATION
1448 SR 333
Russellville, AR 72802
c/o Sandra Barton
N-GSB-45

Or; sbart90@entergy.com Sandy (this goes with the OE programs, Lori will know what to do with it)

Thanks!

Leland Loyd
License Renewal
lloyd90@entergy.com
479/858/4696

GE Nuclear Energy

Technical Services Business
General Electric Company
175 Curtner Avenue, San Jose, CA 95125

GE-NE-B1100732-01, Revision 1
Final Report
Class II
February 1998

PLANT FITZPATRICK RPV SURVEILLANCE MATERIALS TESTING AND ANALYSIS OF 120° CAPSULE AT 13.4 EFPY

Prepared by: Timothy J. Griesbach
T. J. Griesbach, Director
ATI Consulting

Verified by: R. G. Carey
R. G. Carey, Engineer
Structural Mechanics and Materials

Approved by: B. J. Branlund
B. J. Branlund, Project Manager
Structural Mechanics and Materials

NEW YORK POWER AUTHORITY
DOCUMENT REVIEW STATUS

STATUS NO:
1 ☑ ACCEPTED
2 ☐ ACCEPTED AS NOTED RESUBMITTAL NOT REQUIRED
3 ☐ ACCEPTED AS NOTED RESUBMITTAL REQUIRED
4 ☐ NOT ACCEPTED

Permission to proceed does not constitute acceptance or approval of desig details, calculations, analysis, test methods or materials developed or selecte by the supplier and does not relieve supplier from full compliance wi contractual negotiations.

REVIEWED BY: William Hunter TITLE: Consulting Engr

123 Main Street
White Plains, New York 10601
914 681.6200

New York Power Authority

February 13, 1998 DCME-98-0086

To: GE NUCLEAR ENERGY Contract No. C95-Z0013
175 Curtner Ave
San Jose CA 95125

Attn: Ms. B. J. Branlund, Project Manager

The document(s) listed below are being returned to you with the status indicated on each document.

Document No.	Rev.	Status
GE-NE-B1100732-01	1	1 ACCEPTED

JAF RPV SURVEILLANCE MATERIALS TESTING & ANALYSIS OF 120 DEGREE CAPSULE AT 13.4 EFPY (EFFECTIVE FULL POWER YEARS)

Very truly yours,

William H Spataro

W. Spataro
Consulting Metallurgist

copies (transmittal only): G. Grochowski
w. attachment: G. Rorke, J. Ellmers, C. Doc

IMPORTANT NOTICE REGARDING CONTENTS OF THIS REPORT PLEASE READ CAREFULLY

This report was prepared by General Electric solely for the use of the New York Power Authority. The information contained in this report is believed by General Electric to be an accurate and true representation of the facts known, obtained, or provided to General Electric at the time this report was prepared.

The only undertakings of the General Electric Company respecting information in this document are contained in the contract between the customer and General Electric Company, as identified in the purchase order for this report and nothing contained in this document shall be construed as changing the contract. The use of this information by anyone other than the customer or for any purpose other than that for which it is intended, is not authorized; and with respect to any unauthorized use, General Electric Company makes no representation or warranty, and assumes no liability as to the completeness, accuracy, or usefulness of the information contained in this document.

TABLE OF CONTENTS

TABLE OF TABLES

TABLE OF FIGURES

TABLE OF FIGURES
(continued)

ABSTRACT

The surveillance capsule at the 120° azimuthal location was removed at 13.4 EFPY from the FitzPatrick reactor in November 1996. The capsule contained flux wires for neutron fluence measurement, and Charpy test specimens and tensile test specimens for material property evaluations. The flux wires were evaluated to determine the fluence experienced by the test specimens. Charpy V-Notch impact testing and tensile testing were performed to establish the properties of the irradiated surveillance materials.

The irradiated Charpy data for the base material specimens were compared to available unirradiated data to determine the shift in Charpy curves due to irradiation. The results indicate a shift lower than the predictions of Regulatory Guide 1.99 Revision 2 [Rev. 2]. Since two sets of credible data sets were available for the plate material, the Adjusted Reference Temperature (ART) calculations for vessel base materials were adjusted in accordance with Rev. 2. For the vessel weld metal, no unirradiated data was available and the predictions of Rev. 2 were used to calculate ART.

The flux wire results combined with the lead factor were used to estimate the 32 EFPY fluence. The fluence calculations included the effects of a 105% power uprate. The resulting estimated fluence showed a reduction of 22 percent compared with the previous nominal 32 EFPY fluence estimate consistent with the fluence used for the Technical Specification Pressure-Temperature (P-T) Curves.

P-T Curves were prepared based on the new projected fluence levels for both 32 EFPY and 24 EFPY.

ACKNOWLEDGMENTS

The author gratefully acknowledges the efforts of other people towards completion of the contents of this report.

Cask shipping & receipt, and capsule disassembly were performed by J. B. Myers and R. D. Rimmer. Charpy testing was completed by G. E. Dunning and B. D. Frew. Tensile testing was performed by S. B. Wisner. Chemical composition analysis was performed by P. S. Wall. Flux wire testing and analysis was performed by L. Kessler, R. M. Kruger and R. D. Reager. Fluence and lead factor calculations were performed by D. R. Rogers, H. A. Careway and S. S. Wang. Assistance with the capsule evaluation was provided by B. N. Burgos of ATI Consulting. Project management was conducted by B. J. Branlund.

1. INTRODUCTION

Part of the effort to assure reactor vessel integrity involves evaluation of the fracture toughness of the vessel ferritic materials. The key values which characterize a material's fracture toughness are the reference temperature of nil-ductility transition (RT_{NDT}) and the upper shelf energy (USE). These are defined in 10CFR50 Appendix G [1] and in Appendix G of the ASME Boiler and Pressure Vessel Code, Section XI [2].

Appendix H of 10CFR50 [3] and ASTM E185-70 [4] establish the methods to be used for surveillance of the James A. FitzPatrick (FitzPatrick) reactor vessel materials. The second vessel surveillance specimen capsule required by 10CFR50 Appendix H [3] was removed from FitzPatrick in November 1996. The irradiated capsule was sent to the GE Vallecitos Nuclear Center (VNC) for testing. The surveillance capsule contained flux wires for neutron flux monitoring and Charpy V-Notch impact and tensile test specimens fabricated using base metal from the beltline region, as well as weld metal from a similar heat of material as the beltline welds. The impact and tensile specimens were tested to establish properties for the irradiated materials.

The results of the surveillance specimen testing are presented in this report, as required per 10CFR50 Appendices G and H [1 & 3]. The irradiated material properties are compared to available unirradiated properties to determine the effect of irradiation on material toughness for the base and weld materials, through Charpy testing. Irradiated tensile testing results are provided and are compared with unirradiated data to determine the effect of irradiation on the stress-strain relationship of the materials.

Pressure-temperature (P-T) curves are included in this report which have been developed to present steam dome pressure versus minimum vessel metal temperature incorporating appropriate non-beltline limits and irradiation embrittlement effects in the beltline. The P-T curves are established to the requirements of 10CFR50, Appendix G [1] to assure that brittle fracture of the reactor vessel is prevented.

2. SUMMARY AND CONCLUSIONS

2.1 SUMMARY OF RESULTS

The 120° azimuth position surveillance capsule was removed and shipped to VNC. The flux wires, Charpy V-Notch and tensile test specimens removed from the capsule were tested according to ASTM E185-82 [6]. The methods and results of the testing are presented in this report as follows:

Section 3: Surveillance Program Background

- RPV Materials and Fabrication
- Material Properties
- Surveillance Specimen Chemical Composition
- Specimen Description

Section 4: Peak RPV Fluence Evaluation

Section 5: Charpy V-Notch Impact Testing

Section 6: Tensile Testing

Section 7: Adjusted Reference Temperature and Upper Shelf Energy

Section 8: Pressure-Temperature Curves

The significant results of the evaluation are below:

a. The 120° azimuth position capsule was removed from the reactor after 13.4 EFPY (Effective Full Power Years) of operation. The capsule contained 2 sets of 3 flux wires: nickel (Ni), copper (Cu), and iron (Fe). There were 24 Charpy V-Notch specimens in the capsule: eight (8) each of plate (base) material, weld material, and heat affected zone (HAZ) material. The capsule also contained eight (8) tensile specimens: three plate material, three weld material, and two HAZ material. (See Sections 3.1 and 3.3)

b. The chemical composition of copper (Cu) and nickel (Ni) for the irradiated surveillance materials was determined from a chemical composition analysis. The best estimate values for the surveillance material chemistries were calculated as averages of the available baseline and irradiated data. The best estimate values for the surveillance plate are 0.11% Cu and 0.60% Ni, and are 0.29% Cu and 0.71% Ni for the surveillance weld. (See Table 3.4)

c. The purpose of the flux wire testing was to determine the neutron flux at the surveillance capsule location. The flux wire results show that the fluence (from E >1 MeV flux) received by the surveillance specimens was 5.0×10^{17} n/cm^2 at removal (13.4 EFPY-See Section 4.1.2).

d. A neutron transport computation had been performed based on the first surveillance capsule. Relative flux distributions in the azimuthal and axial directions were previously developed in Reference 8. The lead factor was 0.79, relating the surveillance capsule flux to the peak inside surface flux. The lead factor was calculated after the second capsule was removed at 13.4 EFPY, and determined to be 0.68. A lead factor of 0.68 was used for all calculations in this report (See Section 4.2.2).

e. The surveillance Charpy V-Notch specimens were impact tested at temperatures selected to define the upper shelf energy (USE) and the transition of the Charpy V-Notch curves for the plate, weld, and HAZ materials. Measurements were taken of absorbed energy, lateral expansion and percentage shear. From absorbed energy and lateral expansion curve-fit results, the values of USE and of index temperature for 30 ft-lb, 50 ft-lb and 35 mils lateral expansion (MLE) were obtained (see Table 5-3). Fracture surface photographs of each specimen are presented in Appendix A.

f. The irradiated tensile specimens were tested at room temperature (70°F), at reactor operating temperature (550°F) and at 185°F as an intermediate temperature. Unirradiated base material results, as well as results from the first capsule, were available for comparison (See Tables 6-1 through 6-4.)

g. The curves of irradiated and unirradiated Charpy specimens established the 30 ft-lb shifts. The plate material showed a 15°F shift and a 12 ft-lb decrease in USE (9% decrease). These values were not calculated for the weld, as no unirradiated data was available (See Table 5-3).

h. The measured shift of 15°F for plate material for a fluence of 5.0×10^{17} n/cm^2, was within the Rev. 2 [7] range predictions ($\Delta RT_{NDT} \pm 2\sigma$) of -12°F to 56°F. Since two credible data sets are available for the plate material, the surveillance adjustment (Section 7) was applied to the vessel base plates. The measured shift values were not obtained for the weld as no unirradiated data was available. The best estimate chemical composition for the surveillance weld material was used for evaluating the projected shift of the surveillance weld data (See Table 5-3).

i. The 32 EFPY RPV peak fluence prediction is 1.81×10^{18} n/cm^2 at the vessel wall, based on the flux wire test and lead factor. This is 22% less than the previously established nominal 32 EFPY fluence prediction (2.32×10^{18} n/cm^2) [5]. The 32 EFPY fluence prediction is 1.31×10^{18} n/cm^2 at 1/4 T. (See Section 4.3)

j. The adjusted reference temperature (ART = Initial RT_{NDT} + ΔRT_{NDT} + Margin) was predicted for each beltline material, based on the methods of Regulatory Guide 1.99, Rev. 2. The ART for the limiting material, Axial Weld Heat 27204/12008, at 32 EFPY is 109°F and is lower than the 200°F requirement of 10CFR50 Appendix G [1] and Rev. 2 [7]. (See Table 7-1)

k. An update of the beltline material USE values at 32 EFPY was performed using the Reg. Guide 1.99, Rev. 2 methodology. The equivalent margin analyses demonstrate that 10CFR50, Appendix G safety requirements are satisfactorily met for FitzPatrick. (See Tables 7-2 and 7-3)

l. P-T curves were developed for three reactor conditions: pressure test (Curve A), non-nuclear heatup and cooldown core not critical operation (Curve B), and core critical operation (Curve C) curves which are valid for up to 32 EFPY of operation. The beltline curve is more limiting for Curve A at pressures above approximately 550 psig. For Curves B and C, the beltline curves are limiting for pressures above approximately 600 psig. The P-T curves for 32 EFPY are shown in Figures 8-1 through 8-3, and the P-T curves for 24 EFPY are shown in Appendix B, Figures B-1 through B-3

2.2 CONCLUSIONS

The requirements of 10CFR50 Appendix G [1] deal with vessel design life conditions and with limits of operation designed to prevent brittle fracture. Based on the evaluation of surveillance testing results, and the associated analyses, the following conclusions are made:

a. The 30 ft-lb shift for the base material was less than the Rev. 2 prediction, and therefore the ART values for beltline plates were modified in accordance with Position 2 of Rev. 2. The changes in USE for the survillance plate are bounded by the Regulatory Guide 1.99 Revision 2 predictions and associated deviations.

b. The values of ART and USE for the reactor vessel beltline materials are expected to remain within the limits of 10CFR50 Appendix G [1] for at least 32 EFPY of operation.

3. SURVEILLANCE PROGRAM BACKGROUND

3.1 CAPSULE RECOVERY

The reactor pressure vessel (RPV) surveillance program consists of three surveillance capsules at 30°, 120°, and 300° azimuths at the core midplane. The specimen capsules are held against the RPV inside surface by a spring loaded specimen holder. Each capsule is expected to receive equal irradiation because of core symmetry. The first capsule (30° azimuth) was removed in April 1985 after 5.98 EFPY. During the November 1996 outage, the second surveillance capsule was removed from the 120° azimuthal location. The capsule was cut from its holder assembly and shipped by cask to the GE Vallecitos Nuclear Center (VNC), where testing was performed.

Upon arrival at VNC, the capsule was examined for identification. The identification number stamped on the capsule corresponded to FitzPatrick, as specified by GE drawings, 117C3739 (Outline Specimen Holder) and 921D465 (Surveillance Program), for the FitzPatrick 120° surveillance materials. The general condition of the capsule as received is shown in Figure 3-1. The specimen holder contained 2 sets of 3 flux wires (iron, copper, and nickel), three Charpy specimen capsules each containing 8 plate, weld, or HAZ Charpy specimens in a sealed helium environment, and four tensile specimen capsules (together containing 3 base, 3 weld and 2 HAZ tensile specimens in a sealed helium environment).

3.2 RPV MATERIALS AND FABRICATION

3.2.1 Fabrication History

The FitzPatrick RPV is a 220.75 inch inside diameter BWR/4 design. Construction was performed by Combustion Engineering (CE) under the 1965 edition of the ASME Code through the 1966 Winter Addenda. The shell and head plate materials are ASME SA533, Grade B, Class 1 low alloy steel (LAS). The nozzles and closure flanges are ASME SA508 Class 2 LAS, and the closure flange bolting materials are ASME A540 Grade B24 LAS [8]. Submerged arc or shielded metal arc welding of plates was followed by post-weld heat treatment at 1150°F. The fabrication impact test specimens were given a simulated post weld heat treatment at

1150°F ± 25°F, held 40 hours followed by furnace cooling to below 600°F, then air cooled. The identification of plates and welds in the beltline region is shown in Figure 3-2.

3.2.2 Material Properties of RPV at Fabrication

Material certification records were retrieved from GE Quality Assurance (QA) records to determine chemical and mechanical properties of the vessel materials. The retrieved information for the beltline materials is documented in [5]. Table 3-1 shows the chemistry data for the beltline materials. Properties of the beltline materials and materials at other locations of interest are presented in Tables 3-2 and 3-3.

3.2.3 Surveillance Capsule Specimen Chemical Composition

Samples were taken from the irradiated base and weld Charpy specimens after they were tested. Chemical analyses were performed using a Spectraspan III plasma emission spectrometer. Each sample was dissolved in an acid solution to a concentration of 40 mg steel per ml solution. The spectrometer was calibrated for determination of Mn, P, Ni, Mo, V, Cr, Si and Cu by diluting National Institute of Standards and Technology (NIST) Spectrometric Standard Solutions. The phosphorus calibration involved analysis of five reference materials from NIST with known phosphorus levels. Analysis accuracies are ±0.005% (absolute) of reported value for phosphorus and ±5% (relative) of reported value for other elements. The chemical composition results are given in Table 3-4 for both irradiated and baseline surveillance plate and irradiated weld materials. The baseline plate data was taken from CE material certification records as documented in [5] for the plate surveillance specimens; no baseline data was available for the weld material.

3.3 SPECIMEN DESCRIPTION

The surveillance capsule holder contained 24 Charpy specimens: base metal (8), weld metal (8), and HAZ (8). The holder also contained 2 sets of 3 flux wires (iron, nickel, and copper) and eight (8) tensile specimens (three base, three weld and two HAZ). The chemistry and fabrication history for the Charpy and tensile specimens are described in this section.

3.3.1 Charpy Specimens

The fabrication of the Charpy specimens is described in the CE drawings of the surveillance test program. All materials used for specimens were beltline materials taken from the lower intermediate shell course.

The base metal specimens were cut from plate G-3414-2, heat number C3278-2. The test plates received the same heat treatment as plate heat no. C3278-2, including the post-weld heat treatment for 40 hours at 1150°F ± 25°F. The Charpy specimens were removed from plate heat no. C3278-2 and machined from the 1/4 T and 3/4 T positions in the plate, in the longitudinal orientation (long axis parallel to the rolling direction). The Charpy specimens had been stamped on one end with the fabrication codes as listed in GE surveillance program drawings for FitzPatrick.

The weld metal and HAZ Charpy specimens were fabricated by welding together pieces of plates G-3414-1 and G-3414-2 with a weld identical to longitudinal seam weld 1-233 in the RPV beltline. Welding records obtained from CE indicate the surveillance weld to be a submerged arc weld representive of the vessel beltline circumferential weld. The welded test plates received stress relief heat treatment at 1150°F ±25°F to simulate the RPV fabrication conditions. The weld and HAZ specimens were cut from the material avoiding the volume near the root of the welds. The base metal orientation in the weld and HAZ specimens was longitudinal.

3.3.2 Tensile Specimens

Fabrication of the surveillance tensile specimens is also described in the CE surveillance program drawings. The materials, chemical compositions, and heat treatments for the tensile specimens are the same as the corresponding Charpy specimens. The identifications of the base, weld and HAZ surveillance specimens are described in Reference 8.

TABLE 3-1: CHEMICAL COMPOSITION OF RPV BELTLINE MATERIALS[a]

		Composition by Weight Percent							
Identification	Heat/Lot No.	Cu	Ni	C	Mn	P	S	Si	Mo
PLATES:									
Lower Shell:									
G-3415-1R	C3394-1	0.11[f]	0.56	0.21	1.32	0.015	0.017	0.26	0.47
G-3415-3	C3376-2	0.13[b]	0.60	0.22	1.33	0.015	0.017	0.22	0.48
G-3415-2	C3103-2	0.14[b]	0.57	0.23	1.36	0.012	0.015	0.26	0.46
Lower-Intermed. Shell:									
G-3413-7	C3368-1	0.12[b]	0.50	0.19	1.30	0.015	0.017	0.22	0.45
G-3414-2[c]	C3278-2	0.11[e]	0.60[e]	0.20	1.26	0.011	0.016	0.22	0.48
G-3414-1	C3301-1	0.18[b]	0.57	0.18	1.36	0.008	0.015	0.29	0.46
WELDS:									
Lower Longitudinal: 2-233 A,B,C	27204/12008 Flux 1092 Lot 3774	0.219[d]	0.996[d]	N/A	1.16	0.013	0.007	0.21	0.46
Lower Int. Long.: 1-233 A,B,C	13253/12008 Flux 1092 Lot 3947	0.210[d]	0.873[d]	N/A	N/A	N/A	N/A	N/A	N/A
Lower to Lower -Int. Girth: 1-240	305414 Flux 1092 Lot 3947	0.337[d]	0.609[d]	0.14	1.45	0.012	0.01	0.18	0.51

[a] Data from CMTR Reports, GE QA Records and [5] except as noted below
[b] Cu values taken from Lukens Steel letter to NYPA dated 10/14/85 [19]
[c] Surveillance plate
[d] Best estimate Cu and Ni weld values obtained from CE Owners Group report [18]
[e] Average chemistry of surveillance plate from Table 3-4
[f] Cu content from Generic Letter 92-01 response [21]

TABLE 3-2: RT_{NDT} OF VESSEL MATERIALS

COMPONENT	ID	HEAT	TEST TEMP. (°F)	CHARPY ENERGY (FT-LB)			$(T_{50T}-60)$ (°F)	DROP WEIGHT NDT (°F)	RT_{NDT} (°F)
PLATES & FORGINGS:									
Top Head & Flange									
Dollar Plate	G-3412	C-2869-5	10	83	70	72	-20	-10	-10
Top Head Torus	G-3411-1	C-3055-1	10	98	73	118	-20	-10	-10
	G-3411-2	C-3055-1	10	98	73	118	-20	-10	-10
Top Head Flange	G-3402	4P-1885	10	66	87	96	-50	30	30
Shell Courses									
Upper Shell Flange	G-3401	2V595	10	117	94	117	-50	10	10
Upper Shell	G-3413-4	B-7255-1	10	70	76	71	-20	-10	-10
	G-3413-5	C-3229-2	10	50	68	82	-20	-10	-10
	G-3413-6	B-7291-1	10	81	69	65	-20	-10	-10
Upper Int. Shell	G-3413-1	C-3116-1	10	65	91	79	-20	-10	-10
	G-3413-2	C-3121-2	10	31	48	35	18	10	18
	G-3413-3	C-3158-2	10	95	87	76	-20	-10	-10
Low-Int. Shell	G-3413-7	C-3368-1	10	61	55	45	-10	-50	-10
	G-3414-1	C-3301-1	10	60	63	49	-18	-40	-18
	G-3414-2	C-3278-2	10	45	77	58	-10	-30	-10
Lower Shell	G-3415-1R	C-3394-1	10	53	71	52	-20	-10	-10
	G-3415-2	C-3103-2	10	41	48	49	-2	-10	-2
	G-3415-3	C-3376-2	40	43	51	49	24	-10	24
Bottom Head									
Dollar Plate	G-3410	C-2917-3	10	38	36	36	8	-10	8
Bottom Head Torus	G-3407-1	C-2851-1	10	83	72	75	-20	-10	-10
	G-3408-1	C-3055-2	10	53	73	66	-20	-10	-10
	G-3409	C-2906-3	10	36	43	35	10	-10	10

TABLE 3-3: RT_{NDT} OF NOZZLE, WELD AND STUD MATERIALS

COMPONENT	ID	HEAT	TEST TEMP. (°F)	CHARPY ENERGY (FT-LB)			$(T_{50T}-60)$ (°F)	DROP WEIGHT NDT (°F)	RT_{NDT} (°F)
Nozzles:									
Recirc. Outlet Nozzle	G-3419-1	EV-9781	10	70	71	76	-20	-10	-10
	G-3419-2	AV-1872	10	93	86	72	-20	0	0
Recirc. Inlet Nozzle	G-3436-1	E21VW-104J10	10	103	111	110	-20	<40	30
	G-3436-2	E21VW-104J2	10	82	94	96	-20	<40	30
	G-3436-3	E21VW-104J9	10	95	101	107	-20	<40	30
	G-3436-4	E21VW-104J7	10	86	76	79	-20	<40	30
	G-3436-5	E21VW-104J6	10	84	109	107	-20	<40	30
	G-3436-6	E21VW-104J3	10	89	94	77	-20	<40	30
	G-3436-7	E21VW-104J4	10	106	109	116	-20	<40	30
	G-3436-8	E21VW-104J8	10	101	114	102	-20	<40	30
	G-3436-9	E21VW-104J5	10	73	116	118	-20	<40	30
	G-3436-10	E21VW-104J1	10	110	93	103	-20	<40	30
Steam Outlet Nozzle	G-3420-1	EV-9754	10	82	105	82	-20	-10	-10
	G-3420-2	EV-9775	10	66	40	36	8	-10	8
	G-3420-3	EV-9775	10	62	75	78	-20	-10	-10
	G-3420-4	AV-1576	10	30	52	48	20	0	20
Feedwater Nozzle	G-3421-1	EV-9741	10	65	75	73	-20	10	10
	G-3421-2	EV-9741	10	92	75	90	-20	10	10
	G-3421-3	EV-9741	10	69	67	68	-20	-20	-20
	G-3421-4	AV-1607	10	30	36	32	-20	0	20
Core Spray Nozzle	G-3422-1	EV-9741	10	40	56	65	-30	0	0
	G-3422-2	EV-9741	10	54	89	74	-50	10	10
Top Head Instrumentation Nozzle	G-2921-3	EV-9781	10	82	69	72	-20	0	0
	G-2921-4	AV-2379	10	117	90	108	-20	-10	-10
Vent Nozzle	G-2920-2	AV-2374	10	145	182	185	-20	0	0
Jet Pump Instrumentation Nozzle	G-3424-1	EV-9792	10	144	144	144	-20	0	0
CRD Hyd. Sys. Return	G-3423	EV-9143	10	112	94	80	-20	-20	-20
Drain Nozzle	G-2085	2106172	10	96	108	92	-20		20

COMPONENT	ID	HEAT	TEST TEMP. (°F)	CHARPY ENERGY (FT-LB)			(T_{50T}-60) (°F)	DROP WEIGHT NDT (°F)	RT_{NDT} (°F)
WELDS:									
Vertical Welds									
Lower Shell	2-233 A,B,C	27204/12008	10	63	60	49	-48		-48
Lower-Int Shell	1-233 A,B,C	13253/12008	10	60	64	56	-50		-50
Girth Welds									
Lower to Lower-Int Shells	1-240	305414	10	82	66	80	-50		-50
							LST		
STUDS:	G-3134-1	37385	10	39	40	39	70	OK	
	G-3134-2	37677	10	60	55	57	70	OK	

TABLE 3-4: CHEMICAL COMPOSITION OF FITZPATRICK SURVEILLANCE MATERIALS FROM SURVEILLANCE SPECIMEN CHEMICAL TESTS

Metal Sample ID	Metal Sample Type	Mn (wt%)	Ni (wt%)	Cu (wt%)	Mo (wt%)	Si (wt%)	Cr (wt%)	P (wt%)
5CL[a]	Base	1.40	0.62	0.11	0.48	0.07[b]	0.11	0.011
5CM[a]	Base	1.30	0.63	0.12	0.50	0.06[b]	0.11	0.010
29283	Base	1.17	0.58	0.11	0.45	0.36	0.09	0.013
29285	Base	1.25	0.61	0.11	0.46	0.16	0.10	0.013
29286	Base	1.20	0.60	0.11	0.46	0.19	0.10	0.011
LP1-28[c]	Base	1.43	0.62	0.10	0.42	0.24	N/A	0.018
Baseline[d]	Base	1.26	0.57	0.13[e]	0.48	0.22	N/A	0.011
	Data Avg.	1.29	0.60	0.11	0.46	0.23	0.10	0.012
	Std. Dev.	0.10	0.02	0.01	0.03	0.08	0.01	0.003
5DL[a]	Weld	1.50	0.72	0.31	0.50	0.06[b]	0.04	0.015
5DM[a]	Weld	1.40	0.72	0.31	0.51	0.06[b]	0.04	0.014
29289	Weld	1.36	0.70	0.30	0.48	0.38	0.04	0.014
29295	Weld	1.25	0.70	0.23	0.47	0.41	0.04	0.014
29297	Weld	1.39	0.74	0.31	0.49	0.52	0.04	0.012
	Data Avg.	1.38	0.72	0.29	0.49	0.44	0.04	0.014
	Std. Dev.	0.09	0.02	0.03	0.02	0.07	0.001	0.001

[a] Chemical analysis of tensile specimens from 30° azimuthal capsule location (1st capsule report) [8].
[b] Si results may be low due to precipitiation during dissolution heating (Results not used in Average).
[c] Data taken from the BWROG Supplemental Surveillance Program for the FitzPatrick Plant.
[d] Taken from original fabrication records (see Table 3-1).
[e] Cu value taken from Lukens Steel letter to NYPA dated 10/14/85 [19]

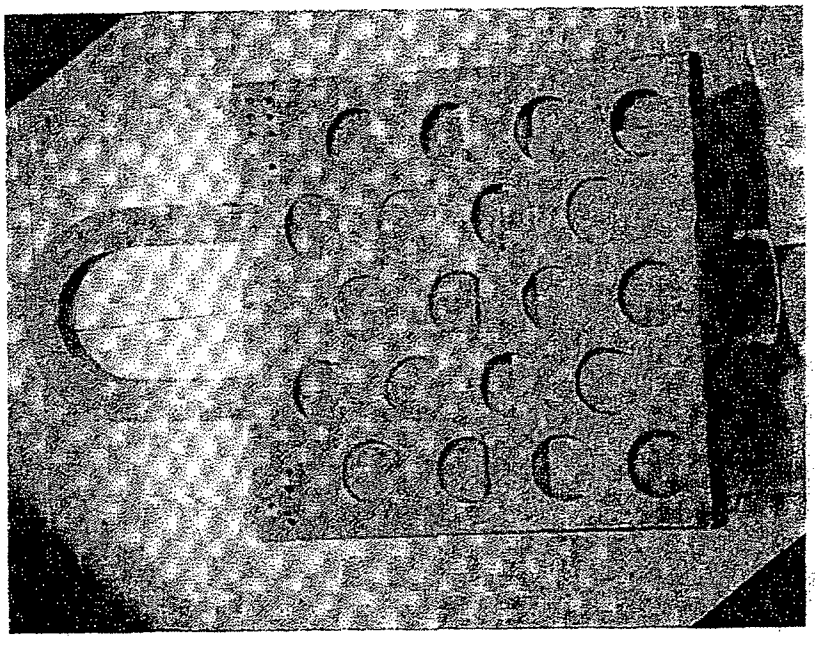

FIGURE 3-1: SURVEILLANCE CAPSULE HOLDER RECOVERED FROM FITZPATRICK (120° AZIMUTHAL LOCATION CAPSULE - REMOVED AT 13.4 EFPY)

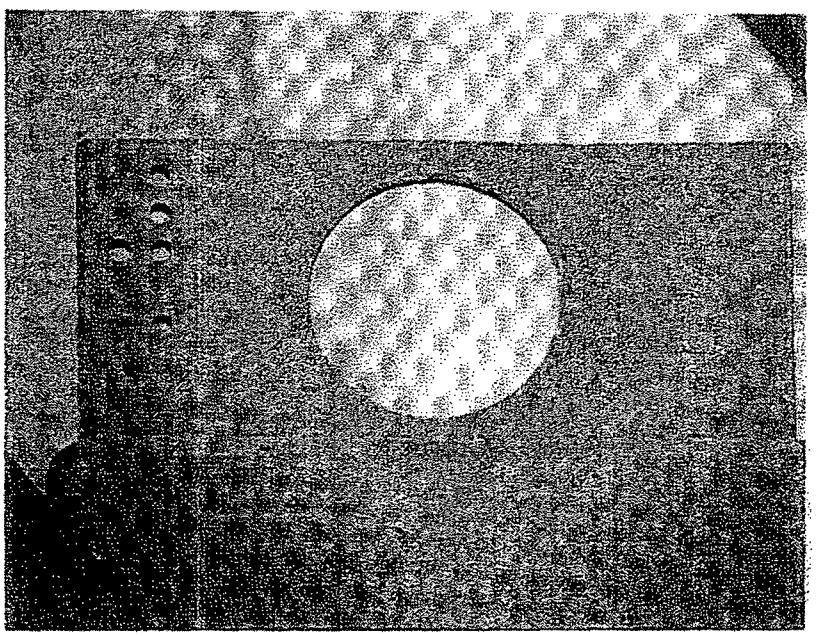

FIGURE 3-1(A): CHARPY SPECIMEN CAPSULE IDENTIFICATION
(120° AZIMUTHAL LOCATION CAPSULE - REMOVED AT 13.4 EFPY)

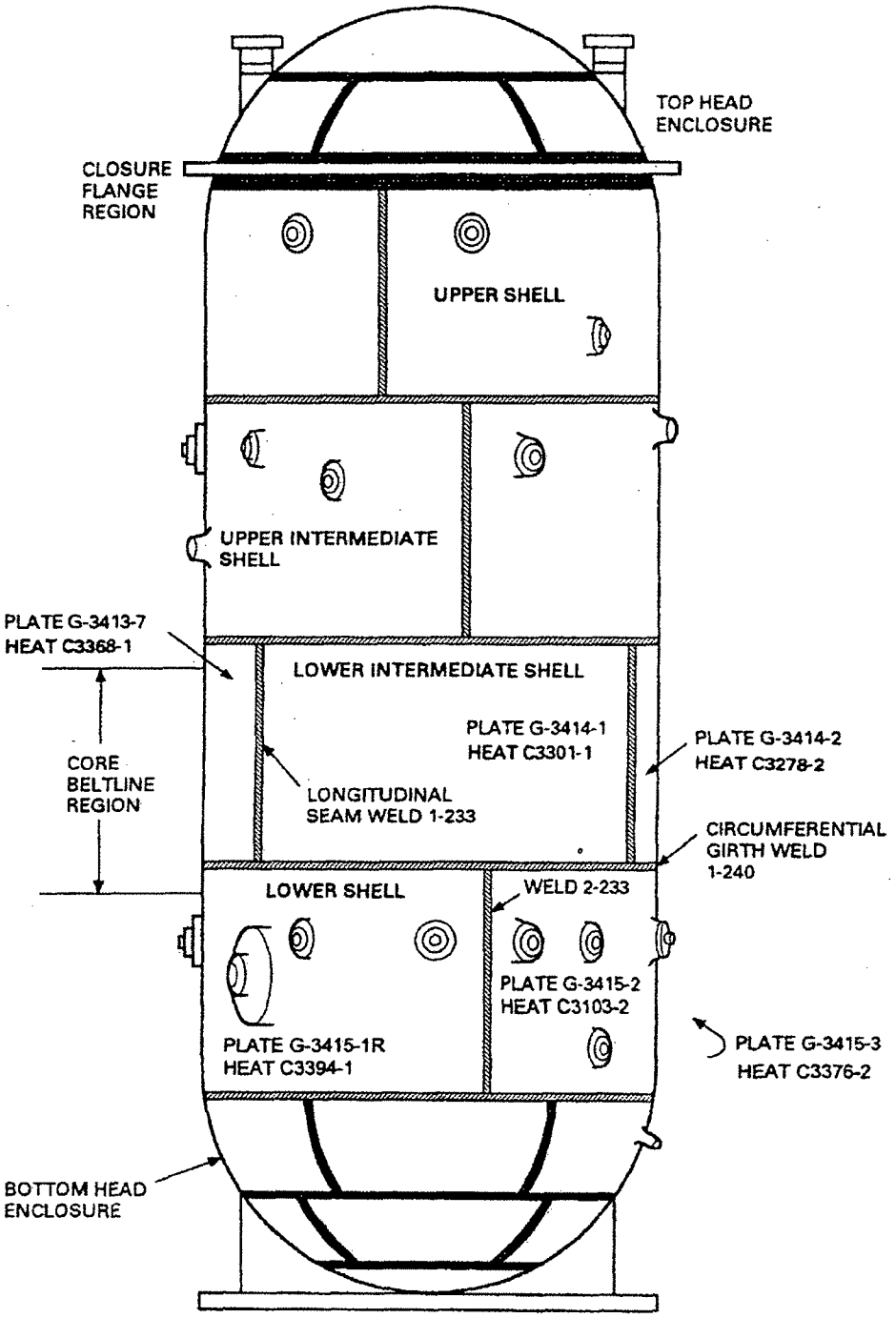

FIGURE 3-2. SCHEMATIC OF RPV SHOWING IDENTIFICATION OF VESSEL BELTLINE PLATES AND WELDS

4. PEAK RPV FLUENCE EVALUATION

Flux wires removed from the 120° location capsule were analyzed, as described in Section 4.1, to determine flux and fluence received by the surveillance capsule. The lead factor, determined as described in Section 4.2, was used to establish the peak vessel fluence from the flux wire results. Section 4.3 includes 32 EFPY peak fluence estimates.

4.1 FLUX WIRE ANALYSIS

4.1.1 Procedure

The surveillance capsule contained 2 sets of 3 flux wires: iron, nickel, and copper. Each wire was removed from the capsule, cleaned with dilute acid, weighed, mounted on a counting card, and analyzed for its radioactivity content by gamma spectrometry. Each iron wire was analyzed for Mn-54 content, each nickel wire was analyzed for Co-58 content, and each copper wire for Co-60 at calibrated source-to-detector distances with 170-cc Ge and 100-cc Ge(Li) gamma detectors used in conjunction with a Nuclear Data 6700 multichannel analyzer system.

To properly predict the flux and fluence at the surveillance capsule from the activity of the flux wires, the periods of full and partial power irradiation and the zero power decay periods were considered. Operating days for each fuel cycle and the reactor average power fraction were derived from records provided by New York Power Authority are shown in Table 4-1. Zero power days between fuel cycles are listed as well.

From the flux wire activity measurements and power history, reaction rates for Fe-54 (n,p) Mn-54, Ni-58 (n,p) Co-58, and Cu-63 (n,α) Co-60 were calculated. The E >1 MeV fast flux reaction empirical cross sections for the iron, nickel, and copper wires are 0.182 barn, 0.234 barn and 0.00318 barn, respectively. The calculated fluence result from the iron flux wire was used. The fluence result from the iron specimen was confirmed by the Ni and Cu flux wires, with all three results differing by less than 10%. The GE empirical activation cross sections are consistent with other transport code cross sections, and parallel calculations were performed using the both the empirical and transport code cross sections [20]. However, the fluence results obtained from the empirical cross sections are recommended since they yield approximately 4% higher estimates of RPV fluence. These data functions were applied to BWR pressure vessel locations based on water gap (fuel to vessel wall) distances. The cross sections for > 0.1 MeV flux were determined from the measured 0.1 to 1 MeV cross section ratio of 1.6 [11].

4.1.2 Results

The measured activity, reaction rate and full-power flux results for the 120° location surveillance capsule are given in Table 4-2. The E > 1 MeV flux values were calculated by dividing the wire reaction rate measurements by the corresponding cross sections, factoring in the local power history for each fuel cycle. The fluence result, 5.0×10^{17} n/cm^2 (E > 1 MeV), was obtained by using the following equation:

$$\Phi_{Cu} = \Phi_{fp} \sum_i t_i p_i \qquad (4\text{-}1)$$

where, Φ_{Cu} = fluence measured by the Cu dosimeters, n/cm^2
Φ_{fp} = full power flux value for Cu, n/cm^2-s
t_i = operating time, s
p_i = full power fraction

as shown in Tables 4-1 through 4-3.

The accuracies of the values in Table 4-2 for a 2σ deviation are influenced by the following sources of error:

± 2%	counting rates
± 15%	power history
± 10%	cross sections

The uncertainty in the E > 1 MeV fluence is approximately ±20% (2σ).

This analysis is performed using the GE empirical activation cross sections. A parallel analysis using cross sections from a transport code was made, but is not preferred, because its resulting fluences were approximately 4% lower for all three of the flux wires.

4.2 DETERMINATION OF LEAD FACTOR

The flux wires from the surveillance capsule are used to determine the fast neutron (E > 1 MeV) fluence at the location of the capsule as described in Section 4.1. However, the capsule and flux wires are not located where the peak vessel fluence occurs. A calculated lead factor is used to

relate the fluence at the location of the wires to the peak fluence at the vessel. The lead factor is defined as the ratio of the fast neutron fluence at the surveillance capsule to the peak fluence at the vessel inside surface. A neutron transport analysis was performed to determine the effective full power fast neutron flux distribution at the reactor pressure vessel. The lead factor was evaluated as the ratio of the calculated effective full power fast neutron fluxes at the capsule and vessel peak flux locations. Calculation of the fluxes and lead factor requires modeling of the reactor geometry and materials and depends on the distributions of power density and coolant voids in the core. The lead factor was calculated for the FitzPatrick geometry, using data for a typical operating cycle to determine power shape and void distribution. The lead factor was not adjusted for the 105% power uprate, as the fluxes were assumed to increase linearly with power. The methods used to calculate the lead factor are discussed below.

The NRC is developing Draft Regulatory Guide DG-1053, "Calculational and Dosimetry Methods for Determining Pressure Vessel Neutron Fluence", which will include guidance concerning acceptable methods and assumptions for determining the pressure vessel fluence. At this time, the draft has not been finalized for issuance as a Regulatory Guide. However, while the specific regulatory requirements are still subject to change, it is believed that the analysis described in this section is consistent with the intent of the draft guide.

4.2.1 Procedure

The lead factor for the RPV inside wall was determined by using a combination of two separate two-dimensional neutron transport computer analyses. The first of these established the azimuthal and radial variation of flux at the fuel midplane elevation. The second analysis determined the relative variation of flux with elevation. The azimuthal and axial distribution results were combined to provide a simulation of the three-dimensional distribution of flux. The ratio of fluxes, or lead factor, between the surveillance capsule location and the peak flux locations was obtained from this distribution.

The DORT computer program, which utilizes the discrete ordinates method to solve the Boltzmann transport equation in two dimensions, was used to calculate the spatial flux distribution produced by a fixed source of neutrons in the core region. The analysis considered neutrons with energies above 0.1 MeV and used 29 energy groups above this threshold. Angular dependence of the neutron scattering cross-sections was approximated by a third-order Legendre polynomial (P-3) expansion. The DORT calculations were run using S_8 angular quadrature.

The azimuthal distribution was obtained with a model specified in (R,θ) geometry, assuming eighth-core symmetry with reflective boundary conditions at 0° and 45°. In this model, θ= 30° is symmetrically equivalent to the 120° capsule location. A schematic of the (R,θ) model is shown in Figure 4-1. The model incorporates inner and outer core regions, bypass water region, shroud, downcomer water region, and a vessel plus liner region. The portion of the core inside a radius of 133 cm was not included because it will not significantly influence the flux distribution at the vessel. The spatial mesh contained 155 steps of varying sizes in the radial dimension. The azimuthal mesh step was specified to be 1/2° and was reduced to 1/4° in the vicinity of the capsule, resulting in a total of 98 azimuthal intervals. The (R,θ) model used core region material compositions and neutron source densities for the core midplane elevation (75 inches above the bottom of active fuel). This is near the elevation of the capsule, which is centered at 72.31 inches above the bottom of the active fuel. The neutron source densities and coolant mass densities were based on cycle-average values for the selected representative operating cycle. The output of this calculation provided the distribution of flux as a function of azimuth and radius at reactor midplane. The azimuth of the peak flux and its magnitude relative to the flux at the 30° capsule/flux wire azimuth were determined from this distribution.

The calculation of the axial flux distribution was performed in (R,Z) geometry, using a simplified cylindrical representation of the core configuration and realistic simulations of the axial variations of power density and coolant mass density. The core cylinder radius was specified to be equal to the radius of the outermost corner of the core, which is located at an azimuth of approximately 39.3°. The core model contained inner and outer material regions for each of 25 axial fuel nodes (total of 50 core regions). Source densities and coolant densities in these regions were based on cycle-average values for the representative cycle. The elevation of the peak flux at the reactor vessel inside surface and the magnitude of the peak flux relative to the flux at the surveillance capsule elevation were determined from the (R,Z) flux distribution results.

4.2.2 Results

The relative distribution of flux at the RPV base metal inside surface vs. azimuthal angle obtained from the (R,θ) calculation is shown in Figure 4-2. The relative distribution of flux versus elevation at the RPV inside surface from the (R,Z) calculation is shown in Figure 4-3. The azimuthal distribution (Figure 4-2) indicates that the 8 flux maxima at the vessel base metal inside surface occur at azimuthal locations which are displaced by 42.75° from the RPV quadrant reference axes (0°, 90°, etc.). From the R,Z results (Figure 4-3), the peak is estimated to occur at

an elevation about 79 inches above the bottom of the active fuel. The calculated core midplane E > 1 MeV flux at the (R,θ) coordinates corresponding to the equivalent capsule center position (θ = 30°, R = 109.19 inches) was 1.382 x10^9 n/cm^2/s. This was multiplied by the ratio of flux at the capsule elevation to flux at midplane (0.996), as determined from the (R,Z) calculation, resulting in a calculated flux at the capsule location which rounds to 1.38 x 10^9 n/cm^2/s. The peak flux at the vessel surface (R = 110.375 inches) was similarly obtained by multiplying the calculated midplane flux of 2.015 x10^9 n/cm^2/s at the peak azimuth by an axial adjustment factor of 1.003 from the (R,Z) calculation. The resulting peak flux estimate is 2.02 x 10^9 n/cm^2/s. Consequently, the lead factor is 1.38 x 10^9 / 2.02 x 10^9 =0.68.

The calculated capsule full power flux of 1.38x10^9 n/cm^2/s obtained with this model is about 16 % higher than the capsule dosimetry result of 1.19x10^9 n/cm^2/s. The indicated agreement between the analytical and experimental results is within the uncertainties associated with those results and is considered good. It is estimated that the 1σ uncertainty in the calculated flux magnitudes is on the order of 25 - 30 %. However, since the lead factor is determined from the ratio of two calculated fluxes which have sources of error in common, the 1σ uncertainty in the lead factor is estimated to be no more than 15 %.

Use of a lead factor calculated on the basis of the model described above is consistent with current GE practice for estimation of the peak vessel fluence. Application of the lead factor to the capsule dosimetry results yields an estimated end-of-cycle 12 peak fluence of 5.0x10^{17} / 0.68=7.4x10^{17} n/cm^2 and an estimated peak full power flux of 1.19x10^9/0.68 = 1.75 x 10^9 n/cm^2/s at the vessel inside surface. Since the estimated 1σ uncertainty in the dosimetry results is 10 % and the estimated 1σ uncertainty in the lead factor is 15%, the combined overall 1σ uncertainty in the projected peak values is estimated to be about $(10^2 + 15^2)^{0.5}$ = 18 %.

The analysis model discussed above did not include the effects of the material specimens and specimen holder on the local neutron flux. A second calculation was performed in (R,θ) geometry with a model which incorporated regions which simulated the material specimens and holder. The densely packed material specimens were represented as solid steel in the model. The perforated wall of the specimen holder was modeled as a steel/water mixture. This model is expected to provide a reasonable upper bound estimate of the effect of the capsule on local fluxes. The results obtained with this model were also used to provide independent confirmation of the reaction rate cross-sections used in the dosimetry analysis described in Section 4.1.

The flux obtained at the capsule midpoint radius with the modified (R,θ) model was $1.53x10^9$ n/cm^2/s. Application of the axial adjustment of 0.996 results in an estimated flux of $1.52x10^9$ n/cm^2/s at the capsule center point. Consequently, the flux calculated at this point with the simulated capsule materials is about 10 % higher than the flux calculated with the base model. The region-averaged flux obtained in the specimen region, $1.51x10^9$ n/cm^2/s, differs only slightly from the center point value. These results indicate that the base model under-predicts the flux within the capsule by a few percent and possibly as much as 10 %. Therefore, a conservative bias exists in the calculated lead factor and projected peak fluences, since underestimation of the lead factor results in overestimation of the vessel peak fluence.

The 29-group neutron energy spectrum obtained at the simulated capsule center point was plotted and applied to ENDF/B-VI library data for the dosimeter activation reaction cross-sections to calculate spectrum-weighted group cross-sections for the reactions. The DORT case was re-run to obtain calculated total reaction rates which, when divided by the E > 1 MeV flux, yield the effective reaction rate cross-sections for the fast flux. The cross-sections used in Section 4.1 to analyze the dosimeter data are derived from fits to empirical data which have been used by GE for analysis of surveillance capsule dosimetry for many years. Region-averaged values obtained for the specimen region in the DORT model are compared with the Section 4.1 cross-sections in the table below.

Comparison of Calculated Activation Cross-Sections in Simulated Capsule Region With Semi-Empirical Cross-Sections Used in Capsule Dosimetry Analysis

Reaction	Effective Cross-Section for E > 1 Mev Flux (barns)		Difference
	Empirical Fit	Calculated	%
Fe54(n,p)Mn54	0.182	0.1899	+4.34
Ni58(n,p)Co58	0.234	0.2425	+3.63
Cu63(n,a)Co60	0.00318	0.003305	+3.93

The close agreement between the calculated cross-sections and the fit-derived cross-sections provides confidence that the empirically derived cross-sections are reliable. It also provides confidence that the calculated neutron spectrum is realistic, even though the magnitude of the calculated flux is somewhat greater than the measured flux. In each instance, the calculated

cross-sections are slightly higher than the empirical cross-sections. Consequently, if the dosimeter material reaction rates are predicted purely from the analysis, the difference between calculated and measured reaction rates will be slightly greater than the difference between the calculated and measured fluxes. The reaction rates are compared below.

Comparison of Calculated Reaction Rates in Simulated Capsule Region With Reaction Rates Determined From Capsule Dosimetry Analysis

Reaction	Dosimeter Reaction Rate (reactions/s/nucleus)		Difference
	Capsule Dosimeters	Calculated	%
Fe54(n,p)Mn54	2.14E-16	2.86E-16	+33.8
Ni58(n,p)Co58	2.70E-16	3.66E-16	+35.4
Cu63(n,a)Co60	3.91E-18	4.98E-18	+27.4

The fracture toughness analysis is based on a 1/4 T depth flaw in the beltline region, so the attenuation of the flux to that depth is considered. This attenuation is calculated according to the Reg. Guide 1.99, Rev. 2 requirements, as shown in the next section.

4.3 ESTIMATE OF 32 EFPY FLUENCE

The inside surface fluence (f_{surf}) at 32 EFPY is determined from the flux wire fluence at a particular EFPY and lead factor according to:

$$f_{surf} = (f_{cap} * 32\ EFPY)/(LF * CEFPY) \qquad (4\text{-}2)$$

where, f_{surf} = 32 EFPY fluence at the peak vessel inside surface
f_{cap} = capsule fluence measured at the CEFPY
32 EFPY = end of life EFPY based on a 40-year operation at an 80% capacity factor
CEFPY = the current EFPY for the capsule
LF = lead factor

The surveillance capsule was removed from FitzPatrick at 13.4 EFPY as calculated in Table 4-2. The fluence at 13.4 EFPY was determined to be 5.0×10^{17} n/cm^2 using Equation 4-1, and the lead factor was determined to be 0.68 as discussed in Section 4.2. In addition, the fluence over the remaining 18.6 EFPY was increased by 5% to account for the 5% power uprate that began in December 1996. Using this information with Equation 4-2, the resulting 32 EFPY fluence value at the peak vessel inside surface is:

$$f_{surf} = [(5.0 \times 10^{17}) + (5.0 \times 10^{17} * 18.6/13.4) * 1.05]/0.68 = 1.81 \times 10^{18} \text{ n/cm}^2 \quad (4\text{-}3)$$

at the peak location.

The peak surface fluence at 32 EFPY is 22% lower than the nominal value (2.32×10^{18} n/cm^2) that was calculated from the first surveillance capsule dosimetry as a result of power uprate as reported in GE report [15]. This variation can be attributed to refinements in the analysis technique since the first capsule was removed.

The 1/4 T fluence (f) is calculated according to the Reg. Guide 1.99 [7] equation:

$$f = f_{surf}(e^{-0.24x}), \quad (4\text{-}4)$$

where x = distance, in inches, to the 1/4 T depth. The vessel beltline lower intermediate shell ring thickness is 5.375 inches minimum requirement. The corresponding depth, x, taken from the minimum required thickness is 1.34 inches for the lower intermediate shell. Equation 4-4 evaluated for this value of x gives the 1/4 T value of 32 EFPY fluence, $f = 1.31 \times 10^{18}$ n/cm^2 for the lower intermediate shell ring.

In the case of the lower shell ring, the axial fluence distribution was also taken into account. The maximum fluence at the top of the lower shell is 0.89 times the peak fluence, or 1.61×10^{18} n/cm^2. The minimum plate thickness of the lower shell is 6.375 inches, which corresponds to an x value of 1.6 inches. The resultant 1/4T fluence at 32 EFPY is 1.10×10^{17} n/cm^2.

TABLE 4-1: SUMMARY OF FITZPATRICK IRRADIATION PERIODS

On	Off	Duration (days)	Days to eoi	MWd	Effective Full Power Days	Full Power Fraction
1/26/75	12/31/77	1071	6874	1301203	534.4	0.499
1/1/78	12/31/78	365	6509	539687	221.6	0.607
1/1/79	12/31/79	365	6144	373919	153.7	0.421
1/1/80	12/31/80	366	5778	541475	222.2	0.607
1/1/81	12/31/81	365	5413	592405	243.1	0.666
1/1/82	12/31/82	365	5048	630106	258.8	0.709
1/1/83	12/31/83	365	4683	592197	243.1	0.666
1/1/84	12/31/84	366	4317	633307	259.9	0.710
1/1/85	12/31/85	365	3952	532365	218.6	0.599
1/1/86	12/31/86	365	3587	767477	315.0	0.863
1/1/87	12/31/87	365	3222	545590	224.1	0.614
1/1/88	12/31/88	366	2856	557082	228.8	0.625
1/1/89	12/31/89	365	2491	781820	320.8	0.879
1/1/90	12/31/90	365	2126	592684	243.5	0.667
1/1/91	1/31/91	31	2095	69083	28.4	0.915
2/1/91	2/28/91	28	2067	56800	23.3	0.833
3/1/91	3/9/91	9	2058	19191	7.9	0.875
3/17/91	3/18/91	2	2049	116	0.1	0.024
4/13/91	4/30/91	18	2006	34493	14.2	0.787
5/1/91	5/7/91	7	1999	16095	6.6	0.944
8/18/91	8/31/91	14	1883	26087	10.7	0.765
9/1/91	9/30/91	30	1853	72905	29.9	0.998
10/1/91	10/31/91	31	1822	74840	30.7	0.991
11/1/91	11/28/91	28	1794	63288	26.0	0.928
11/29/91	1/2/93	401	1393	0	0.0	0.000
1/3/93	1/31/93	29	1364	14983	6.2	0.212
2/1/93	2/28/93	28	1336	58272	23.9	0.854
3/1/93	3/31/93	31	1305	17725	7.3	0.235
4/1/93	4/30/93	30	1275	51219	21.0	0.701
5/1/93	5/31/93	31	1244	46629	19.1	0.617
6/1/93	6/30/93	30	1214	72730	29.8	0.995
7/1/93	7/31/93	31	1183	72348	29.7	0.958
8/1/93	8/31/93	31	1152	75443	31.0	0.999
9/1/93	9/30/93	30	1122	62975	25.9	0.862
10/1/93	10/31/93	31	1091	55927	23.0	0.741
11/1/93	11/30/93	30	1061	13756	5.6	0.188
12/1/93	12/31/93	31	1030	74988	30.8	0.993
1/1/94	1/31/94	31	999	75300	30.9	0.997
2/1/94	2/28/94	28	971	68114	28.0	0.999
3/1/94	3/31/94	31	940	73706	30.3	0.976
4/1/94	4/30/94	30	910	4546	1.9	0.062
5/1/94	5/31/94	31	879	63588	26.1	0.842
6/1/94	6/30/94	30	849	71339	29.3	0.976
7/1/94	7/31/94	31	818	68452	28.1	0.906

8/1/94	8/31/94	31	787	61533	25.3	0.815
9/1/94	9/30/94	30	757	54488	22.4	0.746
10/1/94	10/31/94	31	726	54520	22.4	0.722
11/1/94	11/30/94	30	696	47247	19.4	0.647
12/1/94	12/31/94	31	665	0	0.0	0.000
1/1/95	1/31/95	31	634	0	0.0	0.000
2/1/95	2/28/95	28	606	0	0.0	0.000
3/1/95	3/31/95	31	575	5960	2.5	0.079
4/1/95	4/30/95	30	545	69366	28.5	0.949
5/1/95	5/31/95	31	514	72287	29.7	0.957
6/1/95	6/30/95	30	484	49822	20.5	0.682
7/1/95	7/31/95	31	453	75412	31.0	0.999
8/1/95	8/31/95	31	422	75410	31.0	0.999
9/1/95	9/30/95	30	392	53600	22.0	0.733
10/1/95	10/31/95	31	361	75437	31.0	0.999
11/1/95	11/30/95	30	331	73014	30.0	0.999
12/1/95	12/31/95	31	300	73993	30.4	0.980
1/1/96	1/31/96	31	269	75173	30.9	0.995
2/1/96	2/29/96	29	240	51562	21.2	0.730
3/1/96	3/31/96	31	209	56448	23.2	0.747
4/1/96	4/30/96	30	179	72990	30.0	0.999
5/1/96	5/31/96	31	148	73629	30.2	0.975
6/1/96	6/30/96	30	118	71757	29.5	0.982
7/1/96	7/31/96	31	87	75250	30.9	0.996
8/1/96	8/31/96	31	56	73687	30.3	0.976
9/1/96	9/30/96	30	26	49799	20.4	0.681
10/1/96	10/26/96	26	0	56785	23.3	0.897

Note: Full power was taken as the value prior to uprate of 2436 MW_t

Total Effective Full Power Days= 4907.8
Total Effective Full Power Years = 13.4

TABLE 4-2: SURVEILLANCE CAPSULE FLUX AND FLUENCE FOR IRRADIATION FROM START-UP TO 11/12/96 (13.4 EFPY) USING EMPIRICAL CROSS SECTIONS (GE CORRELATION)

Wire (Element)	Average[a] dps/g Element (at end of irradiation)	Average Reaction Rate [dps/nucleus (saturated)]	Full Power Flux[b] (n/cm^2-s) E>1 MeV	Full Power Flux[c] (n/cm^2-s) E>0.1 MeV	Fluence (n/cm^2) E>1 MeV	Fluence[c] (n/cm^2) E>0.1 MeV
Iron	1.07E05	2.14E-16	1.18E09	1.89E09	5.00E17	7.99E17
Nickel	1.67E06	2.70E-16	1.16E09	1.86E09	4.90E17	7.85E17
Copper	1.56E04	3.91E-18	1.23E09	1.97E09	5.21E17	8.34E17

a Obtained by R.D Reager [20]
b Full power flux, based on thermal power of 2436 MW_t
c 1.6 times the E >1 MeV result

TABLE 4-2: SURVEILLANCE CAPSULE FLUX AND FLUENCE FOR IRRADIATION FROM START-UP TO 11/12/96 (13.4 EFPY) USING EMPIRICAL CROSS SECTIONS (GE CORRELATION)

Wire (Element)	Average[a] dps/g Element (at end of irradiation)	Average Reaction Rate [dps/nucleus (saturated)]	Full Power Flux[b] (n/cm^2-s) E>1 MeV	Full Power Flux[c] (n/cm^2-s) E>0.1 MeV	Fluence (n/cm^2) E>1 MeV	Fluence[c] (n/cm^2) E>0.1 MeV
Iron	1.07E05	2.14E-16	1.18E09	1.89E09	5.00E17	7.99E17
Nickel	1.67E06	2.70E-16	1.16E09	1.86E09	4.90E17	7.85E17
Copper	1.56E04	3.91E-18	1.23E09	1.97E09	5.21E17	8.34E17

a Obtained by R.D Reager [20]
b Full power flux, based on thermal power of 2436 MW_t
c 1.6 times the E >1 MeV result

TABLE 4-3. MEASURED FLUX VS. THEORETICAL FLUX FOR DOSIMETER AND FLUX WIRES

			E > 1 MeV			
	Lead Factor Capsule to ID Surface	EFPY*	Measured Capsule Flux (n/cm^2-s)	Capsule Fluence (n/cm^2)	EOL (32 EFPY) FLUENCE (n/cm^2)	
					ID Surface	1/4T Location
1982 30° Azimuth Dosimeter		~1	$1.5x10^{9}$			
1985 30° Azimuth Flux Wires	0.79	6.0	$1.4x10^{9}$	$2.6x10^{17}$	$1.8x10^{18}$	$1.35x10^{18}$
Upper Bound (1.25 Factor)					$2.2x10^{18}$	$1.7x10^{18}$
Reg. Guide 1.99 Rev.2 Evaluation, no upper bound factor included. Tech Spec P-T curve basis.	0.61				$2.32x10^{18}$	$1.7x10^{18}$
5% Power Uprate based on upper bound value.					$2.44x10^{18}$	$1.76x10^{18}$
1996 120° Azimuth Flux Wires Includes 5% Power Uprate New P-T curve basis.	0.68	13.4	$1.2x10^{9}$	$5.0x10^{17}$	$1.81x10^{18}$	$1.38x10^{18}$

* Effective Full Power Years at 2436 Mw_t

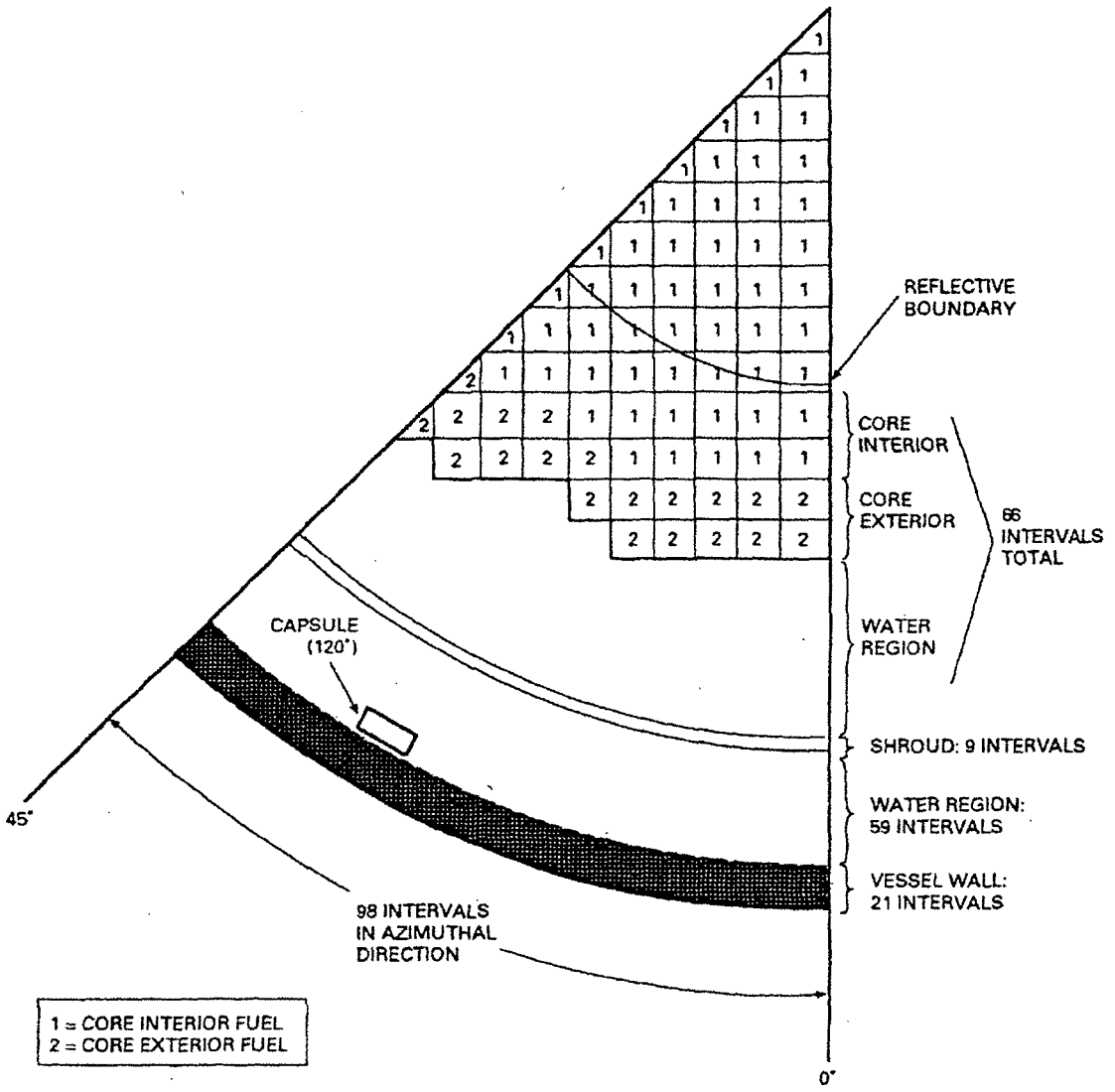

FIGURE 4-1: SCHEMATIC OF MODEL FOR AZIMUTHAL FLUX DISTRIBUTION ANALYSIS

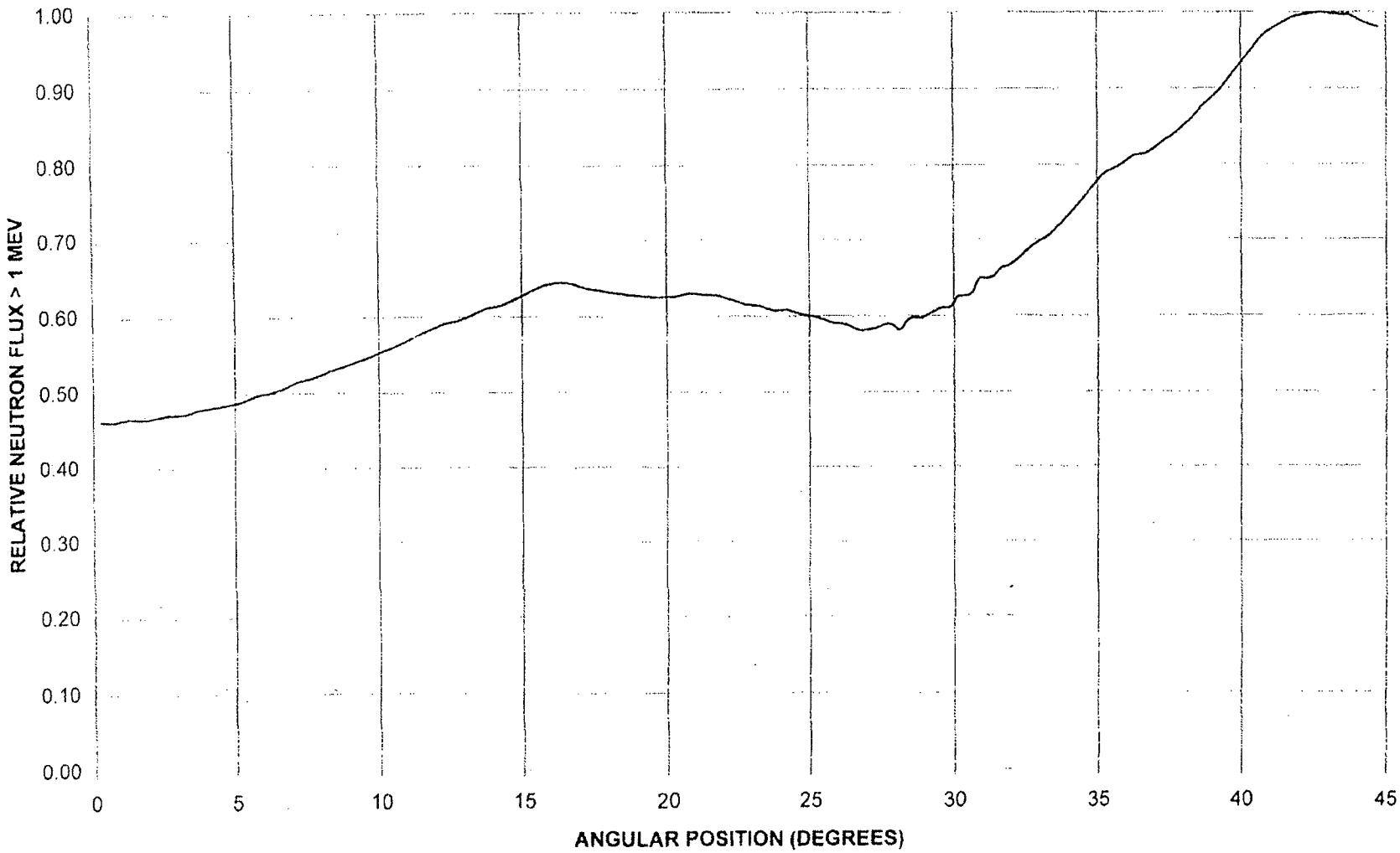

FIGURE 4-2: RELATIVE FLUX VS. ANGLE AT RPV INSIDE SURFACE

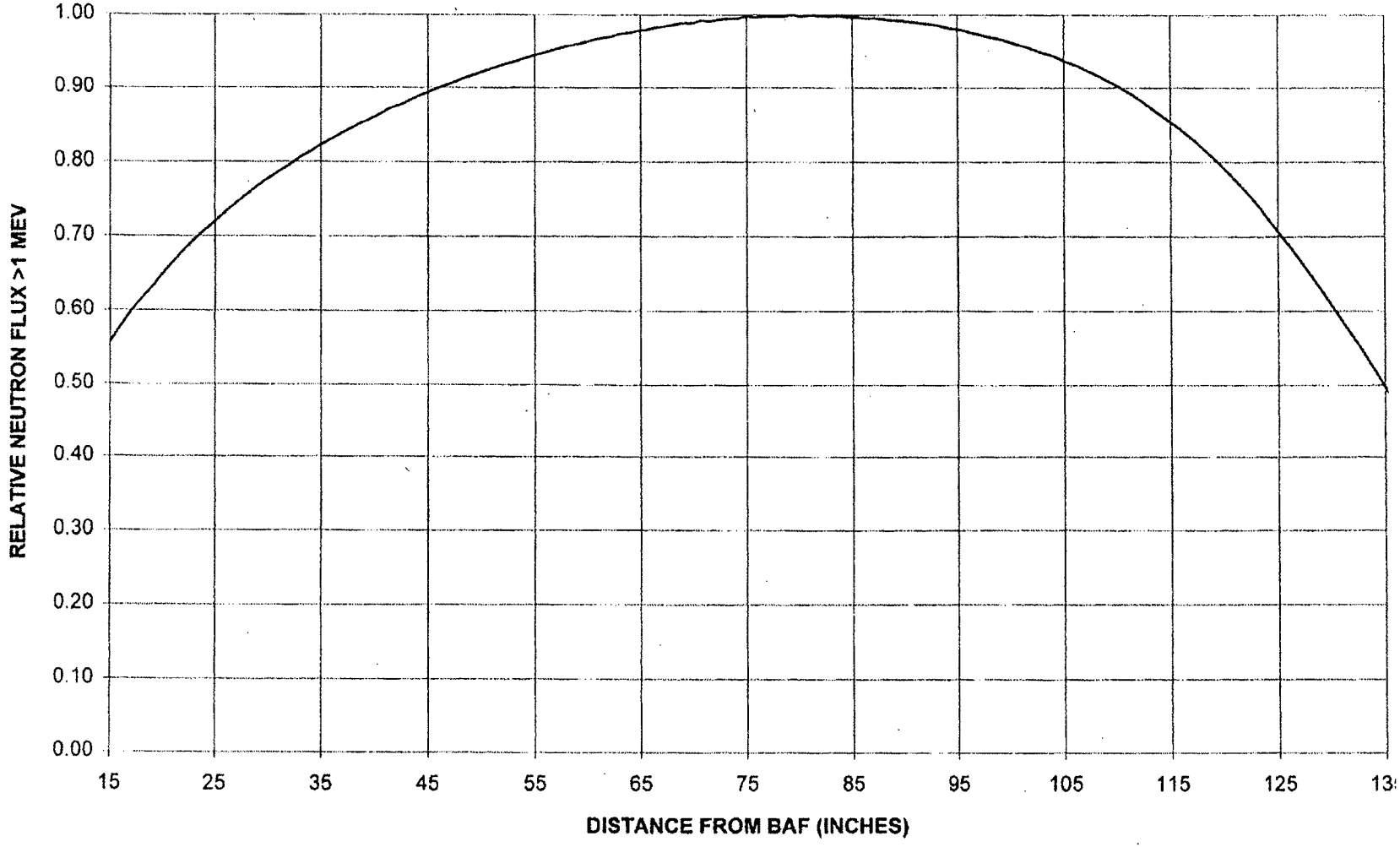

FIGURE 4-3: RELATIVE FLUX VS. ELEVATION AT RPV INSIDE SURFACE

5. CHARPY V-NOTCH IMPACT TESTING

The 24 Charpy specimens recovered from the surveillance capsule were impact tested at temperatures selected to establish the toughness transition and upper shelf of the irradiated RPV materials. Testing was conducted in accordance with ASTM E23-94b [12].

5.1 IMPACT TEST PROCEDURE

The Vallecitos testing machine used for irradiated specimens was a Tinius Olsen impact machine, serial number 175363. The maximum energy capacity of the machine is 300 ft-lb, which produces a test velocity at impact of 19.3 ft/sec.

The Tinius Olsen machine was qualified using NIST standard reference material specimens. The Standard Reference Materials (SRMs) consist of three sets of specimens which cover the energy range of the apparatus. Each set has a designated failure energy and a standard test temperature. According to ASTM E23-94b [12], the test apparatus averaged results must reproduce the NIST standard values within an accuracy of $\pm 5\%$ or ± 1.0 ft-lb, whichever is greater. The results of the qualification of the Tinius Olsen impact machine are summarized in Table 5-1.

Charpy V-Notch tests were conducted at temperatures between -80°F and 400°F. The cooling fluid used for irradiated specimens tested at temperatures at or below 50°F was ethanol. At temperatures between 50°F and 210°F, water was used as the temperature conditioning fluid. The specimens were heated in silicon oil for test temperatures above 210°F. Cooling of the conditioning fluids was done by heat exchange with liquid nitrogen through a copper coil; heating was done by an immersion heater. The bath of fluid was mechanically stirred to maintain uniform temperatures. The fluid temperature was measured with a calibrated Type K thermocouple positioned near the impact samples. After equilibration at the test temperature for at least 5 minutes, the specimens were manually transferred with centering tongs to the Charpy test machine and impacted in less than 5 seconds.

For each Charpy V-Notch specimen the test temperature, energy absorbed, lateral expansion, and percent shear were determined. In addition, photographs were taken for the

irradiated specimens. Lateral expansion and percent shear were measured according to specified methods [12]. Percent shear was determined using method number 1 of Subsection 11.2.4.3 of ASTM E23-94b [12], which involved measuring the length and width of the cleavage surface in inches and determining the percent shear value from Table 2 of ASTM E23-94b [12].

5.2 IMPACT TEST RESULTS

Eight Charpy V-Notch specimens each of irradiated base, weld, and HAZ material were tested at temperatures (-80°F to 400°F) selected to define the toughness transition and upper shelf portions of the fracture toughness curves. The absorbed energy, lateral expansion, and percent shear data are listed for each material in Table 5-2. Plots of absorbed energy and lateral expansion for base, weld, and HAZ materials are presented in Figures 5-1 through 5-6. These curves are plotted along with the corresponding curves from the first capsule (and unirradiated base material data where appropriate) in Figures 5-7 through Figure 5-12. The fracture surface photographs and a summary of the test results for each specimen are contained in Appendix A.

The unirradiated and irradiated plate and weld energy and lateral expansion data are fit with the hyperbolic tangent function developed by Oldfield for the EPRI Irradiated Steel Handbook [13] (HAZ was not fit due to data scatter):

$$Y = A + B * TANH [(T - T_0)/C],$$

where Y = impact energy or lateral expansion
T = test temperature, and
A, B, T_0 and C are determined by non-linear regression.

The TANH function is one of the few continuous functions with a shape characteristic of low alloy steel fracture toughness transition curves.

5.3 IRRADIATED VERSUS UNIRRADIATED CHARPY V-NOTCH PROPERTIES

Ideally, a shift in RT_{NDT} would be established by comparing the irradiated Charpy specimen data to baseline unirradiated Charpy data. For the case of the FitzPatrick base material specimens, data was obtained from the Certified Material Test Report. Additional Charpy test

data for the FitzPatrick surveillance plate (heat number C3278-2) was available from the BWROG Supplemental Surveillance Program report [17]. This program was useful in providing plant-specific data and information for the FitzPatrick base material to establish baseline properties. The unirradiated data for the base material, as well as the results for both the plate and weld materials from the first and second surveillance capsules, were fit to a TANH function as described in the previous section. The unirradiated properties for the surveillance plate were determined from the combined sets of data, as shown in Figure 5-13. For the weld material, no credible unirradiated baseline data was available.

5.4 COMPARISON TO PREDICTED IRRADIATION EFFECTS

5.4.1 Irradiation Shift

The measured transition temperature shifts for the base and weld materials were compared to the predictions calculated according to Rev. 2 [7]. The inputs and calculated values for irradiated shift for the plate and weld materials based upon measurements taken from the 120° azimuth capsule at 13.4 EFPY are as follows:

Plate:	Copper =	0.11%	
	Nickel =	0.60%	
	CF =	74	
	fluence =	5.0×10^{17} n/cm^2	
	Reg. Guide 1.99 ΔRT_{NDT} =		21.7°F
	Reg. Guide 1.99 $\Delta RT_{NDT} \pm 2\sigma_\Delta$(34°F) =		55.7°F max, -12.3°F min
	Measured 30 ft-lb shift =		14.97°F
Weld:	Copper =	0.29%	
	Nickel =	0.71%	
	CF =	208	
	fluence =	5.0×10^{17} n/cm^2	
	Reg. Guide 1.99 ΔRT_{NDT} =		60.9°F
	Reg. Guide 1.99 $\Delta RT_{NDT} \pm 2\sigma_\Delta$(56°F) =		116.9°F max, 4.9°F min

GE Nuclear Energy

Technical Services Business
General Electric Company
175 Curtner Avenue, San Jose, CA 95125

GE-NE-B1100732-01, Revision 1
Final Report
Class II
February 1998

PLANT FITZPATRICK RPV SURVEILLANCE MATERIALS TESTING AND ANALYSIS OF 120° CAPSULE AT 13.4 EFPY

Prepared by: Timothy J. Griesbach
T. J. Griesbach, Director
ATI Consulting

Verified by: R. G. Carey
R. G. Carey, Engineer
Structural Mechanics and Materials

Approved by: B. J. Branlund
B. J. Branlund, Project Manager
Structural Mechanics and Materials

Pagano, Terry

From: Porter, Anne
Sent: Thursday, November 10, 2005 10:33 AM
To: Pagano, Terry
Subject: FW: Fitz Doc

Terry – can you get this please

From: LOYD, LELAND
Sent: Thursday, November 10, 2005 10:21 AM
To: Porter, Anne
Cc: Harrison, Douglas; Herrmann, Terry; BARTON, SANDRA
Subject: Fitz Doc

Good Morning Anne
I need GE-NE-B1100732-01 (JAF RPV surveillance materials testing & analysis of 120 degree capsule at 13.4 EFPY (effective full power years) – including BJB-9907 and attachment to BJB-9907).

If you send it hard copy send to Sandy

ENTERGY CORPORATION
1448 SR 333
Russellville, AR 72802
c/o Sandra Barton
N-GSB-45

Or; sbart90@entergy.com Sandy (this goes with the OE programs, Lori will know what to do with it)

Thanks!

Leland Loyd
License Renewal
lloyd90@entergy.com
479/858/4696

GE Nuclear Energy

Technical Services Business
General Electric Company
175 Curtner Avenue, San Jose, CA 95125

GE-NE-B1100732-01, Revision 1
Final Report
Class II
February 1998

PLANT FITZPATRICK RPV SURVEILLANCE MATERIALS TESTING AND ANALYSIS OF 120° CAPSULE AT 13.4 EFPY

Prepared by: Timothy J. Griesbach
T. J. Griesbach, Director
ATI Consulting

Verified by: R. G. Carey
R. G. Carey, Engineer
Structural Mechanics and Materials

Approved by: B. J. Branlund
B. J. Branlund, Project Manager
Structural Mechanics and Materials

123 Main Street
White Plains, New York 10601
914 681.6200

New York Power Authority

February 13, 1998 DCME-98-0086

To: GE NUCLEAR ENERGY
175 Curtner Ave
San Jose CA 95125

Contract No. C95-Z0013

Attn: Ms. B. J. Branlund, Project Manager

The document(s) listed below are being returned to you with the status indicated on each document.

Document No.	Rev.	Status
GE-NE-B1100732-01 JAF RPV SURVEILLANCE MATERIALS TESTING & ANALYSIS OF 120 DEGREE CAPSULE AT 13.4 EFPY (EFFECTIVE FULL POWER YEARS)	1	1 ACCEPTED

Very truly yours,

William H Spataro

W. Spataro
Consulting Metallurgist

copies (transmittal only): G. Grochowski
w. attachment: G. Rorke, J. Ellmers, C. Doc

**IMPORTANT NOTICE REGARDING
CONTENTS OF THIS REPORT
PLEASE READ CAREFULLY**

This report was prepared by General Electric solely for the use of the New York Power Authority. The information contained in this report is believed by General Electric to be an accurate and true representation of the facts known, obtained, or provided to General Electric at the time this report was prepared.

The only undertakings of the General Electric Company respecting information in this document are contained in the contract between the customer and General Electric Company, as identified in the purchase order for this report and nothing contained in this document shall be construed as changing the contract. The use of this information by anyone other than the customer or for any purpose other than that for which it is intended, is not authorized; and with respect to any unauthorized use, General Electric Company makes no representation or warranty, and assumes no liability as to the completeness, accuracy, or usefulness of the information contained in this document.

TABLE OF CONTENTS

TABLE OF TABLES

TABLE OF FIGURES

TABLE OF FIGURES
(continued)

ABSTRACT

The surveillance capsule at the 120° azimuthal location was removed at 13.4 EFPY from the FitzPatrick reactor in November 1996. The capsule contained flux wires for neutron fluence measurement, and Charpy test specimens and tensile test specimens for material property evaluations. The flux wires were evaluated to determine the fluence experienced by the test specimens. Charpy V-Notch impact testing and tensile testing were performed to establish the properties of the irradiated surveillance materials.

The irradiated Charpy data for the base material specimens were compared to available unirradiated data to determine the shift in Charpy curves due to irradiation. The results indicate a shift lower than the predictions of Regulatory Guide 1.99 Revision 2 [Rev. 2]. Since two sets of credible data sets were available for the plate material, the Adjusted Reference Temperature (ART) calculations for vessel base materials were adjusted in accordance with Rev. 2. For the vessel weld metal, no unirradiated data was available and the predictions of Rev. 2 were used to calculate ART.

The flux wire results combined with the lead factor were used to estimate the 32 EFPY fluence. The fluence calculations included the effects of a 105% power uprate. The resulting estimated fluence showed a reduction of 22 percent compared with the previous nominal 32 EFPY fluence estimate consistent with the fluence used for the Technical Specification Pressure-Temperature (P-T) Curves.

P-T Curves were prepared based on the new projected fluence levels for both 32 EFPY and 24 EFPY.

ACKNOWLEDGMENTS

The author gratefully acknowledges the efforts of other people towards completion of the contents of this report.

Cask shipping & receipt, and capsule disassembly were performed by J. B. Myers and R. D. Rimmer. Charpy testing was completed by G. E. Dunning and B. D. Frew. Tensile testing was performed by S. B. Wisner. Chemical composition analysis was performed by P. S. Wall. Flux wire testing and analysis was performed by L. Kessler, R. M. Kruger and R. D. Reager. Fluence and lead factor calculations were performed by D. R. Rogers, H. A. Careway and S. S. Wang. Assistance with the capsule evaluation was provided by B. N. Burgos of ATI Consulting. Project management was conducted by B. J. Branlund.

1. INTRODUCTION

Part of the effort to assure reactor vessel integrity involves evaluation of the fracture toughness of the vessel ferritic materials. The key values which characterize a material's fracture toughness are the reference temperature of nil-ductility transition (RT_{NDT}) and the upper shelf energy (USE). These are defined in 10CFR50 Appendix G [1] and in Appendix G of the ASME Boiler and Pressure Vessel Code, Section XI [2].

Appendix H of 10CFR50 [3] and ASTM E185-70 [4] establish the methods to be used for surveillance of the James A. FitzPatrick (FitzPatrick) reactor vessel materials. The second vessel surveillance specimen capsule required by 10CFR50 Appendix H [3] was removed from FitzPatrick in November 1996. The irradiated capsule was sent to the GE Vallecitos Nuclear Center (VNC) for testing. The surveillance capsule contained flux wires for neutron flux monitoring and Charpy V-Notch impact and tensile test specimens fabricated using base metal from the beltline region, as well as weld metal from a similar heat of material as the beltline welds. The impact and tensile specimens were tested to establish properties for the irradiated materials.

The results of the surveillance specimen testing are presented in this report, as required per 10CFR50 Appendices G and H [1 & 3]. The irradiated material properties are compared to available unirradiated properties to determine the effect of irradiation on material toughness for the base and weld materials, through Charpy testing. Irradiated tensile testing results are provided and are compared with unirradiated data to determine the effect of irradiation on the stress-strain relationship of the materials.

Pressure-temperature (P-T) curves are included in this report which have been developed to present steam dome pressure versus minimum vessel metal temperature incorporating appropriate non-beltline limits and irradiation embrittlement effects in the beltline. The P-T curves are established to the requirements of 10CFR50, Appendix G [1] to assure that brittle fracture of the reactor vessel is prevented.

2. SUMMARY AND CONCLUSIONS

2.1 SUMMARY OF RESULTS

The 120° azimuth position surveillance capsule was removed and shipped to VNC. The flux wires, Charpy V-Notch and tensile test specimens removed from the capsule were tested according to ASTM E185-82 [6]. The methods and results of the testing are presented in this report as follows:

Section 3: Surveillance Program Background

- RPV Materials and Fabrication
- Material Properties
- Surveillance Specimen Chemical Composition
- Specimen Description

Section 4: Peak RPV Fluence Evaluation

Section 5: Charpy V-Notch Impact Testing

Section 6: Tensile Testing

Section 7: Adjusted Reference Temperature and Upper Shelf Energy

Section 8: Pressure-Temperature Curves

The significant results of the evaluation are below:

a. The 120° azimuth position capsule was removed from the reactor after 13.4 EFPY (Effective Full Power Years) of operation. The capsule contained 2 sets of 3 flux wires: nickel (Ni), copper (Cu), and iron (Fe). There were 24 Charpy V-Notch specimens in the capsule: eight (8) each of plate (base) material, weld material, and heat affected zone (HAZ) material. The capsule also contained eight (8) tensile specimens: three plate material, three weld material, and two HAZ material. (See Sections 3.1 and 3.3)

b. The chemical composition of copper (Cu) and nickel (Ni) for the irradiated surveillance materials was determined from a chemical composition analysis. The best estimate values for the surveillance material chemistries were calculated as averages of the available baseline and irradiated data. The best estimate values for the surveillance plate are 0.11% Cu and 0.60% Ni, and are 0.29% Cu and 0.71% Ni for the surveillance weld. (See Table 3.4)

c. The purpose of the flux wire testing was to determine the neutron flux at the surveillance capsule location. The flux wire results show that the fluence (from E >1 MeV flux) received by the surveillance specimens was 5.0×10^{17} n/cm^2 at removal (13.4 EFPY-See Section 4.1.2).

d. A neutron transport computation had been performed based on the first surveillance capsule. Relative flux distributions in the azimuthal and axial directions were previously developed in Reference 8. The lead factor was 0.79, relating the surveillance capsule flux to the peak inside surface flux. The lead factor was calculated after the second capsule was removed at 13.4 EFPY, and determined to be 0.68. A lead factor of 0.68 was used for all calculations in this report (See Section 4.2.2).

e. The surveillance Charpy V-Notch specimens were impact tested at temperatures selected to define the upper shelf energy (USE) and the transition of the Charpy V-Notch curves for the plate, weld, and HAZ materials. Measurements were taken of absorbed energy, lateral expansion and percentage shear. From absorbed energy and lateral expansion curve-fit results, the values of USE and of index temperature for 30 ft-lb, 50 ft-lb and 35 mils lateral expansion (MLE) were obtained (see Table 5-3). Fracture surface photographs of each specimen are presented in Appendix A.

f. The irradiated tensile specimens were tested at room temperature (70°F), at reactor operating temperature (550°F) and at 185°F as an intermediate temperature. Unirradiated base material results, as well as results from the first capsule, were available for comparison (See Tables 6-1 through 6-4.)

g. The curves of irradiated and unirradiated Charpy specimens established the 30 ft-lb shifts. The plate material showed a 15°F shift and a 12 ft-lb decrease in USE (9% decrease). These values were not calculated for the weld, as no unirradiated data was available (See Table 5-3).

h. The measured shift of 15°F for plate material for a fluence of 5.0×10^{17} n/cm^2, was within the Rev. 2 [7] range predictions ($\Delta RT_{NDT} \pm 2\sigma$) of -12°F to 56°F. Since two credible data sets are available for the plate material, the surveillance adjustment (Section 7) was applied to the vessel base plates. The measured shift values were not obtained for the weld as no unirradiated data was available. The best estimate chemical composition for the surveillance weld material was used for evaluating the projected shift of the surveillance weld data (See Table 5-3).

i. The 32 EFPY RPV peak fluence prediction is 1.81×10^{18} n/cm^2 at the vessel wall, based on the flux wire test and lead factor. This is 22% less than the previously established nominal 32 EFPY fluence prediction (2.32×10^{18} n/cm^2) [5]. The 32 EFPY fluence prediction is 1.31×10^{18} n/cm^2 at 1/4 T. (See Section 4.3)

j. The adjusted reference temperature (ART = Initial RT_{NDT} + ΔRT_{NDT} + Margin) was predicted for each beltline material, based on the methods of Regulatory Guide 1.99, Rev. 2. The ART for the limiting material, Axial Weld Heat 27204/12008, at 32 EFPY is 109°F and is lower than the 200°F requirement of 10CFR50 Appendix G [1] and Rev. 2 [7]. (See Table 7-1)

k. An update of the beltline material USE values at 32 EFPY was performed using the Reg. Guide 1.99, Rev. 2 methodology. The equivalent margin analyses demonstrate that 10CFR50, Appendix G safety requirements are satisfactorily met for FitzPatrick. (See Tables 7-2 and 7-3)

l. P-T curves were developed for three reactor conditions: pressure test (Curve A), non-nuclear heatup and cooldown core not critical operation (Curve B), and core critical operation (Curve C) curves which are valid for up to 32 EFPY of operation. The beltline curve is more limiting for Curve A at pressures above approximately 550 psig. For Curves B and C, the beltline curves are limiting for pressures above approximately 600 psig. The P-T curves for 32 EFPY are shown in Figures 8-1 through 8-3, and the P-T curves for 24 EFPY are shown in Appendix B, Figures B-1 through B-3

2.2 CONCLUSIONS

The requirements of 10CFR50 Appendix G [1] deal with vessel design life conditions and with limits of operation designed to prevent brittle fracture. Based on the evaluation of surveillance testing results, and the associated analyses, the following conclusions are made:

a. The 30 ft-lb shift for the base material was less than the Rev. 2 prediction, and therefore the ART values for beltline plates were modified in accordance with Position 2 of Rev. 2. The changes in USE for the survillance plate are bounded by the Regulatory Guide 1.99 Revision 2 predictions and associated deviations.

b. The values of ART and USE for the reactor vessel beltline materials are expected to remain within the limits of 10CFR50 Appendix G [1] for at least 32 EFPY of operation.

3. SURVEILLANCE PROGRAM BACKGROUND

3.1 CAPSULE RECOVERY

The reactor pressure vessel (RPV) surveillance program consists of three surveillance capsules at 30°, 120°, and 300° azimuths at the core midplane. The specimen capsules are held against the RPV inside surface by a spring loaded specimen holder. Each capsule is expected to receive equal irradiation because of core symmetry. The first capsule (30° azimuth) was removed in April 1985 after 5.98 EFPY. During the November 1996 outage, the second surveillance capsule was removed from the 120° azimuthal location. The capsule was cut from its holder assembly and shipped by cask to the GE Vallecitos Nuclear Center (VNC), where testing was performed.

Upon arrival at VNC, the capsule was examined for identification. The identification number stamped on the capsule corresponded to FitzPatrick, as specified by GE drawings, 117C3739 (Outline Specimen Holder) and 921D465 (Surveillance Program), for the FitzPatrick 120° surveillance materials. The general condition of the capsule as received is shown in Figure 3-1. The specimen holder contained 2 sets of 3 flux wires (iron, copper, and nickel), three Charpy specimen capsules each containing 8 plate, weld, or HAZ Charpy specimens in a sealed helium environment, and four tensile specimen capsules (together containing 3 base, 3 weld and 2 HAZ tensile specimens in a sealed helium environment).

3.2 RPV MATERIALS AND FABRICATION

3.2.1 Fabrication History

The FitzPatrick RPV is a 220.75 inch inside diameter BWR/4 design. Construction was performed by Combustion Engineering (CE) under the 1965 edition of the ASME Code through the 1966 Winter Addenda. The shell and head plate materials are ASME SA533, Grade B, Class 1 low alloy steel (LAS). The nozzles and closure flanges are ASME SA508 Class 2 LAS, and the closure flange bolting materials are ASME A540 Grade B24 LAS [8]. Submerged arc or shielded metal arc welding of plates was followed by post-weld heat treatment at 1150°F. The fabrication impact test specimens were given a simulated post weld heat treatment at

1150°F ± 25°F, held 40 hours followed by furnace cooling to below 600°F, then air cooled. The identification of plates and welds in the beltline region is shown in Figure 3-2.

3.2.2 Material Properties of RPV at Fabrication

Material certification records were retrieved from GE Quality Assurance (QA) records to determine chemical and mechanical properties of the vessel materials. The retrieved information for the beltline materials is documented in [5]. Table 3-1 shows the chemistry data for the beltline materials. Properties of the beltline materials and materials at other locations of interest are presented in Tables 3-2 and 3-3.

3.2.3 Surveillance Capsule Specimen Chemical Composition

Samples were taken from the irradiated base and weld Charpy specimens after they were tested. Chemical analyses were performed using a Spectraspan III plasma emission spectrometer. Each sample was dissolved in an acid solution to a concentration of 40 mg steel per ml solution. The spectrometer was calibrated for determination of Mn, P, Ni, Mo, V, Cr, Si and Cu by diluting National Institute of Standards and Technology (NIST) Spectrometric Standard Solutions. The phosphorus calibration involved analysis of five reference materials from NIST with known phosphorus levels. Analysis accuracies are ±0.005% (absolute) of reported value for phosphorus and ±5% (relative) of reported value for other elements. The chemical composition results are given in Table 3-4 for both irradiated and baseline surveillance plate and irradiated weld materials. The baseline plate data was taken from CE material certification records as documented in [5] for the plate surveillance specimens; no baseline data was available for the weld material.

3.3 SPECIMEN DESCRIPTION

The surveillance capsule holder contained 24 Charpy specimens: base metal (8), weld metal (8), and HAZ (8). The holder also contained 2 sets of 3 flux wires (iron, nickel, and copper) and eight (8) tensile specimens (three base, three weld and two HAZ). The chemistry and fabrication history for the Charpy and tensile specimens are described in this section.

3.3.1 Charpy Specimens

The fabrication of the Charpy specimens is described in the CE drawings of the surveillance test program. All materials used for specimens were beltline materials taken from the lower intermediate shell course.

The base metal specimens were cut from plate G-3414-2, heat number C3278-2. The test plates received the same heat treatment as plate heat no. C3278-2, including the post-weld heat treatment for 40 hours at 1150°F ± 25°F. The Charpy specimens were removed from plate heat no. C3278-2 and machined from the 1/4 T and 3/4 T positions in the plate, in the longitudinal orientation (long axis parallel to the rolling direction). The Charpy specimens had been stamped on one end with the fabrication codes as listed in GE surveillance program drawings for FitzPatrick.

The weld metal and HAZ Charpy specimens were fabricated by welding together pieces of plates G-3414-1 and G-3414-2 with a weld identical to longitudinal seam weld 1-233 in the RPV beltline. Welding records obtained from CE indicate the surveillance weld to be a submerged arc weld representive of the vessel beltline circumferential weld. The welded test plates received stress relief heat treatment at 1150°F ±25°F to simulate the RPV fabrication conditions. The weld and HAZ specimens were cut from the material avoiding the volume near the root of the welds. The base metal orientation in the weld and HAZ specimens was longitudinal.

3.3.2 Tensile Specimens

Fabrication of the surveillance tensile specimens is also described in the CE surveillance program drawings. The materials, chemical compositions, and heat treatments for the tensile specimens are the same as the corresponding Charpy specimens. The identifications of the base, weld and HAZ surveillance specimens are described in Reference 8.

TABLE 3-1: CHEMICAL COMPOSITION OF RPV BELTLINE MATERIALS[a]

		Composition by Weight Percent							
Identification	Heat/Lot No	Cu	Ni	C	Mn	P	S	Si	Mo
PLATES:									
Lower Shell:									
G-3415-1R	C3394-1	0.11[f]	0.56	0.21	1.32	0.015	0.017	0.26	0.47
G-3415-3	C3376-2	0.13[b]	0.60	0.22	1.33	0.015	0.017	0.22	0.48
G-3415-2	C3103-2	0.14[b]	0.57	0.23	1.36	0.012	0.015	0.26	0.46
Lower-Intermed. Shell:									
G-3413-7	C3368-1	0.12[b]	0.50	0.19	1.30	0.015	0.017	0.22	0.45
G-3414-2[c]	C3278-2	0.11[e]	0.60[e]	0.20	1.26	0.011	0.016	0.22	0.48
G-3414-1	C3301-1	0.18[b]	0.57	0.18	1.36	0.008	0.015	0.29	0.46
WELDS:									
Lower Longitudinal: 2-233 A,B,C	27204/12008 Flux 1092 Lot 3774	0.219[d]	0.996[d]	N/A	1.16	0.013	0.007	0.21	0.46
Lower Int. Long.: 1-233 A,B,C	13253/12008 Flux 1092 Lot 3947	0.210[d]	0.873[d]	N/A	N/A	N/A	N/A	N/A	N/A
Lower to Lower -Int. Girth: 1-240	305414 Flux 1092 Lot 3947	0.337[d]	0.609[d]	0.14	1.45	0.012	0.01	0.18	0.51

[a] Data from CMTR Reports, GE QA Records and [5] except as noted below
[b] Cu values taken from Lukens Steel letter to NYPA dated 10/14/85 [19]
[c] Surveillance plate
[d] Best estimate Cu and Ni weld values obtained from CE Owners Group report [18]
[e] Average chemistry of surveillance plate from Table 3-4
[f] Cu content from Generic Letter 92-01 response [21]

TABLE 3-2: RT_{NDT} OF VESSEL MATERIALS

COMPONENT	ID	HEAT	TEST TEMP. (°F)	CHARPY ENERGY (FT-LB)			$(T_{50T}-60)$ (°F)	DROP WEIGHT NDT (°F)	RT_{NDT} (°F)
PLATES & FORGINGS:									
Top Head & Flange									
Dollar Plate	G-3412	C-2869-5	10	83	70	72	-20	-10	-10
Top Head Torus	G-3411-1	C-3055-1	10	98	73	118	-20	-10	-10
	G-3411-2	C-3055-1	10	98	73	118	-20	-10	-10
Top Head Flange	G-3402	4P-1885	10	66	87	96	-50	30	30
Shell Courses									
Upper Shell Flange	G-3401	2V595	10	117	94	117	-50	10	10
Upper Shell	G-3413-4	B-7255-1	10	70	76	71	-20	-10	-10
	G-3413-5	C-3229-2	10	50	68	82	-20	-10	-10
	G-3413-6	B-7291-1	10	81	69	65	-20	-10	-10
Upper Int. Shell	G-3413-1	C-3116-1	10	65	91	79	-20	-10	-10
	G-3413-2	C-3121-2	10	31	48	35	18	10	18
	G-3413-3	C-3158-2	10	95	87	76	-20	-10	-10
Low-Int. Shell	G-3413-7	C-3368-1	10	61	55	45	-10	-50	-10
	G-3414-1	C-3301-1	10	60	63	49	-18	-40	-18
	G-3414-2	C-3278-2	10	45	77	58	-10	-30	-10
Lower Shell	G-3415-1R	C-3394-1	10	53	71	52	-20	-10	-10
	G-3415-2	C-3103-2	10	41	48	49	-2	-10	-2
	G-3415-3	C-3376-2	40	43	51	49	24	-10	24
Bottom Head									
Dollar Plate	G-3410	C-2917-3	10	38	36	36	8	-10	8
Bottom Head Torus	G-3407-1	C-2851-1	10	83	72	75	-20	-10	-10
	G-3408-1	C-3055-2	10	53	73	66	-20	-10	-10
	G-3409	C-2906-3	10	36	43	35	10	-10	10

TABLE 3-3: RT_{NDT} OF NOZZLE, WELD AND STUD MATERIALS

COMPONENT	ID	HEAT	TEST TEMP. (°F)	CHARPY ENERGY (FT-LB)			$(T_{50T}-60)$ (°F)	DROP WEIGHT NDT (°F)	RT_{NDT} (°F)
Nozzles:									
Recirc. Outlet Nozzle	G-3419-1	EV-9781	10	70	71	76	-20	-10	-10
	G-3419-2	AV-1872	10	93	86	72	-20	0	0
Recirc. Inlet Nozzle	G-3436-1	E21VW-104J10	10	103	111	110	-20	<40	30
	G-3436-2	E21VW-104J2	10	82	94	96	-20	<40	30
	G-3436-3	E21VW-104J9	10	95	101	107	-20	<40	30
	G-3436-4	E21VW-104J7	10	86	76	79	-20	<40	30
	G-3436-5	E21VW-104J6	10	84	109	107	-20	<40	30
	G-3436-6	E21VW-104J3	10	89	94	77	-20	<40	30
	G-3436-7	E21VW-104J4	10	106	109	116	-20	<40	30
	G-3436-8	E21VW-104J8	10	101	114	102	-20	<40	30
	G-3436-9	E21VW-104J5	10	73	116	118	-20	<40	30
	G-3436-10	E21VW-104J1	10	110	93	103	-20	<40	30
Steam Outlet Nozzle	G-3420-1	EV-9754	10	82	105	82	-20	-10	-10
	G-3420-2	EV-9775	10	66	40	36	8	-10	8
	G-3420-3	EV-9775	10	62	75	78	-20	-10	-10
	G-3420-4	AV-1576	10	30	52	48	20	0	20
Feedwater Nozzle	G-3421-1	EV-9741	10	65	75	73	-20	10	10
	G-3421-2	EV-9741	10	92	75	90	-20	10	10
	G-3421-3	EV-9741	10	69	67	68	-20	-20	-20
	G-3421-4	AV-1607	10	30	36	32	-20	0	20
Core Spray Nozzle	G-3422-1	EV-9741	10	40	56	65	-30	0	0
	G-3422-2	EV-9741	10	54	89	74	-50	10	10
Top Head Instrumentation Nozzle	G-2921-3	EV-9781	10	82	69	72	-20	0	0
	G-2921-4	AV-2379	10	117	90	108	-20	-10	-10
Vent Nozzle	G-2920-2	AV-2374	10	145	182	185	-20	0	0
Jet Pump Instrumentation Nozzle	G-3424-1	EV-9792	10	144	144	144	-20	0	0
CRD Hyd. Sys. Return	G-3423	EV-9143	10	112	94	80	-20	-20	-20
Drain Nozzle	G-2085	2106172	10	96	108	92	-20		20

COMPONENT	ID	HEAT	TEST TEMP. (°F)	CHARPY ENERGY (FT-LB)			(T_{50T}-60) (°F)	DROP WEIGHT NDT (°F)	RT_{NDT} (°F)
WELDS:									
Vertical Welds									
Lower Shell	2-233 A,B,C	27204/12008	10	63	60	49	-48		-48
Lower-Int Shell	1-233 A,B,C	13253/12008	10	60	64	56	-50		-50
Girth Welds									
Lower to Lower-Int Shells	1-240	305414	10	82	66	80	-50		-50
							LST		
STUDS:	G-3134-1	37385	10	39	40	39	70	OK	
	G-3134-2	37677	10	60	55	57	70	OK	

TABLE 3-4: CHEMICAL COMPOSITION OF FITZPATRICK SURVEILLANCE MATERIALS FROM SURVEILLANCE SPECIMEN CHEMICAL TESTS

Metal Sample ID	Metal Sample Type	Mn (wt%)	Ni (wt%)	Cu (wt%)	Mo (wt%)	Si (wt%)	Cr (wt%)	P (wt%)
5CL[a]	Base	1.40	0.62	0.11	0.48	0.07[b]	0.11	0.011
5CM[a]	Base	1.30	0.63	0.12	0.50	0.06[b]	0.11	0.010
29283	Base	1.17	0.58	0.11	0.45	0.36	0.09	0.013
29285	Base	1.25	0.61	0.11	0.46	0.16	0.10	0.013
29286	Base	1.20	0.60	0.11	0.46	0.19	0.10	0.011
LP1-28[c]	Base	1.43	0.62	0.10	0.42	0.24	N/A	0.018
Baseline[d]	Base	1.26	0.57	0.13[e]	0.48	0.22	N/A	0.011
	Data Avg.	1.29	0.60	0.11	0.46	0.23	0.10	0.012
	Std. Dev.	0.10	0.02	0.01	0.03	0.08	0.01	0.003
5DL[a]	Weld	1.50	0.72	0.31	0.50	0.06[b]	0.04	0.015
5DM[a]	Weld	1.40	0.72	0.31	0.51	0.06[b]	0.04	0.014
29289	Weld	1.36	0.70	0.30	0.48	0.38	0.04	0.014
29295	Weld	1.25	0.70	0.23	0.47	0.41	0.04	0.014
29297	Weld	1.39	0.74	0.31	0.49	0.52	0.04	0.012
	Data Avg.	1.38	0.72	0.29	0.49	0.44	0.04	0.014
	Std. Dev.	0.09	0.02	0.03	0.02	0.07	0.001	0.001

[a] Chemical analysis of tensile specimens from 30° azimuthal capsule location (1st capsule report) [8].
[b] Si results may be low due to precipitiation during dissolution heating (Results not used in Average).
[c] Data taken from the BWROG Supplemental Surveillance Program for the FitzPatrick Plant.
[d] Taken from original fabrication records (see Table 3-1).
[e] Cu value taken from Lukens Steel letter to NYPA dated 10/14/85 [19]

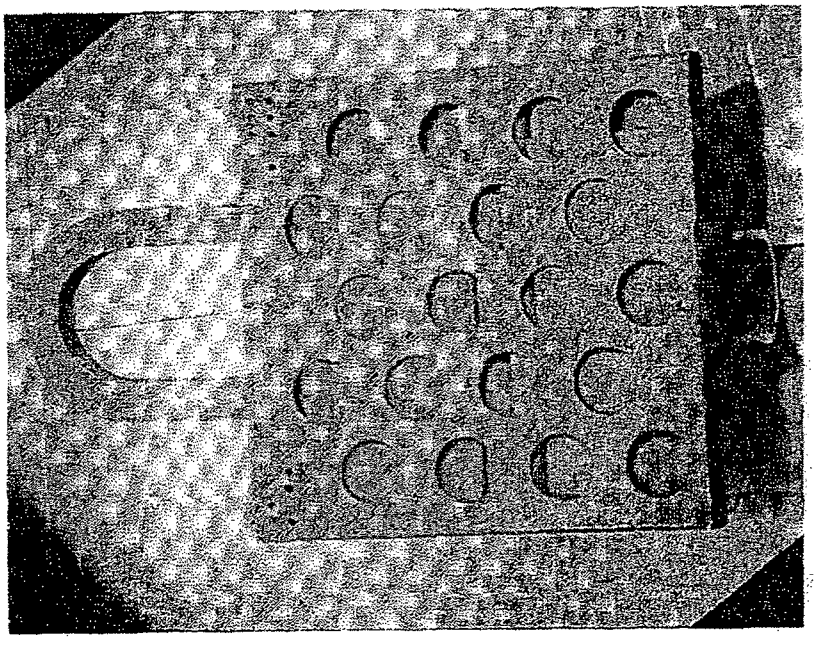

FIGURE 3-1: SURVEILLANCE CAPSULE HOLDER RECOVERED FROM FITZPATRICK (120° AZIMUTHAL LOCATION CAPSULE - REMOVED AT 13.4 EFPY)

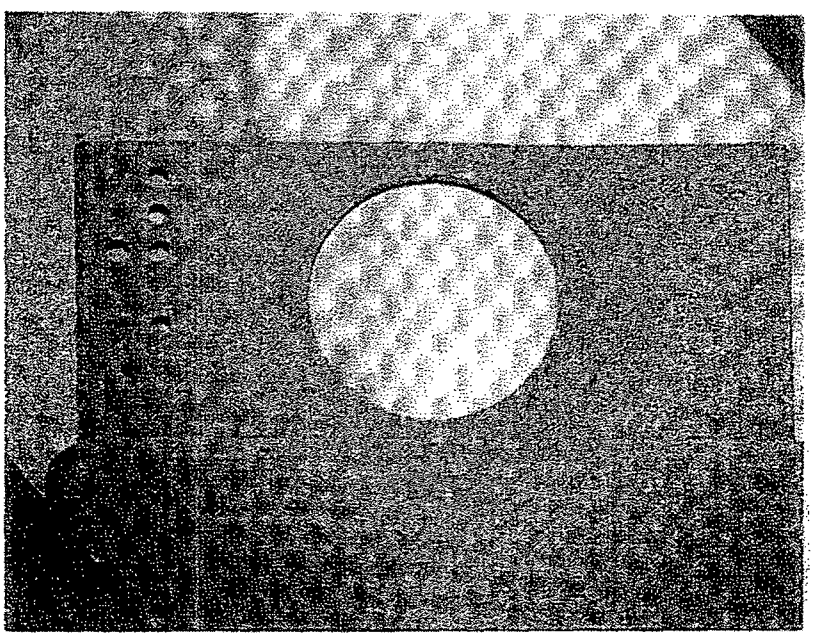

FIGURE 3-1(A): CHARPY SPECIMEN CAPSULE IDENTIFICATION
(120° AZIMUTHAL LOCATION CAPSULE - REMOVED AT 13.4 EFPY)

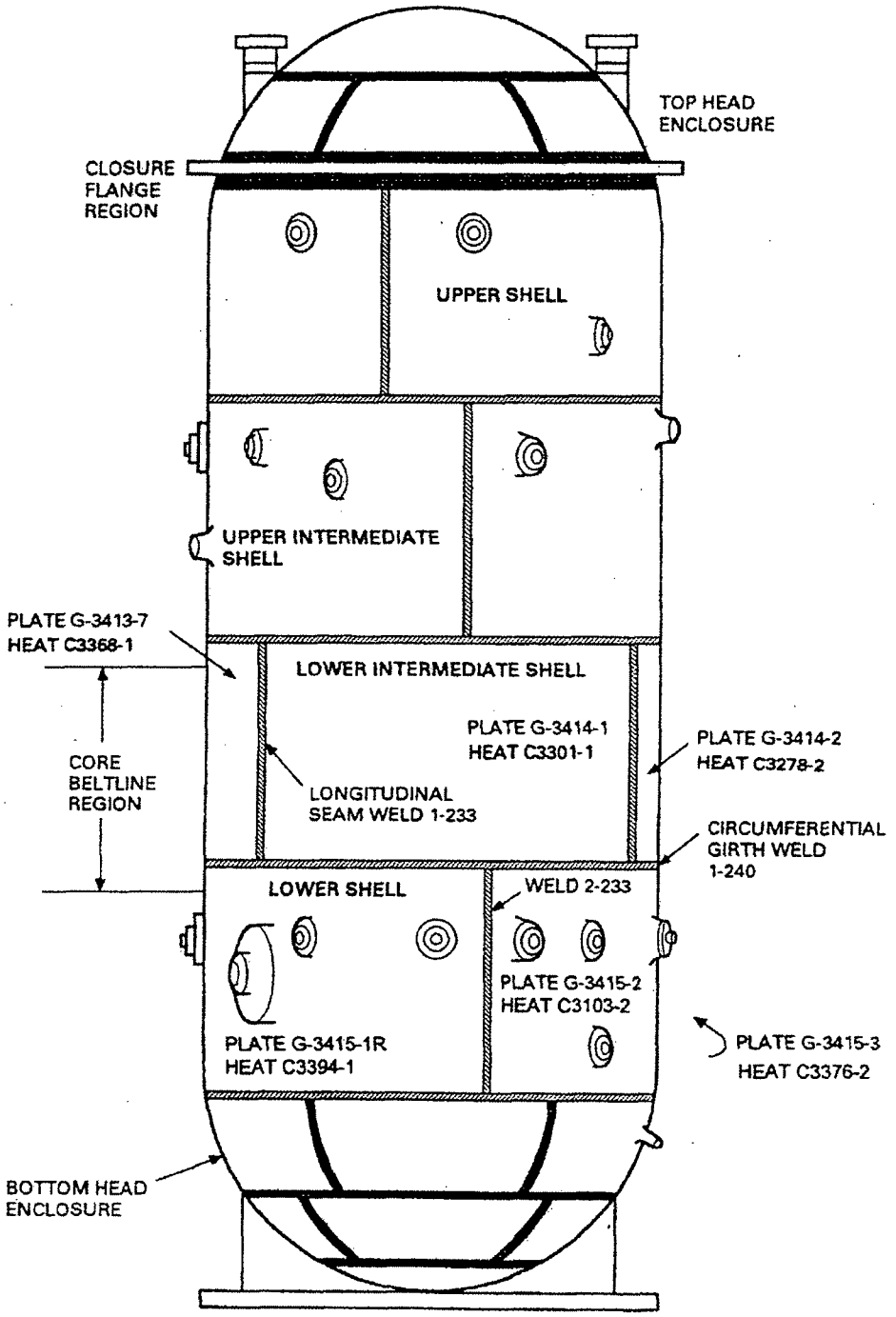

FIGURE 3-2. SCHEMATIC OF RPV SHOWING IDENTIFICATION OF VESSEL BELTLINE PLATES AND WELDS

4. PEAK RPV FLUENCE EVALUATION

Flux wires removed from the 120° location capsule were analyzed, as described in Section 4.1, to determine flux and fluence received by the surveillance capsule. The lead factor, determined as described in Section 4.2, was used to establish the peak vessel fluence from the flux wire results. Section 4.3 includes 32 EFPY peak fluence estimates.

4.1 FLUX WIRE ANALYSIS

4.1.1 Procedure

The surveillance capsule contained 2 sets of 3 flux wires: iron, nickel, and copper. Each wire was removed from the capsule, cleaned with dilute acid, weighed, mounted on a counting card, and analyzed for its radioactivity content by gamma spectrometry. Each iron wire was analyzed for Mn-54 content, each nickel wire was analyzed for Co-58 content, and each copper wire for Co-60 at calibrated source-to-detector distances with 170-cc Ge and 100-cc Ge(Li) gamma detectors used in conjunction with a Nuclear Data 6700 multichannel analyzer system.

To properly predict the flux and fluence at the surveillance capsule from the activity of the flux wires, the periods of full and partial power irradiation and the zero power decay periods were considered. Operating days for each fuel cycle and the reactor average power fraction were derived from records provided by New York Power Authority are shown in Table 4-1. Zero power days between fuel cycles are listed as well.

From the flux wire activity measurements and power history, reaction rates for Fe-54 (n,p) Mn-54, Ni-58 (n,p) Co-58, and Cu-63 (n,α) Co-60 were calculated. The E >1 MeV fast flux reaction empirical cross sections for the iron, nickel, and copper wires are 0.182 barn, 0.234 barn and 0.00318 barn, respectively. The calculated fluence result from the iron flux wire was used. The fluence result from the iron specimen was confirmed by the Ni and Cu flux wires, with all three results differing by less than 10%. The GE empirical activation cross sections are consistent with other transport code cross sections, and parallel calculations were performed using the both the empirical and transport code cross sections [20]. However, the fluence results obtained from the empirical cross sections are recommended since they yield approximately 4% higher estimates of RPV fluence. These data functions were applied to BWR pressure vessel locations based on water gap (fuel to vessel wall) distances. The cross sections for > 0.1 MeV flux were determined from the measured 0.1 to 1 MeV cross section ratio of 1.6 [11].

4.1.2 Results

The measured activity, reaction rate and full-power flux results for the 120° location surveillance capsule are given in Table 4-2. The E > 1 MeV flux values were calculated by dividing the wire reaction rate measurements by the corresponding cross sections, factoring in the local power history for each fuel cycle. The fluence result, 5.0×10^{17} n/cm^2 (E > 1 MeV), was obtained by using the following equation:

$$\Phi_{Cu} = \Phi_{fp} \sum_i t_i p_i \qquad (4\text{-}1)$$

where, Φ_{Cu} = fluence measured by the Cu dosimeters, n/cm^2
Φ_{fp} = full power flux value for Cu, n/cm^2-s
t_i = operating time, s
p_i = full power fraction

as shown in Tables 4-1 through 4-3.

The accuracies of the values in Table 4-2 for a 2σ deviation are influenced by the following sources of error:

± 2%	counting rates
± 15%	power history
± 10%	cross sections

The uncertainty in the E > 1 MeV fluence is approximately ±20% (2σ).

This analysis is performed using the GE empirical activation cross sections. A parallel analysis using cross sections from a transport code was made, but is not preferred, because its resulting fluences were approximately 4% lower for all three of the flux wires.

4.2 DETERMINATION OF LEAD FACTOR

The flux wires from the surveillance capsule are used to determine the fast neutron (E > 1 MeV) fluence at the location of the capsule as described in Section 4.1. However, the capsule and flux wires are not located where the peak vessel fluence occurs. A calculated lead factor is used to

relate the fluence at the location of the wires to the peak fluence at the vessel. The lead factor is defined as the ratio of the fast neutron fluence at the surveillance capsule to the peak fluence at the vessel inside surface. A neutron transport analysis was performed to determine the effective full power fast neutron flux distribution at the reactor pressure vessel. The lead factor was evaluated as the ratio of the calculated effective full power fast neutron fluxes at the capsule and vessel peak flux locations. Calculation of the fluxes and lead factor requires modeling of the reactor geometry and materials and depends on the distributions of power density and coolant voids in the core. The lead factor was calculated for the FitzPatrick geometry, using data for a typical operating cycle to determine power shape and void distribution. The lead factor was not adjusted for the 105% power uprate, as the fluxes were assumed to increase linearly with power. The methods used to calculate the lead factor are discussed below.

The NRC is developing Draft Regulatory Guide DG-1053, "Calculational and Dosimetry Methods for Determining Pressure Vessel Neutron Fluence", which will include guidance concerning acceptable methods and assumptions for determining the pressure vessel fluence. At this time, the draft has not been finalized for issuance as a Regulatory Guide. However, while the specific regulatory requirements are still subject to change, it is believed that the analysis described in this section is consistent with the intent of the draft guide.

4.2.1 Procedure

The lead factor for the RPV inside wall was determined by using a combination of two separate two-dimensional neutron transport computer analyses. The first of these established the azimuthal and radial variation of flux at the fuel midplane elevation. The second analysis determined the relative variation of flux with elevation. The azimuthal and axial distribution results were combined to provide a simulation of the three-dimensional distribution of flux. The ratio of fluxes, or lead factor, between the surveillance capsule location and the peak flux locations was obtained from this distribution.

The DORT computer program, which utilizes the discrete ordinates method to solve the Boltzmann transport equation in two dimensions, was used to calculate the spatial flux distribution produced by a fixed source of neutrons in the core region. The analysis considered neutrons with energies above 0.1 MeV and used 29 energy groups above this threshold. Angular dependence of the neutron scattering cross-sections was approximated by a third-order Legendre polynomial (P-3) expansion. The DORT calculations were run using S_8 angular quadrature.

The azimuthal distribution was obtained with a model specified in (R,θ) geometry, assuming eighth-core symmetry with reflective boundary conditions at 0° and 45°. In this model, θ= 30° is symmetrically equivalent to the 120° capsule location. A schematic of the (R,θ) model is shown in Figure 4-1. The model incorporates inner and outer core regions, bypass water region, shroud, downcomer water region, and a vessel plus liner region. The portion of the core inside a radius of 133 cm was not included because it will not significantly influence the flux distribution at the vessel. The spatial mesh contained 155 steps of varying sizes in the radial dimension. The azimuthal mesh step was specified to be 1/2° and was reduced to 1/4° in the vicinity of the capsule, resulting in a total of 98 azimuthal intervals. The (R,θ) model used core region material compositions and neutron source densities for the core midplane elevation (75 inches above the bottom of active fuel). This is near the elevation of the capsule, which is centered at 72.31 inches above the bottom of the active fuel. The neutron source densities and coolant mass densities were based on cycle-average values for the selected representative operating cycle. The output of this calculation provided the distribution of flux as a function of azimuth and radius at reactor midplane. The azimuth of the peak flux and its magnitude relative to the flux at the 30° capsule/flux wire azimuth were determined from this distribution.

The calculation of the axial flux distribution was performed in (R,Z) geometry, using a simplified cylindrical representation of the core configuration and realistic simulations of the axial variations of power density and coolant mass density. The core cylinder radius was specified to be equal to the radius of the outermost corner of the core, which is located at an azimuth of approximately 39.3°. The core model contained inner and outer material regions for each of 25 axial fuel nodes (total of 50 core regions). Source densities and coolant densities in these regions were based on cycle-average values for the representative cycle. The elevation of the peak flux at the reactor vessel inside surface and the magnitude of the peak flux relative to the flux at the surveillance capsule elevation were determined from the (R,Z) flux distribution results.

4.2.2 Results

The relative distribution of flux at the RPV base metal inside surface vs. azimuthal angle obtained from the (R,θ) calculation is shown in Figure 4-2. The relative distribution of flux versus elevation at the RPV inside surface from the (R,Z) calculation is shown in Figure 4-3. The azimuthal distribution (Figure 4-2) indicates that the 8 flux maxima at the vessel base metal inside surface occur at azimuthal locations which are displaced by 42.75° from the RPV quadrant reference axes (0°, 90°, etc.). From the R,Z results (Figure 4-3), the peak is estimated to occur at

an elevation about 79 inches above the bottom of the active fuel. The calculated core midplane E > 1 MeV flux at the (R,θ) coordinates corresponding to the equivalent capsule center position (θ = 30°, R = 109.19 inches) was 1.382 x10^9 n/cm^2/s. This was multiplied by the ratio of flux at the capsule elevation to flux at midplane (0.996), as determined from the (R,Z) calculation, resulting in a calculated flux at the capsule location which rounds to 1.38 x 10^9 n/cm^2/s. The peak flux at the vessel surface (R = 110.375 inches) was similarly obtained by multiplying the calculated midplane flux of 2.015 x10^9 n/cm^2/s at the peak azimuth by an axial adjustment factor of 1.003 from the (R,Z) calculation. The resulting peak flux estimate is 2.02 x 10^9 n/cm^2/s. Consequently, the lead factor is 1.38 x 10^9 / 2.02 x 10^9 =0.68.

The calculated capsule full power flux of 1.38x10^9 n/cm^2/s obtained with this model is about 16 % higher than the capsule dosimetry result of 1.19x10^9 n/cm^2/s. The indicated agreement between the analytical and experimental results is within the uncertainties associated with those results and is considered good. It is estimated that the 1σ uncertainty in the calculated flux magnitudes is on the order of 25 - 30 %. However, since the lead factor is determined from the ratio of two calculated fluxes which have sources of error in common, the 1σ uncertainty in the lead factor is estimated to be no more than 15 %.

Use of a lead factor calculated on the basis of the model described above is consistent with current GE practice for estimation of the peak vessel fluence. Application of the lead factor to the capsule dosimetry results yields an estimated end-of-cycle 12 peak fluence of 5.0x10^{17} / 0.68=7.4x10^{17} n/cm^2 and an estimated peak full power flux of 1.19x10^9/0.68 = 1.75 x 10^9 n/cm^2/s at the vessel inside surface. Since the estimated 1σ uncertainty in the dosimetry results is 10 % and the estimated 1σ uncertainty in the lead factor is 15%, the combined overall 1σ uncertainty in the projected peak values is estimated to be about $(10^2 + 15^2)^{0.5}$ = 18 %.

The analysis model discussed above did not include the effects of the material specimens and specimen holder on the local neutron flux. A second calculation was performed in (R,θ) geometry with a model which incorporated regions which simulated the material specimens and holder. The densely packed material specimens were represented as solid steel in the model. The perforated wall of the specimen holder was modeled as a steel/water mixture. This model is expected to provide a reasonable upper bound estimate of the effect of the capsule on local fluxes. The results obtained with this model were also used to provide independent confirmation of the reaction rate cross-sections used in the dosimetry analysis described in Section 4.1.

The flux obtained at the capsule midpoint radius with the modified (R,θ) model was $1.53x10^9$ n/cm^2/s. Application of the axial adjustment of 0.996 results in an estimated flux of $1.52x10^9$ n/cm^2/s at the capsule center point. Consequently, the flux calculated at this point with the simulated capsule materials is about 10 % higher than the flux calculated with the base model. The region-averaged flux obtained in the specimen region, $1.51x10^9$ n/cm^2/s, differs only slightly from the center point value. These results indicate that the base model under-predicts the flux within the capsule by a few percent and possibly as much as 10 %. Therefore, a conservative bias exists in the calculated lead factor and projected peak fluences, since underestimation of the lead factor results in overestimation of the vessel peak fluence.

The 29-group neutron energy spectrum obtained at the simulated capsule center point was plotted and applied to ENDF/B-VI library data for the dosimeter activation reaction cross-sections to calculate spectrum-weighted group cross-sections for the reactions. The DORT case was re-run to obtain calculated total reaction rates which, when divided by the E > 1 MeV flux, yield the effective reaction rate cross-sections for the fast flux. The cross-sections used in Section 4.1 to analyze the dosimeter data are derived from fits to empirical data which have been used by GE for analysis of surveillance capsule dosimetry for many years. Region-averaged values obtained for the specimen region in the DORT model are compared with the Section 4.1 cross-sections in the table below.

Comparison of Calculated Activation Cross-Sections in Simulated Capsule Region With Semi-Empirical Cross-Sections Used in Capsule Dosimetry Analysis

Reaction	Effective Cross-Section for E > 1 Mev Flux (barns)		Difference
	Empirical Fit	Calculated	%
Fe54(n,p)Mn54	0.182	0.1899	+4.34
Ni58(n,p)Co58	0.234	0.2425	+3.63
Cu63(n,a)Co60	0.00318	0.003305	+3.93

The close agreement between the calculated cross-sections and the fit-derived cross-sections provides confidence that the empirically derived cross-sections are reliable. It also provides confidence that the calculated neutron spectrum is realistic, even though the magnitude of the calculated flux is somewhat greater than the measured flux. In each instance, the calculated

cross-sections are slightly higher than the empirical cross-sections. Consequently, if the dosimeter material reaction rates are predicted purely from the analysis, the difference between calculated and measured reaction rates will be slightly greater than the difference between the calculated and measured fluxes. The reaction rates are compared below.

Comparison of Calculated Reaction Rates in Simulated Capsule Region With Reaction Rates Determined From Capsule Dosimetry Analysis

Reaction	Dosimeter Reaction Rate (reactions/s/nucleus)		Difference
	Capsule Dosimeters	Calculated	%
Fe54(n,p)Mn54	2.14E-16	2.86E-16	+33.8
Ni58(n,p)Co58	2.70E-16	3.66E-16	+35.4
Cu63(n,a)Co60	3.91E-18	4.98E-18	+27.4

The fracture toughness analysis is based on a 1/4 T depth flaw in the beltline region, so the attenuation of the flux to that depth is considered. This attenuation is calculated according to the Reg. Guide 1.99, Rev. 2 requirements, as shown in the next section.

4.3 ESTIMATE OF 32 EFPY FLUENCE

The inside surface fluence (f_{surf}) at 32 EFPY is determined from the flux wire fluence at a particular EFPY and lead factor according to:

$$f_{surf} = (f_{cap} * 32\ EFPY)/(LF * CEFPY) \qquad (4\text{-}2)$$

where, f_{surf} = 32 EFPY fluence at the peak vessel inside surface
f_{cap} = capsule fluence measured at the CEFPY
32 EFPY = end of life EFPY based on a 40-year operation at an 80% capacity factor
CEFPY = the current EFPY for the capsule
LF = lead factor

The surveillance capsule was removed from FitzPatrick at 13.4 EFPY as calculated in Table 4-2. The fluence at 13.4 EFPY was determined to be 5.0×10^{17} n/cm^2 using Equation 4-1, and the lead factor was determined to be 0.68 as discussed in Section 4.2. In addition, the fluence over the remaining 18.6 EFPY was increased by 5% to account for the 5% power uprate that began in December 1996. Using this information with Equation 4-2, the resulting 32 EFPY fluence value at the peak vessel inside surface is:

$$f_{surf} = [(5.0 \times 10^{17}) + (5.0 \times 10^{17} * 18.6/13.4) * 1.05]/0.68 = 1.81 \times 10^{18} \text{ n/cm}^2 \quad (4\text{-}3)$$

at the peak location.

The peak surface fluence at 32 EFPY is 22% lower than the nominal value (2.32×10^{18} n/cm^2) that was calculated from the first surveillance capsule dosimetry as a result of power uprate as reported in GE report [15]. This variation can be attributed to refinements in the analysis technique since the first capsule was removed.

The 1/4 T fluence (f) is calculated according to the Reg. Guide 1.99 [7] equation:

$$f = f_{surf}(e^{-0.24x}), \quad (4\text{-}4)$$

where x = distance, in inches, to the 1/4 T depth. The vessel beltline lower intermediate shell ring thickness is 5.375 inches minimum requirement. The corresponding depth, x, taken from the minimum required thickness is 1.34 inches for the lower intermediate shell. Equation 4-4 evaluated for this value of x gives the 1/4 T value of 32 EFPY fluence, $f = 1.31 \times 10^{18}$ n/cm^2 for the lower intermediate shell ring.

In the case of the lower shell ring, the axial fluence distribution was also taken into account. The maximum fluence at the top of the lower shell is 0.89 times the peak fluence, or 1.61×10^{18} n/cm^2. The minimum plate thickness of the lower shell is 6.375 inches, which corresponds to an x value of 1.6 inches. The resultant 1/4T fluence at 32 EFPY is 1.10×10^{17} n/cm^2.

TABLE 4-1: SUMMARY OF FITZPATRICK IRRADIATION PERIODS

On	Off	Duration (days)	Days to eoi	MWd	Effective Full Power Days	Full Power Fraction
1/26/75	12/31/77	1071	6874	1301203	534.4	0.499
1/1/78	12/31/78	365	6509	539687	221.6	0.607
1/1/79	12/31/79	365	6144	373919	153.7	0.421
1/1/80	12/31/80	366	5778	541475	222.2	0.607
1/1/81	12/31/81	365	5413	592405	243.1	0.666
1/1/82	12/31/82	365	5048	630106	258.8	0.709
1/1/83	12/31/83	365	4683	592197	243.1	0.666
1/1/84	12/31/84	366	4317	633307	259.9	0.710
1/1/85	12/31/85	365	3952	532365	218.6	0.599
1/1/86	12/31/86	365	3587	767477	315.0	0.863
1/1/87	12/31/87	365	3222	545590	224.1	0.614
1/1/88	12/31/88	366	2856	557082	228.8	0.625
1/1/89	12/31/89	365	2491	781820	320.8	0.879
1/1/90	12/31/90	365	2126	592684	243.5	0.667
1/1/91	1/31/91	31	2095	69083	28.4	0.915
2/1/91	2/28/91	28	2067	56800	23.3	0.833
3/1/91	3/9/91	9	2058	19191	7.9	0.875
3/17/91	3/18/91	2	2049	116	0.1	0.024
4/13/91	4/30/91	18	2006	34493	14.2	0.787
5/1/91	5/7/91	7	1999	16095	6.6	0.944
8/18/91	8/31/91	14	1883	26087	10.7	0.765
9/1/91	9/30/91	30	1853	72905	29.9	0.998
10/1/91	10/31/91	31	1822	74840	30.7	0.991
11/1/91	11/28/91	28	1794	63288	26.0	0.928
11/29/91	1/2/93	401	1393	0	0.0	0.000
1/3/93	1/31/93	29	1364	14983	6.2	0.212
2/1/93	2/28/93	28	1336	58272	23.9	0.854
3/1/93	3/31/93	31	1305	17725	7.3	0.235
4/1/93	4/30/93	30	1275	51219	21.0	0.701
5/1/93	5/31/93	31	1244	46629	19.1	0.617
6/1/93	6/30/93	30	1214	72730	29.8	0.995
7/1/93	7/31/93	31	1183	72348	29.7	0.958
8/1/93	8/31/93	31	1152	75443	31.0	0.999
9/1/93	9/30/93	30	1122	62975	25.9	0.862
10/1/93	10/31/93	31	1091	55927	23.0	0.741
11/1/93	11/30/93	30	1061	13756	5.6	0.188
12/1/93	12/31/93	31	1030	74988	30.8	0.993
1/1/94	1/31/94	31	999	75300	30.9	0.997
2/1/94	2/28/94	28	971	68114	28.0	0.999
3/1/94	3/31/94	31	940	73706	30.3	0.976
4/1/94	4/30/94	30	910	4546	1.9	0.062
5/1/94	5/31/94	31	879	63588	26.1	0.842
6/1/94	6/30/94	30	849	71339	29.3	0.976
7/1/94	7/31/94	31	818	68452	28.1	0.906

8/1/94	8/31/94	31	787	61533	25.3	0.815
9/1/94	9/30/94	30	757	54488	22.4	0.746
10/1/94	10/31/94	31	726	54520	22.4	0.722
11/1/94	11/30/94	30	696	47247	19.4	0.647
12/1/94	12/31/94	31	665	0	0.0	0.000
1/1/95	1/31/95	31	634	0	0.0	0.000
2/1/95	2/28/95	28	606	0	0.0	0.000
3/1/95	3/31/95	31	575	5960	2.5	0.079
4/1/95	4/30/95	30	545	69366	28.5	0.949
5/1/95	5/31/95	31	514	72287	29.7	0.957
6/1/95	6/30/95	30	484	49822	20.5	0.682
7/1/95	7/31/95	31	453	75412	31.0	0.999
8/1/95	8/31/95	31	422	75410	31.0	0.999
9/1/95	9/30/95	30	392	53600	22.0	0.733
10/1/95	10/31/95	31	361	75437	31.0	0.999
11/1/95	11/30/95	30	331	73014	30.0	0.999
12/1/95	12/31/95	31	300	73993	30.4	0.980
1/1/96	1/31/96	31	269	75173	30.9	0.995
2/1/96	2/29/96	29	240	51562	21.2	0.730
3/1/96	3/31/96	31	209	56448	23.2	0.747
4/1/96	4/30/96	30	179	72990	30.0	0.999
5/1/96	5/31/96	31	148	73629	30.2	0.975
6/1/96	6/30/96	30	118	71757	29.5	0.982
7/1/96	7/31/96	31	87	75250	30.9	0.996
8/1/96	8/31/96	31	56	73687	30.3	0.976
9/1/96	9/30/96	30	26	49799	20.4	0.681
10/1/96	10/26/96	26	0	56785	23.3	0.897

Note: Full power was taken as the value prior to uprate of 2436 MW_t

Total Effective Full Power Days= 4907.8
Total Effective Full Power Years = 13.4

TABLE 4-2: SURVEILLANCE CAPSULE FLUX AND FLUENCE FOR IRRADIATION FROM START-UP TO 11/12/96 (13.4 EFPY) USING EMPIRICAL CROSS SECTIONS (GE CORRELATION)

Wire (Element)	Average[a] dps/g Element (at end of irradiation)	Average Reaction Rate [dps/nucleus (saturated)]	Full Power Flux[b] (n/cm^2-s) E>1 MeV	Full Power Flux[c] (n/cm^2-s) E>0.1 MeV	Fluence (n/cm^2) E>1 MeV	Fluence[c] (n/cm^2) E>0.1 MeV
Iron	1.07E05	2.14E-16	1.18E09	1.89E09	5.00E17	7.99E17
Nickel	1.67E06	2.70E-16	1.16E09	1.86E09	4.90E17	7.85E17
Copper	1.56E04	3.91E-18	1.23E09	1.97E09	5.21E17	8.34E17

a Obtained by R.D Reager [20]
b Full power flux, based on thermal power of 2436 MW_t
c 1.6 times the E >1 MeV result

TABLE 4-2: SURVEILLANCE CAPSULE FLUX AND FLUENCE FOR IRRADIATION FROM START-UP TO 11/12/96 (13.4 EFPY) USING EMPIRICAL CROSS SECTIONS (GE CORRELATION)

Wire (Element)	Average[a] dps/g Element (at end of irradiation)	Average Reaction Rate [dps/nucleus (saturated)]	Full Power Flux[b] (n/cm^2-s) E>1 MeV	Full Power Flux[c] (n/cm^2-s) E>0.1 MeV	Fluence (n/cm^2) E>1 MeV	Fluence[c] (n/cm^2) E>0.1 MeV
Iron	1.07E05	2.14E-16	1.18E09	1.89E09	5.00E17	7.99E17
Nickel	1.67E06	2.70E-16	1.16E09	1.86E09	4.90E17	7.85E17
Copper	1.56E04	3.91E-18	1.23E09	1.97E09	5.21E17	8.34E17

a Obtained by R.D Reager [20]
b Full power flux, based on thermal power of 2436 MW_t
c 1.6 times the E >1 MeV result

TABLE 4-3. MEASURED FLUX VS. THEORETICAL FLUX FOR DOSIMETER AND FLUX WIRES

			E > 1 MeV			
	Lead Factor Capsule to ID Surface	EFPY*	Measured Capsule Flux (n/cm^2-s)	Capsule Fluence (n/cm^2)	EOL (32 EFPY) FLUENCE (n/cm^2)	
					ID Surface	1/4T Location
1982 30° Azimuth Dosimeter		~1	$1.5x10^9$			
1985 30° Azimuth Flux Wires	0.79	6.0	$1.4x10^9$	$2.6x10^{17}$	$1.8x10^{18}$	$1.35x10^{18}$
Upper Bound (1.25 Factor)					$2.2x10^{18}$	$1.7x10^{18}$
Reg. Guide 1.99 Rev.2 Evaluation, no upper bound factor included. Tech Spec P-T curve basis.	0.61				$2.32x10^{18}$	$1.7x10^{18}$
5% Power Uprate based on upper bound value.					$2.44x10^{18}$	$1.76x10^{18}$
1996 120° Azimuth Flux Wires Includes 5% Power Uprate New P-T curve basis.	0.68	13.4	$1.2x10^9$	$5.0x10^{17}$	$1.81x10^{18}$	$1.38x10^{18}$

* Effective Full Power Years at 2436 Mw_t

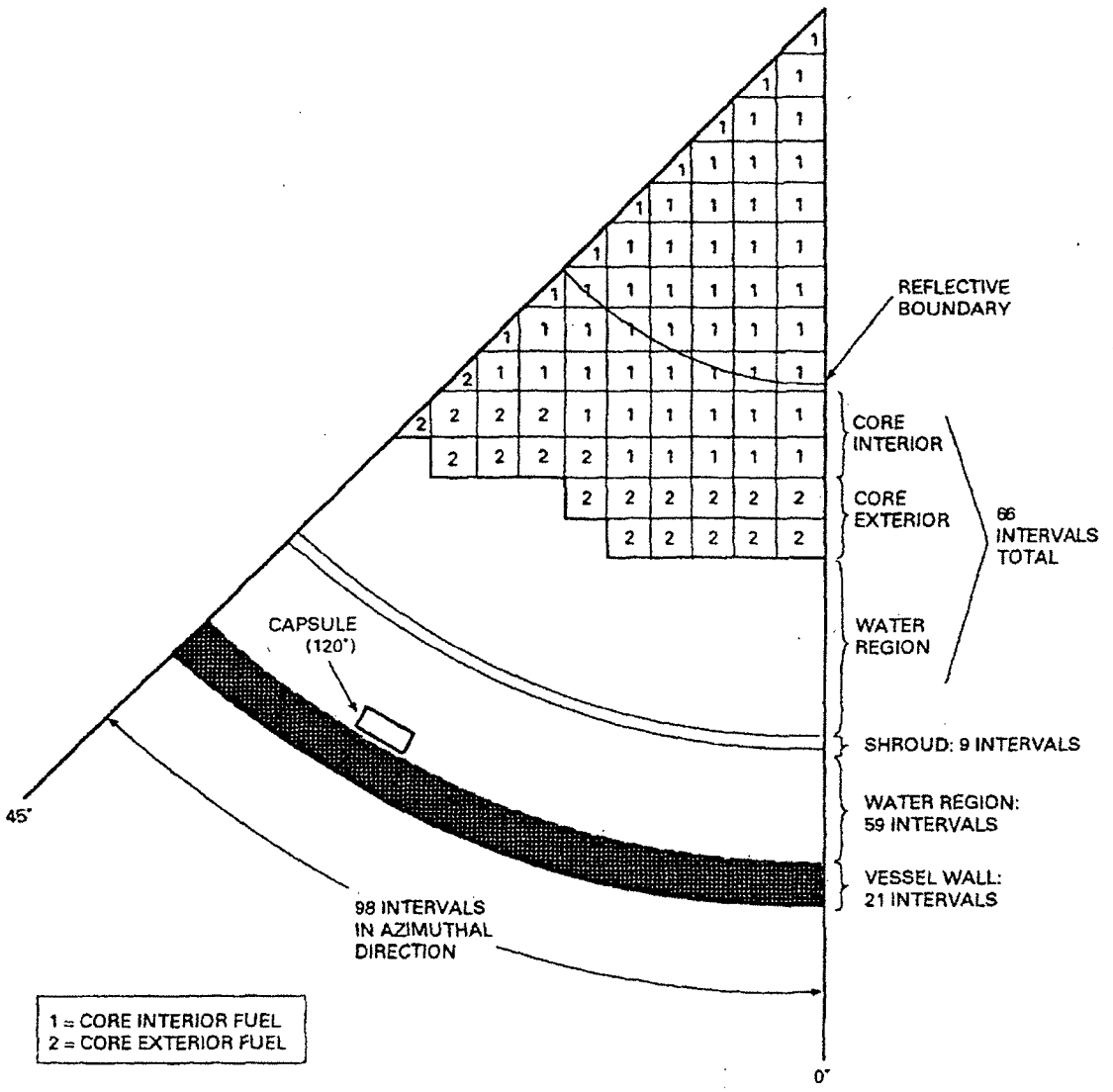

FIGURE 4-1: SCHEMATIC OF MODEL FOR AZIMUTHAL FLUX DISTRIBUTION ANALYSIS

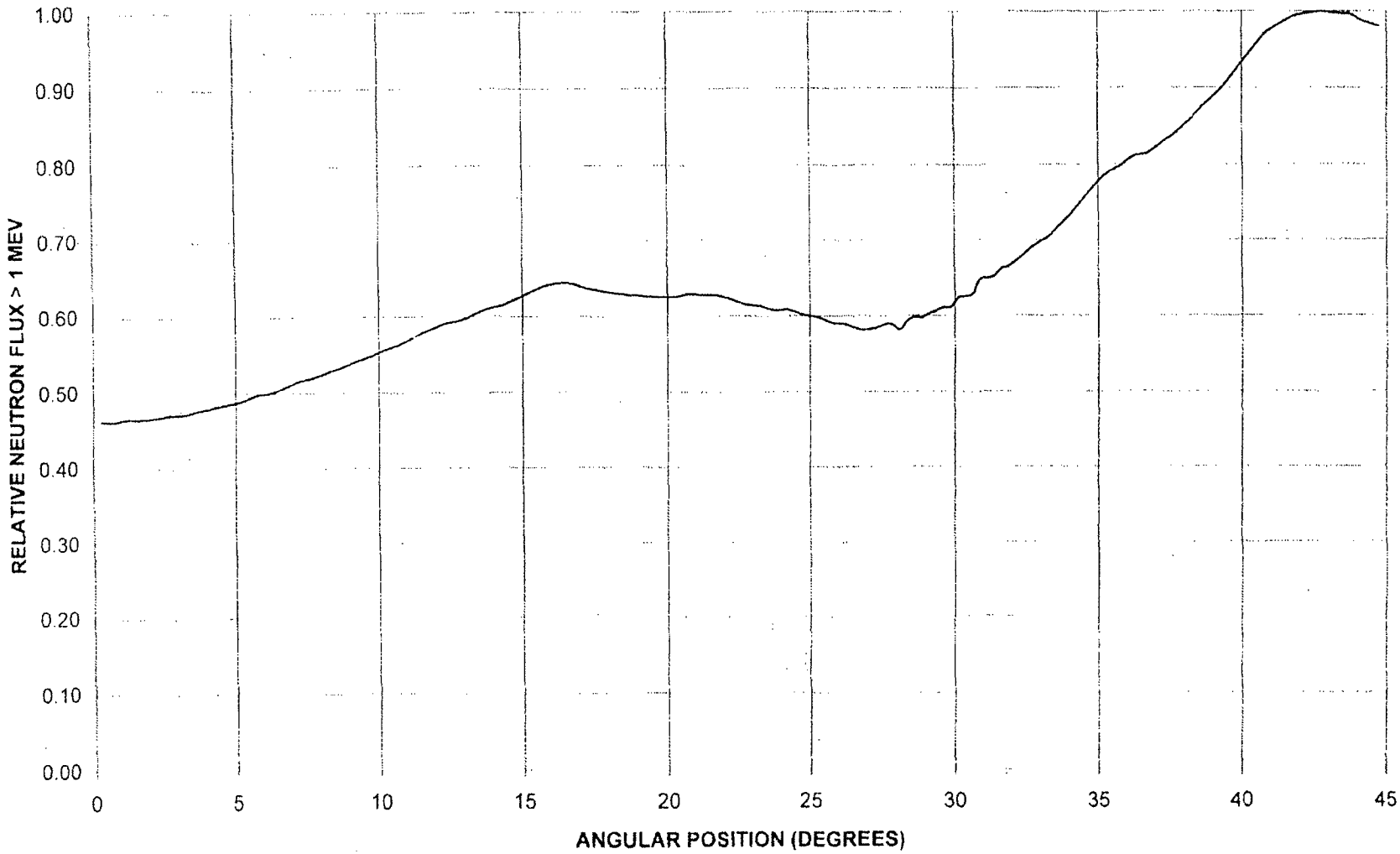

FIGURE 4-2: RELATIVE FLUX VS. ANGLE AT RPV INSIDE SURFACE

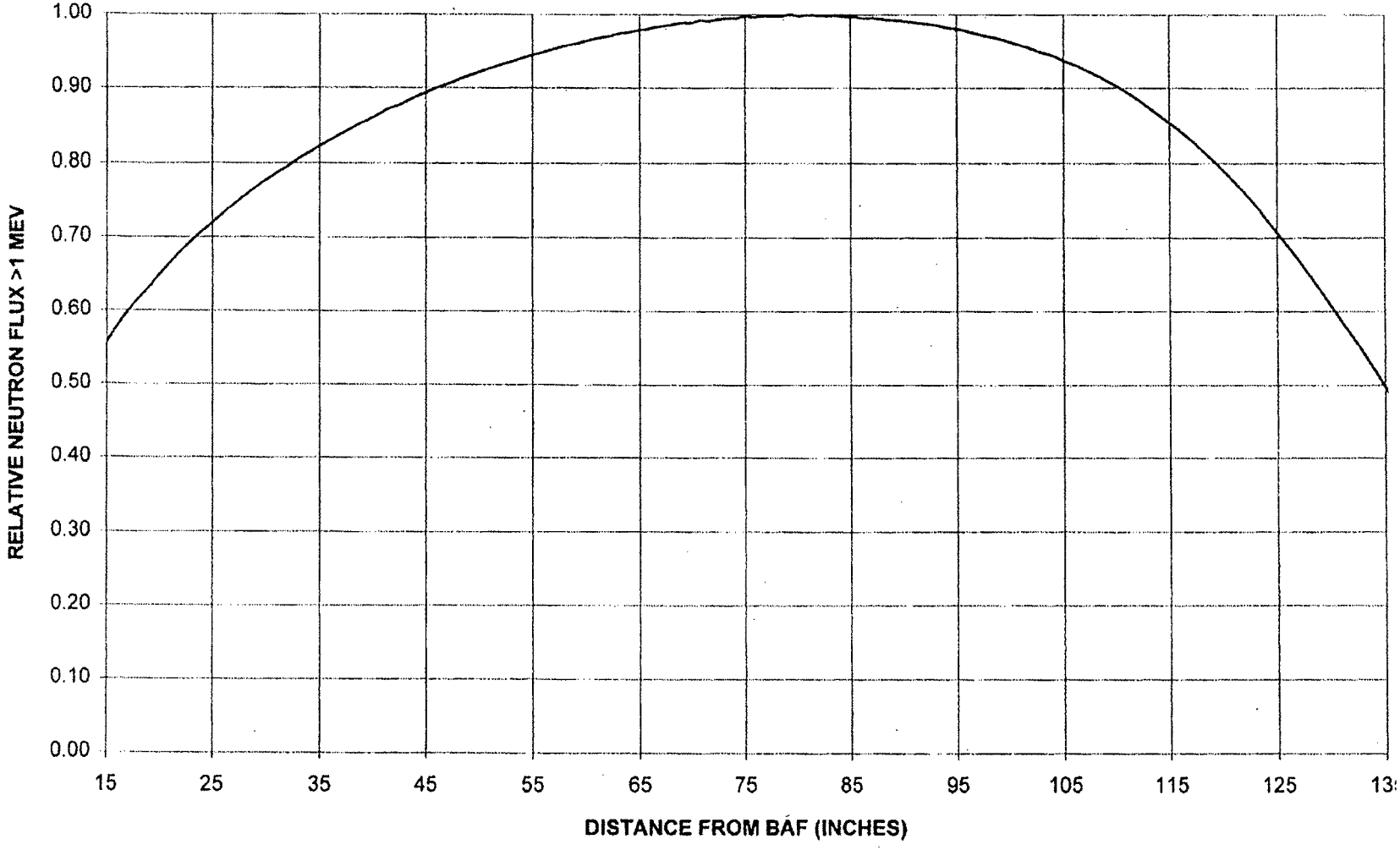

FIGURE 4-3: RELATIVE FLUX VS. ELEVATION AT RPV INSIDE SURFACE

5. CHARPY V-NOTCH IMPACT TESTING

The 24 Charpy specimens recovered from the surveillance capsule were impact tested at temperatures selected to establish the toughness transition and upper shelf of the irradiated RPV materials. Testing was conducted in accordance with ASTM E23-94b [12].

5.1 IMPACT TEST PROCEDURE

The Vallecitos testing machine used for irradiated specimens was a Tinius Olsen impact machine, serial number 175363. The maximum energy capacity of the machine is 300 ft-lb, which produces a test velocity at impact of 19.3 ft/sec.

The Tinius Olsen machine was qualified using NIST standard reference material specimens. The Standard Reference Materials (SRMs) consist of three sets of specimens which cover the energy range of the apparatus. Each set has a designated failure energy and a standard test temperature. According to ASTM E23-94b [12], the test apparatus averaged results must reproduce the NIST standard values within an accuracy of $\pm 5\%$ or ± 1.0 ft-lb, whichever is greater. The results of the qualification of the Tinius Olsen impact machine are summarized in Table 5-1.

Charpy V-Notch tests were conducted at temperatures between -80°F and 400°F. The cooling fluid used for irradiated specimens tested at temperatures at or below 50°F was ethanol. At temperatures between 50°F and 210°F, water was used as the temperature conditioning fluid. The specimens were heated in silicon oil for test temperatures above 210°F. Cooling of the conditioning fluids was done by heat exchange with liquid nitrogen through a copper coil; heating was done by an immersion heater. The bath of fluid was mechanically stirred to maintain uniform temperatures. The fluid temperature was measured with a calibrated Type K thermocouple positioned near the impact samples. After equilibration at the test temperature for at least 5 minutes, the specimens were manually transferred with centering tongs to the Charpy test machine and impacted in less than 5 seconds.

For each Charpy V-Notch specimen the test temperature, energy absorbed, lateral expansion, and percent shear were determined. In addition, photographs were taken for the

irradiated specimens. Lateral expansion and percent shear were measured according to specified methods [12]. Percent shear was determined using method number 1 of Subsection 11.2.4.3 of ASTM E23-94b [12], which involved measuring the length and width of the cleavage surface in inches and determining the percent shear value from Table 2 of ASTM E23-94b [12].

5.2 IMPACT TEST RESULTS

Eight Charpy V-Notch specimens each of irradiated base, weld, and HAZ material were tested at temperatures (-80°F to 400°F) selected to define the toughness transition and upper shelf portions of the fracture toughness curves. The absorbed energy, lateral expansion, and percent shear data are listed for each material in Table 5-2. Plots of absorbed energy and lateral expansion for base, weld, and HAZ materials are presented in Figures 5-1 through 5-6. These curves are plotted along with the corresponding curves from the first capsule (and unirradiated base material data where appropriate) in Figures 5-7 through Figure 5-12. The fracture surface photographs and a summary of the test results for each specimen are contained in Appendix A.

The unirradiated and irradiated plate and weld energy and lateral expansion data are fit with the hyperbolic tangent function developed by Oldfield for the EPRI Irradiated Steel Handbook [13] (HAZ was not fit due to data scatter):

$$Y = A + B * TANH [(T - T_0)/C],$$

where Y = impact energy or lateral expansion
T = test temperature, and
A, B, T_0 and C are determined by non-linear regression.

The TANH function is one of the few continuous functions with a shape characteristic of low alloy steel fracture toughness transition curves.

5.3 IRRADIATED VERSUS UNIRRADIATED CHARPY V-NOTCH PROPERTIES

Ideally, a shift in RT_{NDT} would be established by comparing the irradiated Charpy specimen data to baseline unirradiated Charpy data. For the case of the FitzPatrick base material specimens, data was obtained from the Certified Material Test Report. Additional Charpy test

data for the FitzPatrick surveillance plate (heat number C3278-2) was available from the BWROG Supplemental Surveillance Program report [17]. This program was useful in providing plant-specific data and information for the FitzPatrick base material to establish baseline properties. The unirradiated data for the base material, as well as the results for both the plate and weld materials from the first and second surveillance capsules, were fit to a TANH function as described in the previous section. The unirradiated properties for the surveillance plate were determined from the combined sets of data, as shown in Figure 5-13. For the weld material, no credible unirradiated baseline data was available.

5.4 COMPARISON TO PREDICTED IRRADIATION EFFECTS

5.4.1 Irradiation Shift

The measured transition temperature shifts for the base and weld materials were compared to the predictions calculated according to Rev. 2 [7]. The inputs and calculated values for irradiated shift for the plate and weld materials based upon measurements taken from the 120° azimuth capsule at 13.4 EFPY are as follows:

Plate:	Copper =	0.11%	
	Nickel =	0.60%	
	CF =	74	
	fluence =	5.0×10^{17} n/cm^2	
	Reg. Guide 1.99 ΔRT_{NDT} =		21.7°F
	Reg. Guide 1.99 $\Delta RT_{NDT} \pm 2\sigma_\Delta$(34°F) =		55.7°F max, -12.3°F min
	Measured 30 ft-lb shift =		14.97°F
Weld:	Copper =	0.29%	
	Nickel =	0.71%	
	CF =	208	
	fluence =	5.0×10^{17} n/cm^2	
	Reg. Guide 1.99 ΔRT_{NDT} =		60.9°F
	Reg. Guide 1.99 $\Delta RT_{NDT} \pm 2\sigma_\Delta$(56°F) =		116.9°F max, 4.9°F min

The weight percents of Cu and Ni are best estimates based on averaging (see Table 3-4). The CF values shown above are the chemistry factors for the materials obtained from Rev. 2. The fluence factor for the Reg. Guide calculation of 30 ft-lb shift may either be calculated according to the Rev. 2 definition

$$\text{fluence factor} = f^{(0.28 - 0.10 \log f)} \qquad (5\text{-}1)$$

or it may be obtained from Rev. 2 Figure 1 [7]. Using Equation 5-1, the fluence factor was calculated to be 0.293. These values are used to calculate the Reg. Guide 1.99 prediction for 30 ft-lb shift and USE decrease for comparison to the measured shift and USE decrease for the irradiated surveillance materials. The predicted 30 ft-lb temperature shift (ΔRT_{NDT}) was also calculated according to Rev. 2 using the equation

$$\Delta RT_{NDT} = (CF)\, f^{(0.28 - 0.10 \log f)} \qquad (5\text{-}2)$$

The measured 30 ft-lb temperature shift (Table 5-3) of 14.97°F for the plate material is within the bounds of the Reg. Guide prediction. Since two credible data sets are available for the plate material, the ART prediction was modified in a manner consistent with Position 2 of Rev. 2, as described in Section 7.

A least squares fit to the 30 ft-lb shift (ΔT_{30}) values was performed as shown in Figure 5-14. This figure shows the comparison of the ΔT_{30} vs. fluence relation predicted by Reg. Guide 1.99, Rev. 2 and the actual fitted results for the surveillance plate. It is noted that the fitted curve exhibits less embrittlement than that predicted by the Reg. Guide for this plate material.

5.4.2 Change in USE

Using the copper and fluence data above with Figure 2 of Rev. 2, decreases in USE of approximately 9% are predicted for the plate and 19% for the weld material for the first capsule. For the second capsule, the predicted decreases in USE are 10% and 22% for the base and weld materials, respectively. In the base metal, the USE increased from the unirradiated to the second capsule. (Since unirradiated weld data was not available, no value was used.) The USE decreased for both the plate material and the weld material from the first to the second capsule.

TABLE 5-1: VALLECITOS QUALIFICATION TEST RESULTS USING NIST STANDARD REFERENCE SPECIMENS

	Specimen Identification	Energy Absorbed (ft-lb)		Variance[1]
		VNC	NIST	
Vallecitos Tinius Olsen Machine (tested 6/96)	LL-45 1	12.71		
	LL-45 2	13.75		
	LL-45 3	14.20		
	LL-45 4	13.10		
	LL-45 5	14.10		
	Average:	13.572	12.836	+0.736 ft-lbs
	HH-46 1	71.0		
	HH-46 2	75.5		
	HH-46 3	76.0		
	HH-46 4	76.5		
	HH-46 5	75.0		
	Average:	74.808	74.284	+0.71%
	SH-6 1	170.5		
	SH-6 2	168.0		
	SH-6 3	154.0		
	SH-6 4	154.0		
	SH-6 5	165.0		
	Average:	162.327	165.831	-2.11%

[1] Allowable Variance is 1.4J (1 ft-lb) or 5%, whichever is greater (ASTM STD-E23)

TABLE 5-2: IRRADIATED CHARPY V-NOTCH IMPACT TEST RESULTS SECOND CAPSULE

	VNC ID	Specimen Identification	Test Temperature (°F)	Fracture Energy (ft-lb)	Lateral Expansion (mils)	Shear (Method 1) [12] (%)
Base:	29292	53U	-50	10.0	8	1
Heat C3278-2,	29291	53M	0	35.4	31	29
Longitudinal	29287	53P	24	44.2	39	31
	29283	53Y	49	81.0	65	46
	29285	53B	103	96.5	77	78
	24286	52D	150	117.4	89	100
	29293	53L	250	120.4	91	100
	29284	527	400	126.7	93	100
Weld:						
	29288	56A	0	3.2	3	1
	29298	565	80	18.9	18	30
	29297	563	103	29.4	27	34
	29289	56L	120	33.7	32	55
	29295	55Y	163	56.8	43	75
	29290	55B	202	68.1	61	88
	29294	54M	250	72.5	66	100
	29295	54T	400	75.0	73	100
HAZ:	29301	5AT	-80	36.0	29	38
	29305	5AY	-50	36.6	30	41
	29303	5AK	0	44.0	41	22
	29306	5AU	48	98.3*	78	30
	29302	57P	80	77.6	67	82
	29300	575	120	74.1	69	100
	29299	5AB	202	102.2	82	100
	29304	5A6	400	112.6	95	100

* Note: HAZ data exhibits scatter in fracture energy due to material inhomogeneity and location of notch in relation to the fusion line. Because of these effects, the latest version of ASTM E185-94 recommends not testing the HAZ samples. This version of ASTM E185 has not yet been approved for use by NRC.

TABLE 5-3: SIGNIFICANT RESULTS OF IRRADIATED AND UNIRRADIATED CHARPY V-NOTCH DATA

Material	Index Temp (°F) E=30 ft-lb	Index Temp (°F) E=50 ft-lb	Index Temp (°F) MLE=35 mil	USE (ft-lb)
PLATE: Heat C3278-2				
Unirradiated	-21.83	7.91	8.6	133.8
1st Capsule [a]	-25.14	16.07	-19.0	133.3
Difference Unirrad. to 1st	-3.31	8.16	-27.6	-0.5 (-0.37%)
2nd Capsule [b]	-6.86	22.5	10.1	121.5
Difference Unirrad. to 2nd	14.97	14.59	1.5	-12.3 (-9.2%)

	1st Capsule[a]	2nd Capsule[b]	Difference
Reg. Guide 1.99, Rev. 2 ΔRT_{NDT} :	15°F	22°F [c]	7 °F
Reg. Guide 1.99, Rev. 2 ($\Delta \pm 2\sigma$) :	-19°F to 49°F	-12°F to 56°F [c]	
Reg. Guide 1.99, Rev. 2 Decrease in USE [d]:	9%	10%	1%

Material	Index Temp (°F) E=30 ft-lb	Index Temp (°F) E=50 ft-lb	Index Temp (°F) MLE=35 mil	USE (ft-lb)
SURVEILLANCE WELD: [e]				
1st Capsule [a]	44.4	95.7	54.0	85.1
2nd Capsule [b]	107.7	147.9	130.7	74.8
Difference 1st to 2nd	63.3	52.2	76.7	-10.3(-12.1%)

	1st Capsule[a]	2nd Capsule[b]	Difference
Reg. Guide 1.99, Rev. 2 ΔRT_{NDT} :	42°F	61°F [c]	19°F
Reg. Guide 1.99, Rev. 2 ($\Delta \pm 2\sigma$) :	-14°F to 98°F	5°F to 117°F [c]	
Reg. Guide 1.99, Rev. 2 Decrease in USE [d]:	19%	22%	3%

[a] 1st Capsule pulled from 30° at 5.98 EFPY or 2.6×10^{17} n/cm^2
[b] 2nd Capsule pulled from 120° at 13.4 EFPY or 5.0×10^{17} n/cm^2
[c] Determined in Section 5.4.1
[d] Determined in Section 5.4.2
[e] No Unirradiated data available

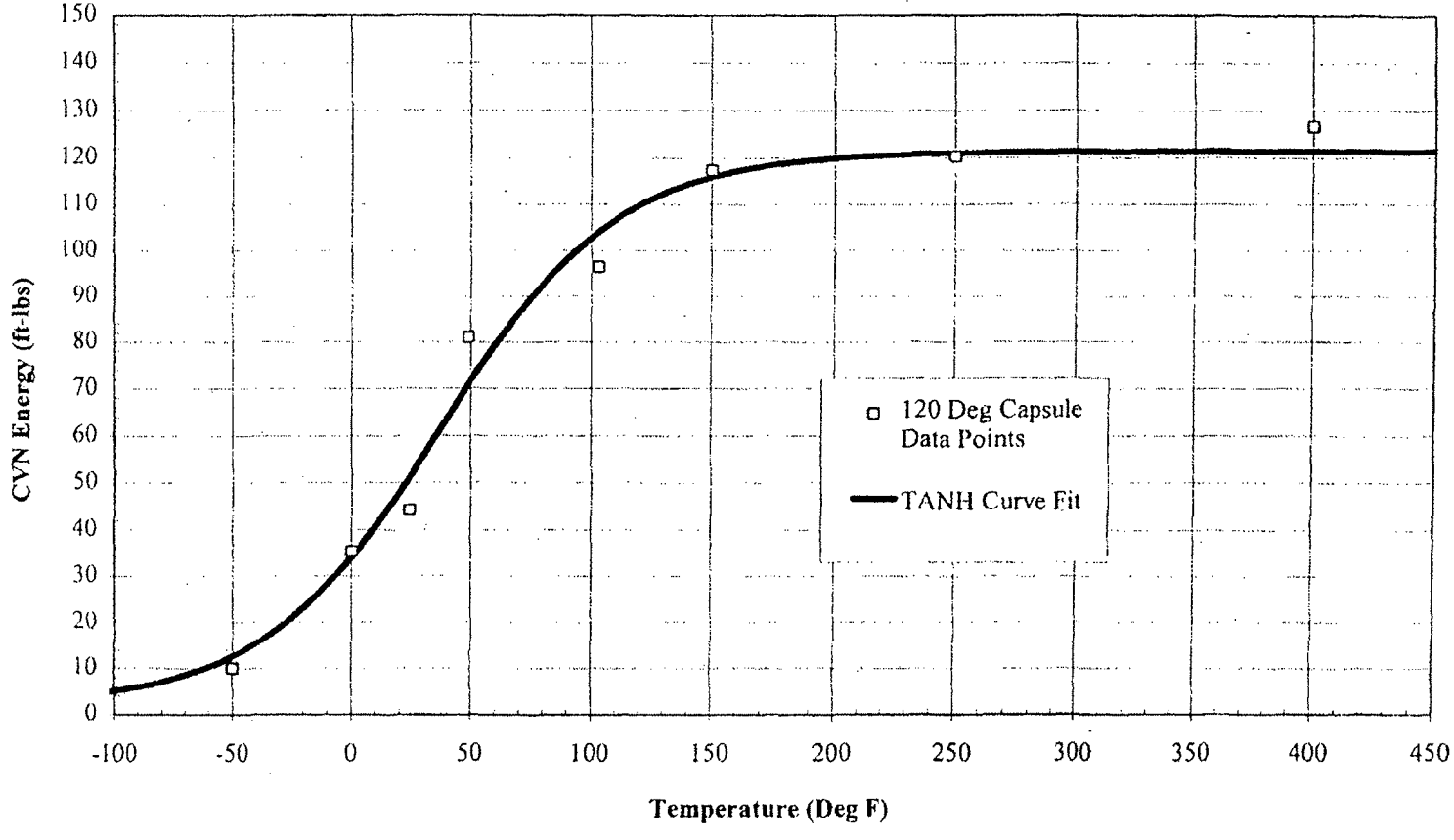

FIGURE 5-1: ABSORBED ENERGY VS. TEMPERATURE (PLATE-120° CAPSULE)

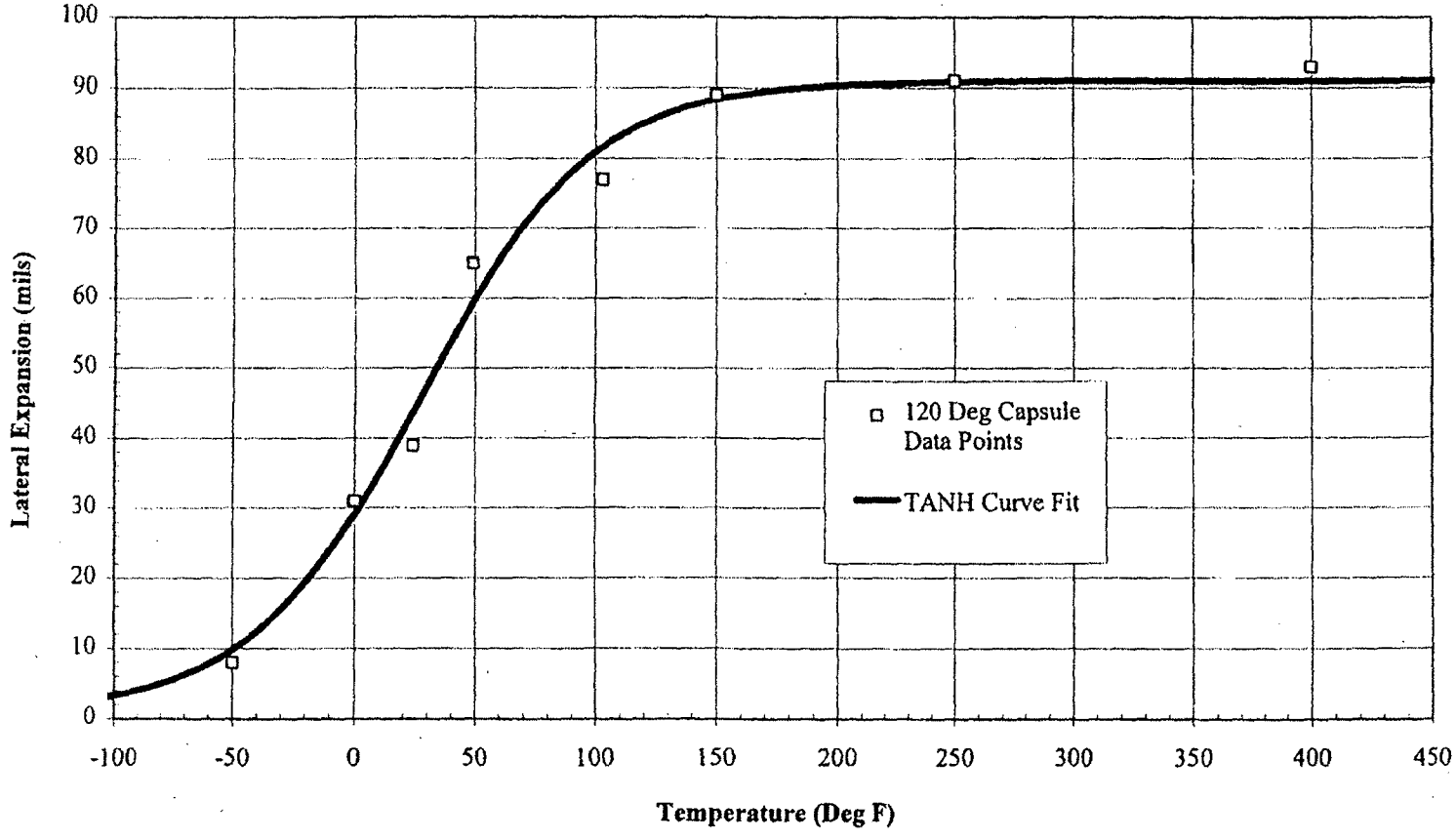

FIGURE 5-2: LATERAL EXPANSION VS. TEMPERATURE (PLATE-120° CAPSULE)

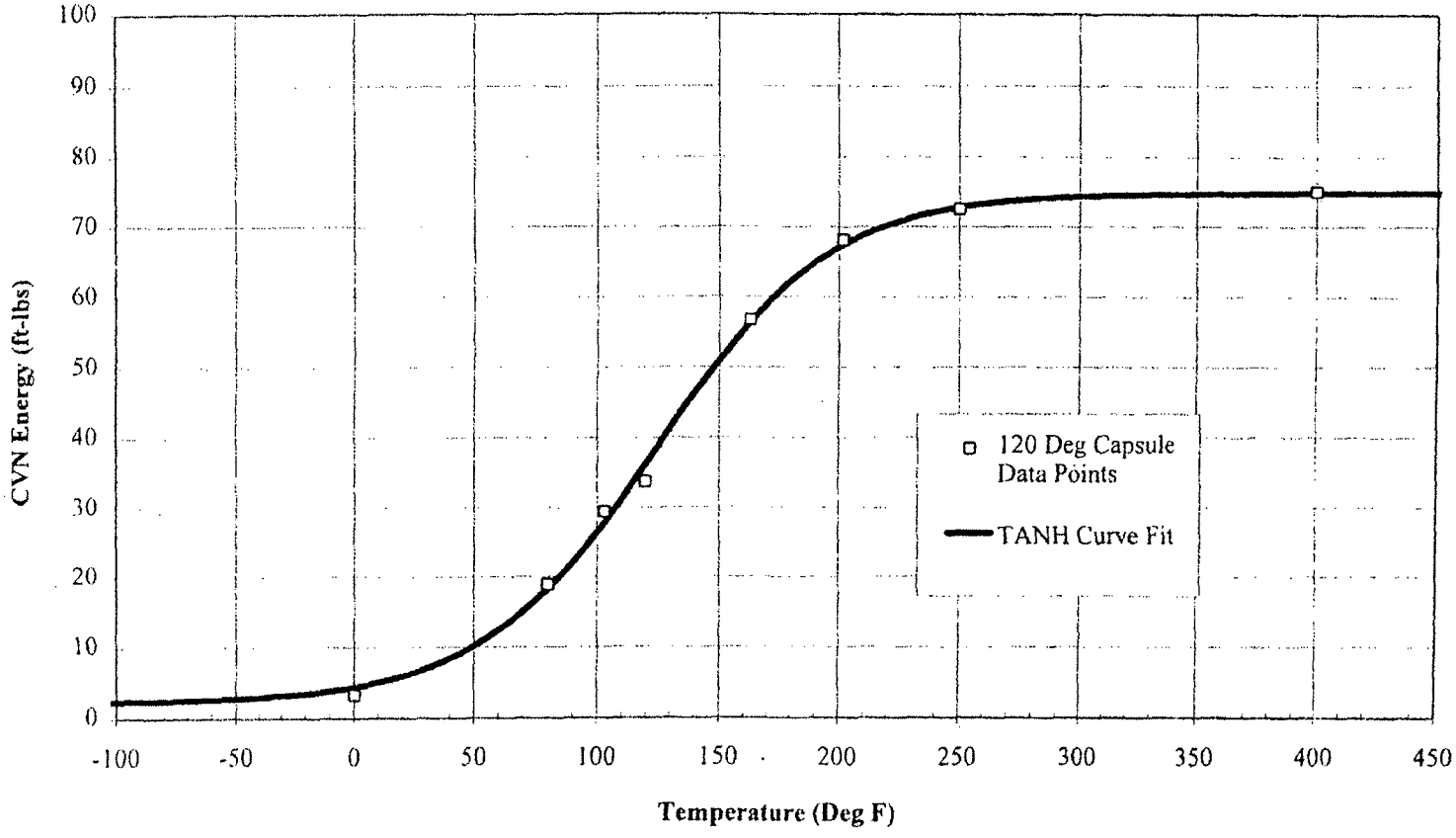

FIGURE 5-3: ABSORBED ENERGY VS. TEMPERATURE (WELD-120° CAPSULE)

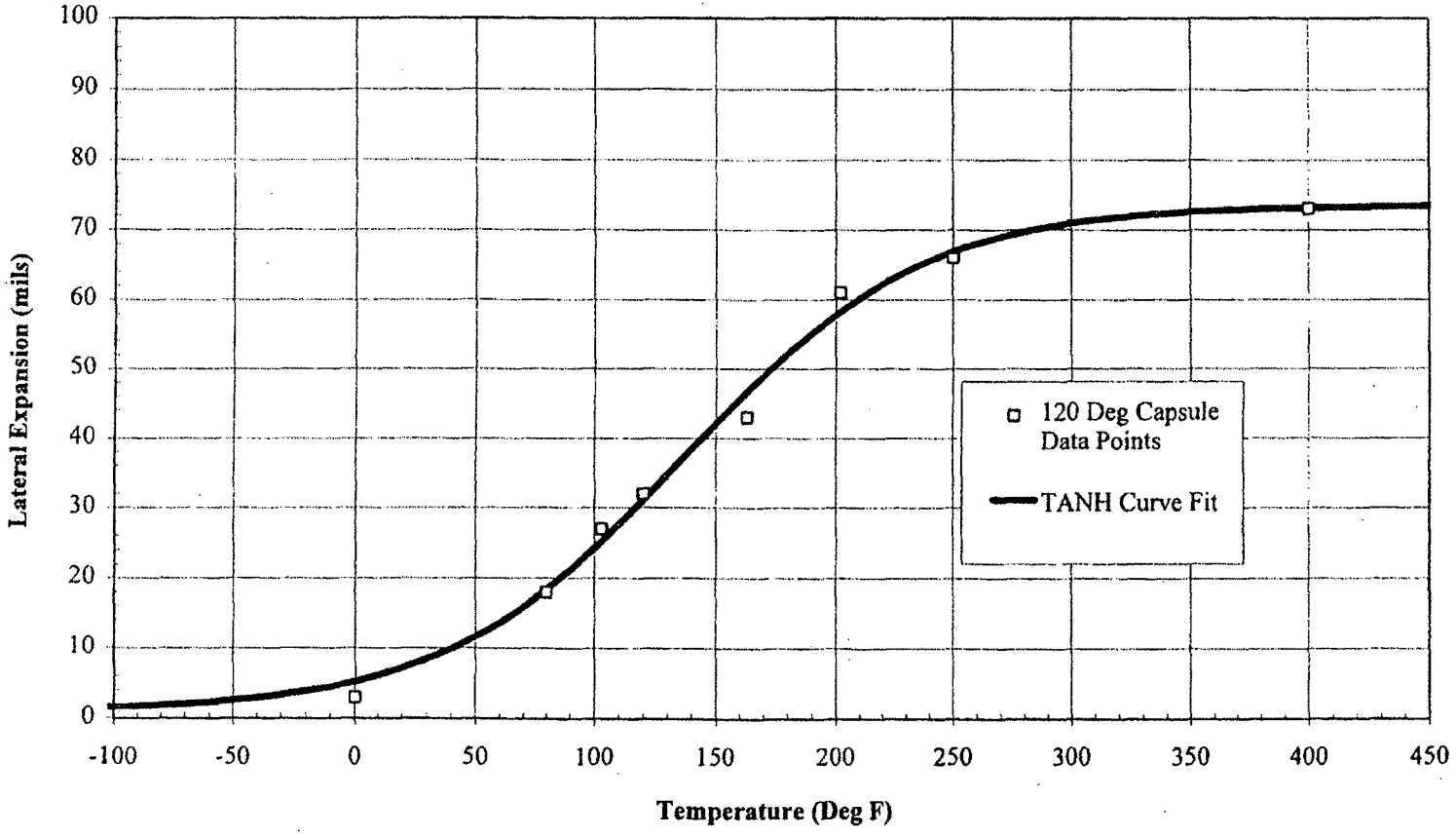

FIGURE 5-4: LATERAL EXPANSION VS. TEMPERATURE (WELD-120° CAPSULE)

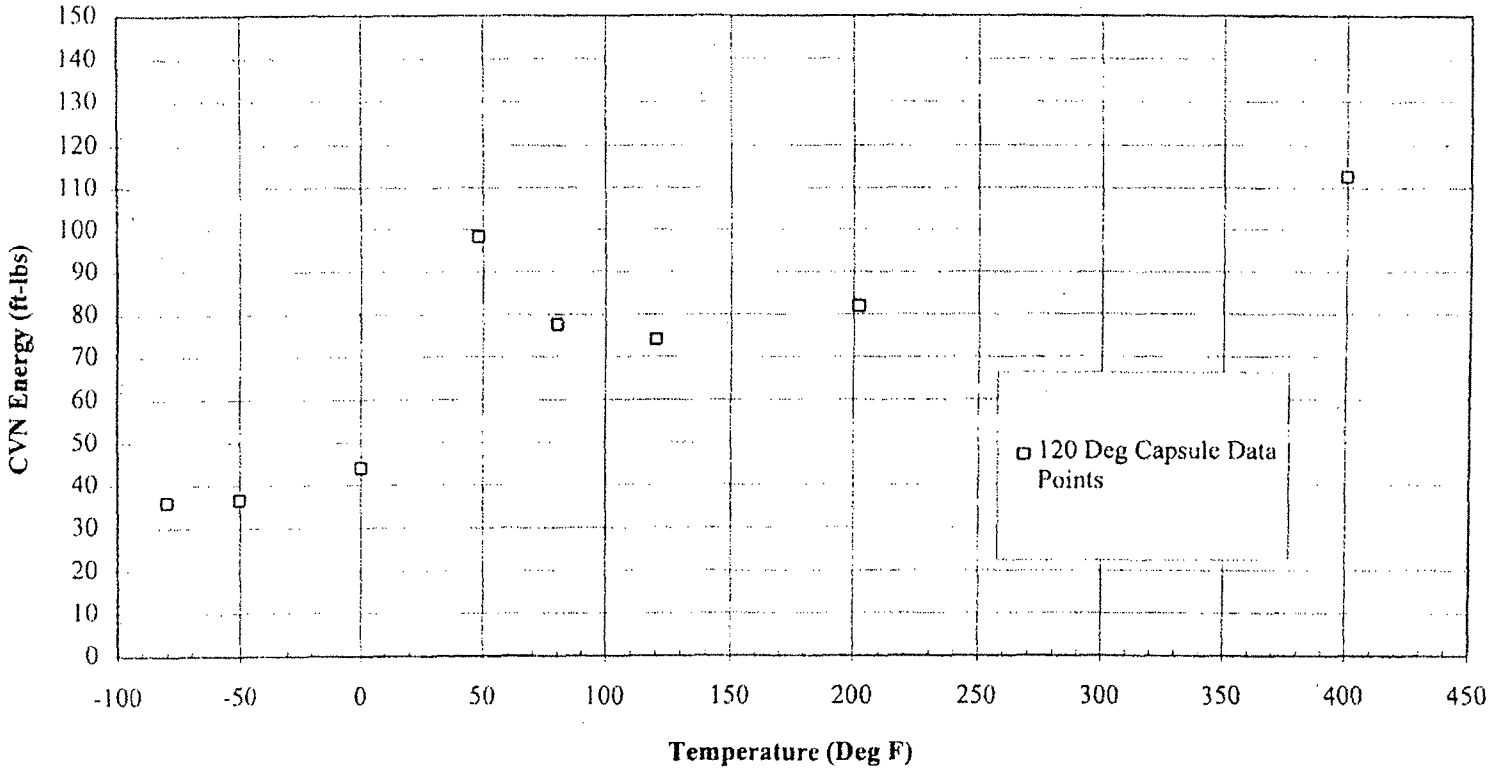

FIGURE 5-5: ABSORBED ENERGY VS. TEMPERATURE (HAZ-120° CAPSULE)

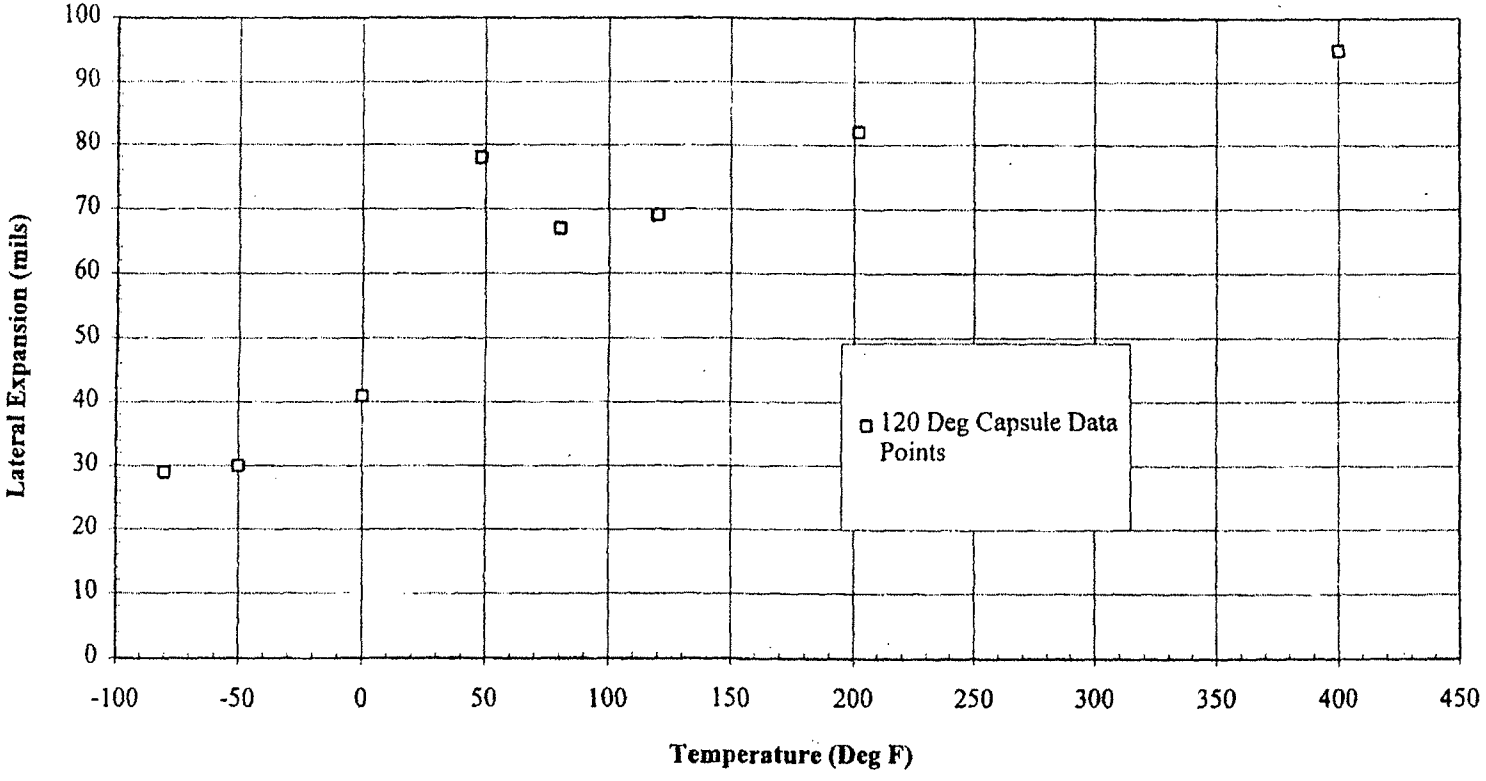

FIGURE 5-6: LATERAL EXPANSION VS. TEMPERATURE (HAZ-120° CAPSULE)

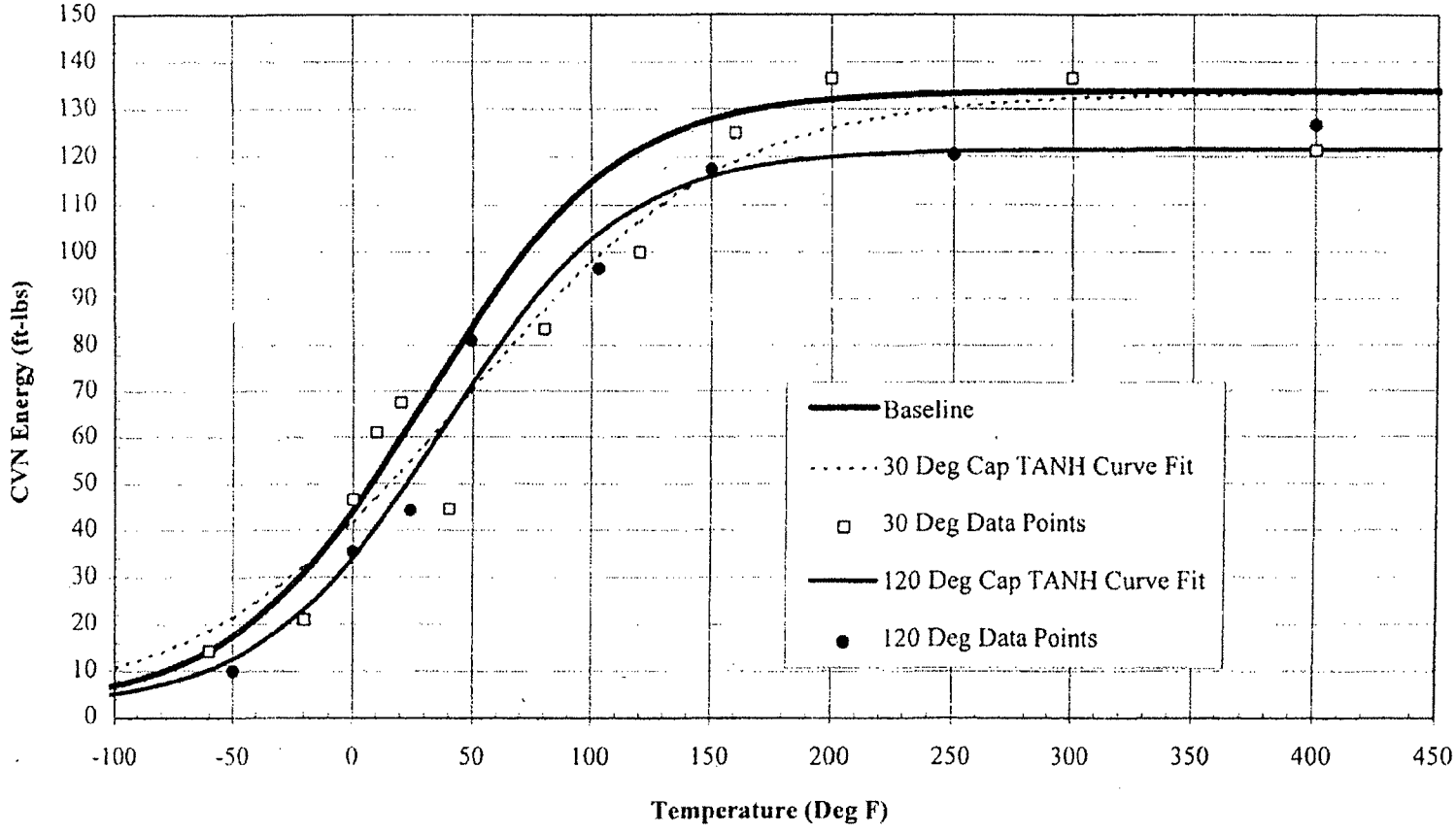

FIGURE 5-7: COMPARISON OF UNIRRADIATED AND IRRADIATED ENERGY DATA (PLATE)

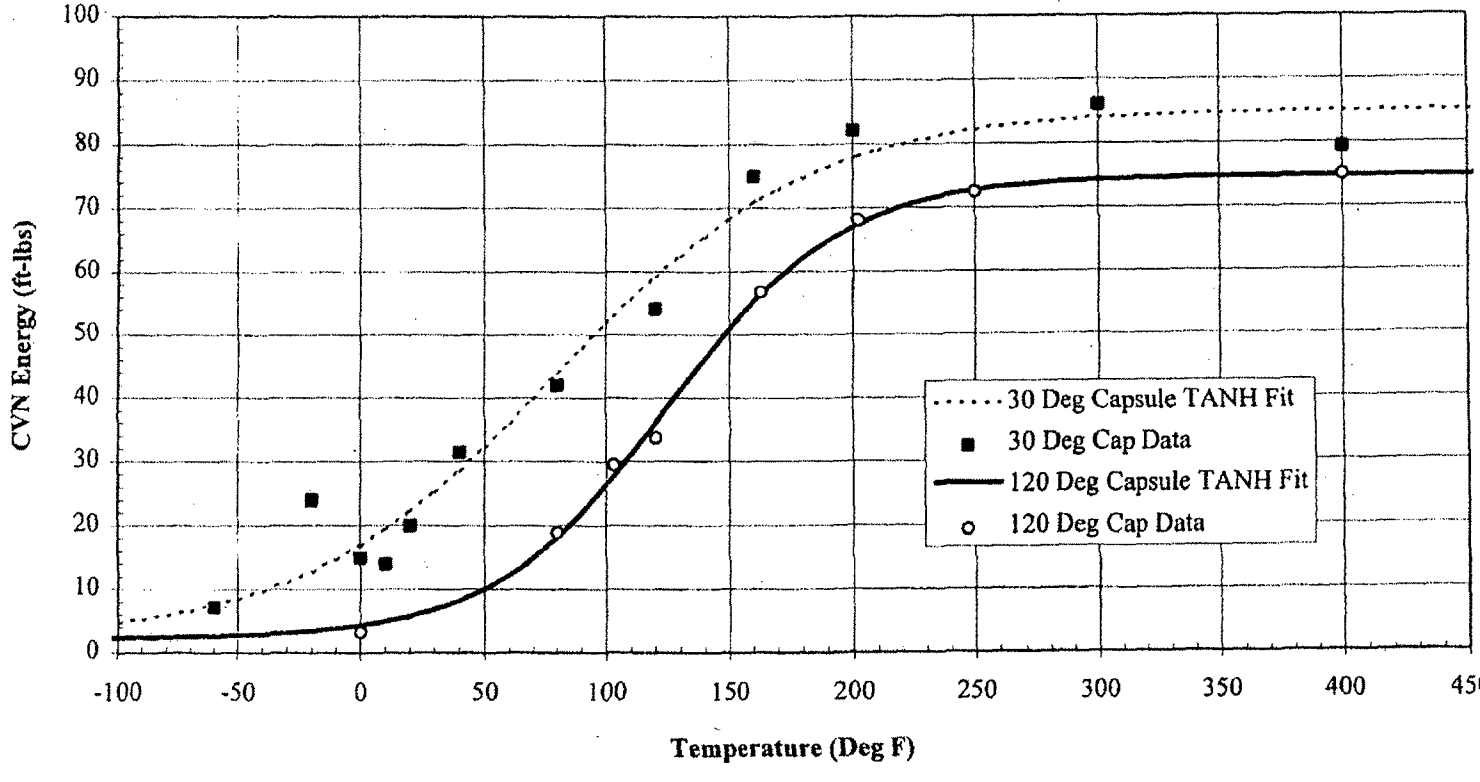

FIGURE 5-8: COMPARISON OF 1ST AND 2ND CAPSULE ENERGY RESULTS (WELD)

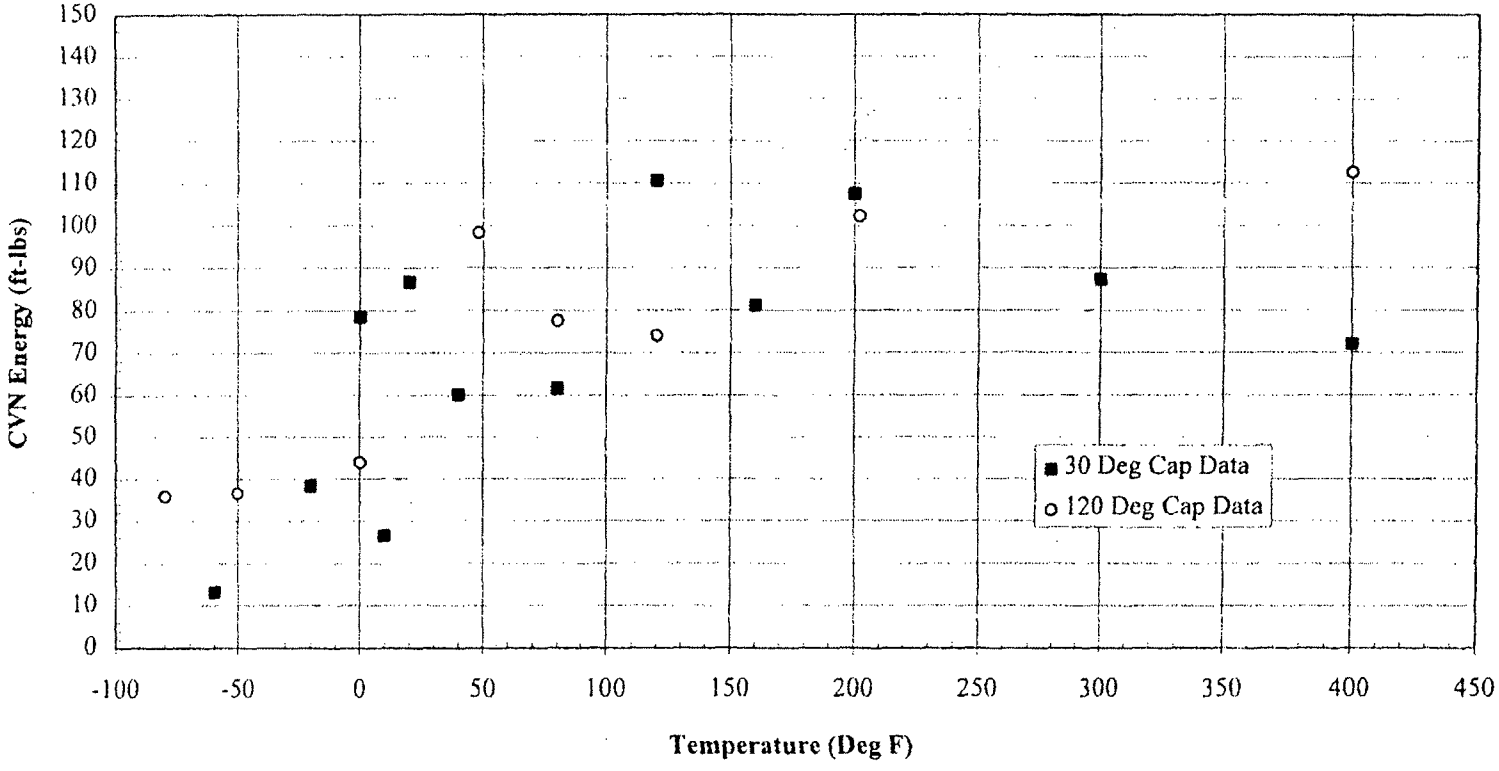

FIGURE 5-9: COMPARISON OF 1ST AND 2ND CAPSULE ENERGY RESULTS (HAZ)

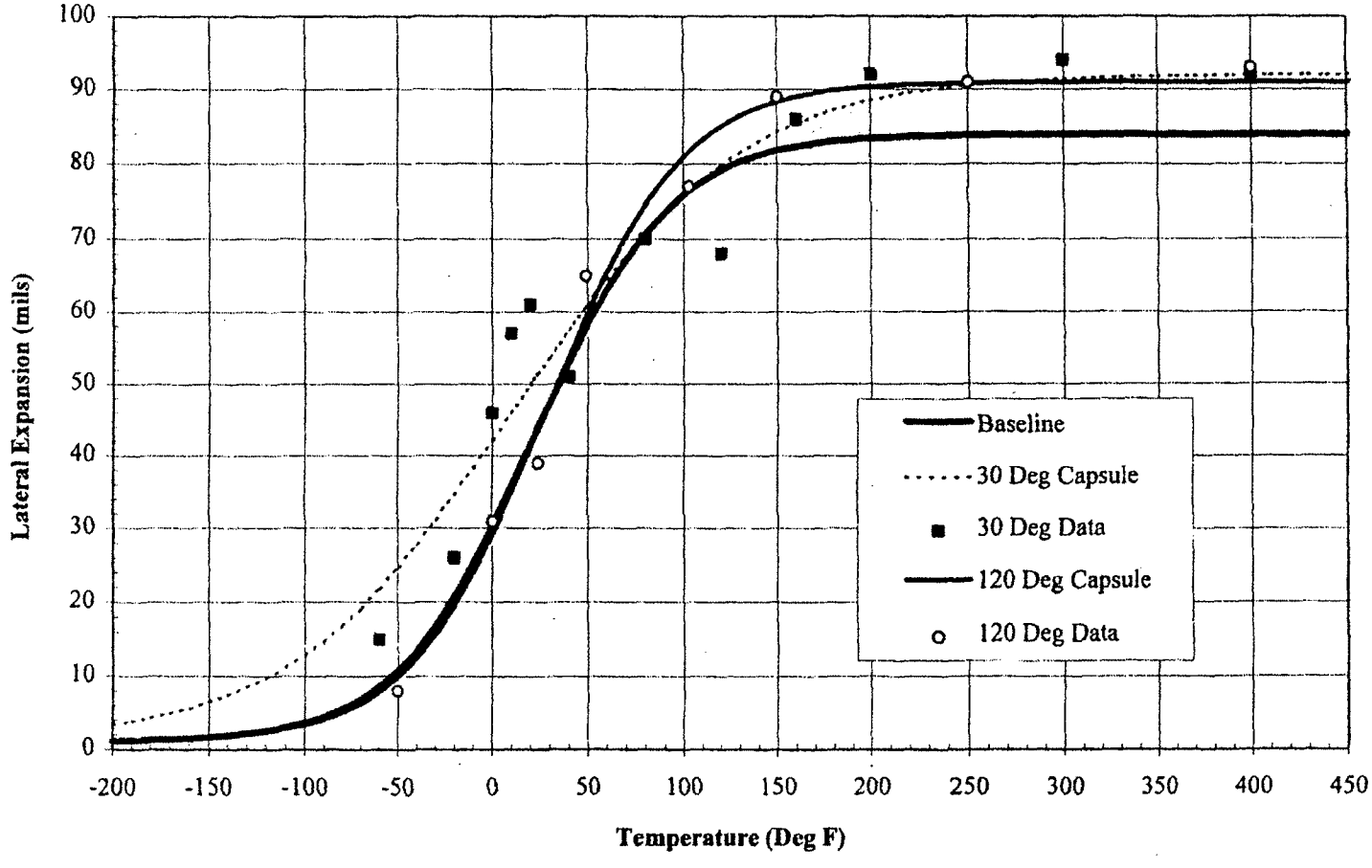

FIGURE 5-10: COMPARISON OF LATERAL EXPANSION RESULTS (PLATE)

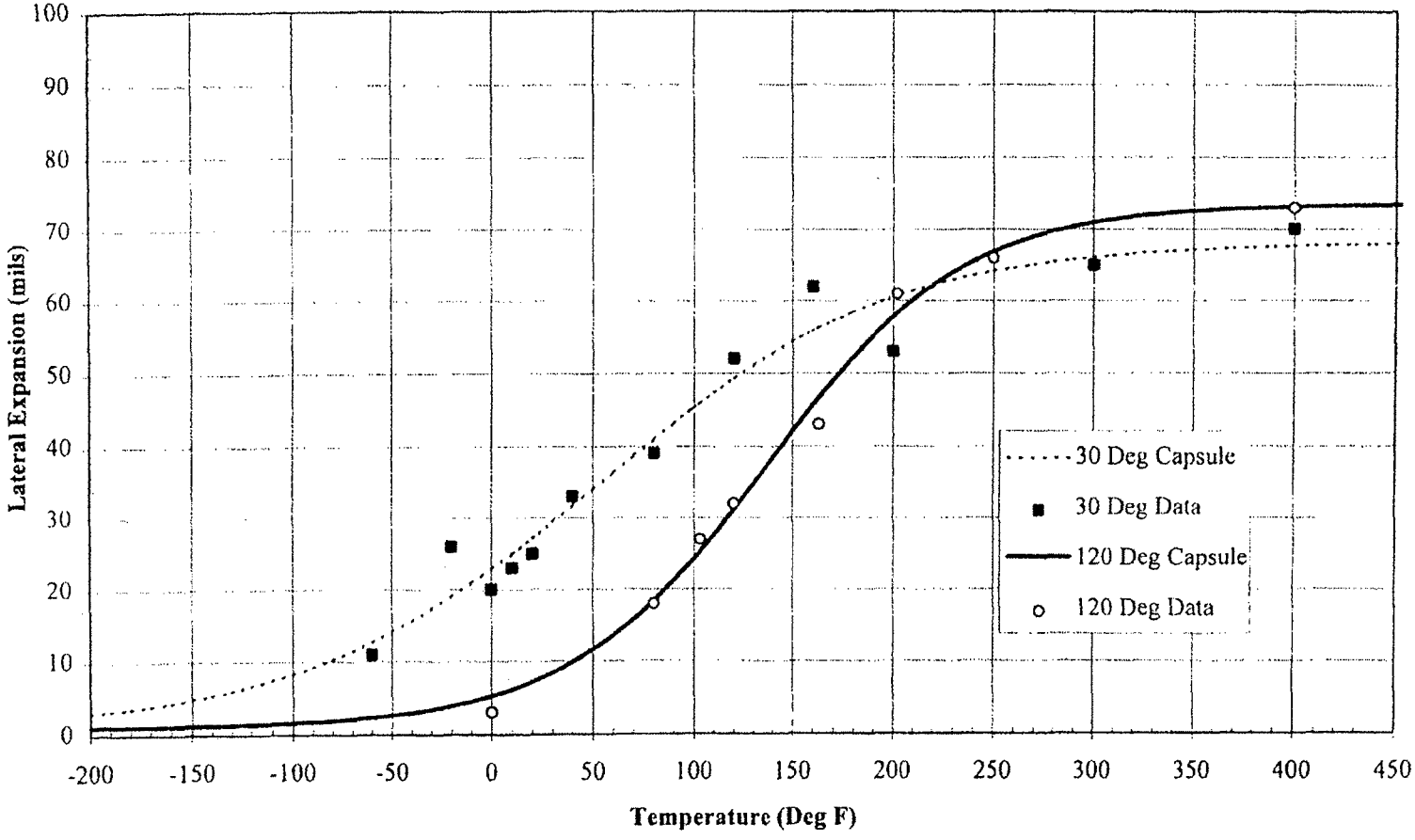

FIGURE 5-11: COMPARISON OF LATERAL EXPANSION RESULTS (WELD)

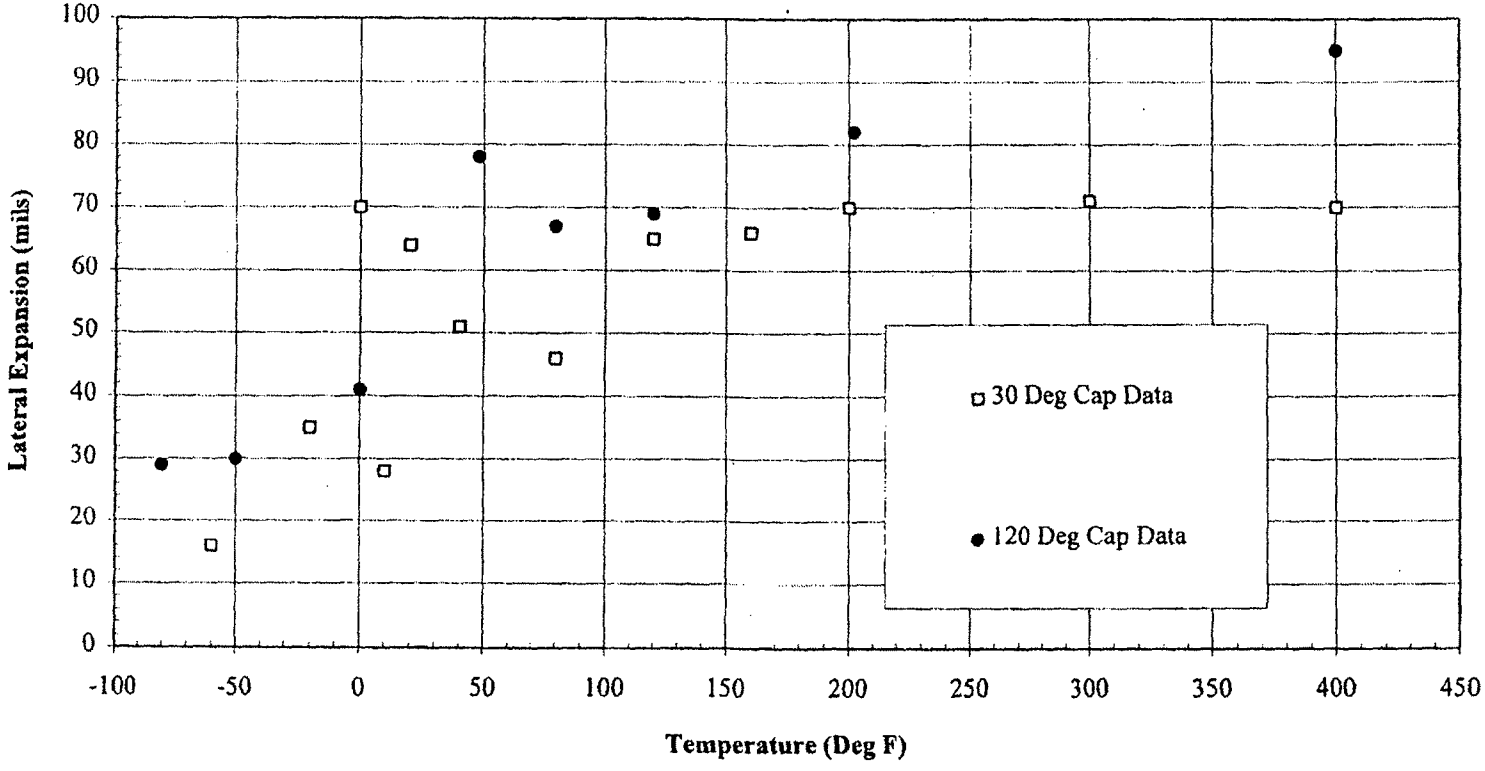

FIGURE 5-12: COMPARISON OF LATERAL EXPANSION RESULTS (HAZ)

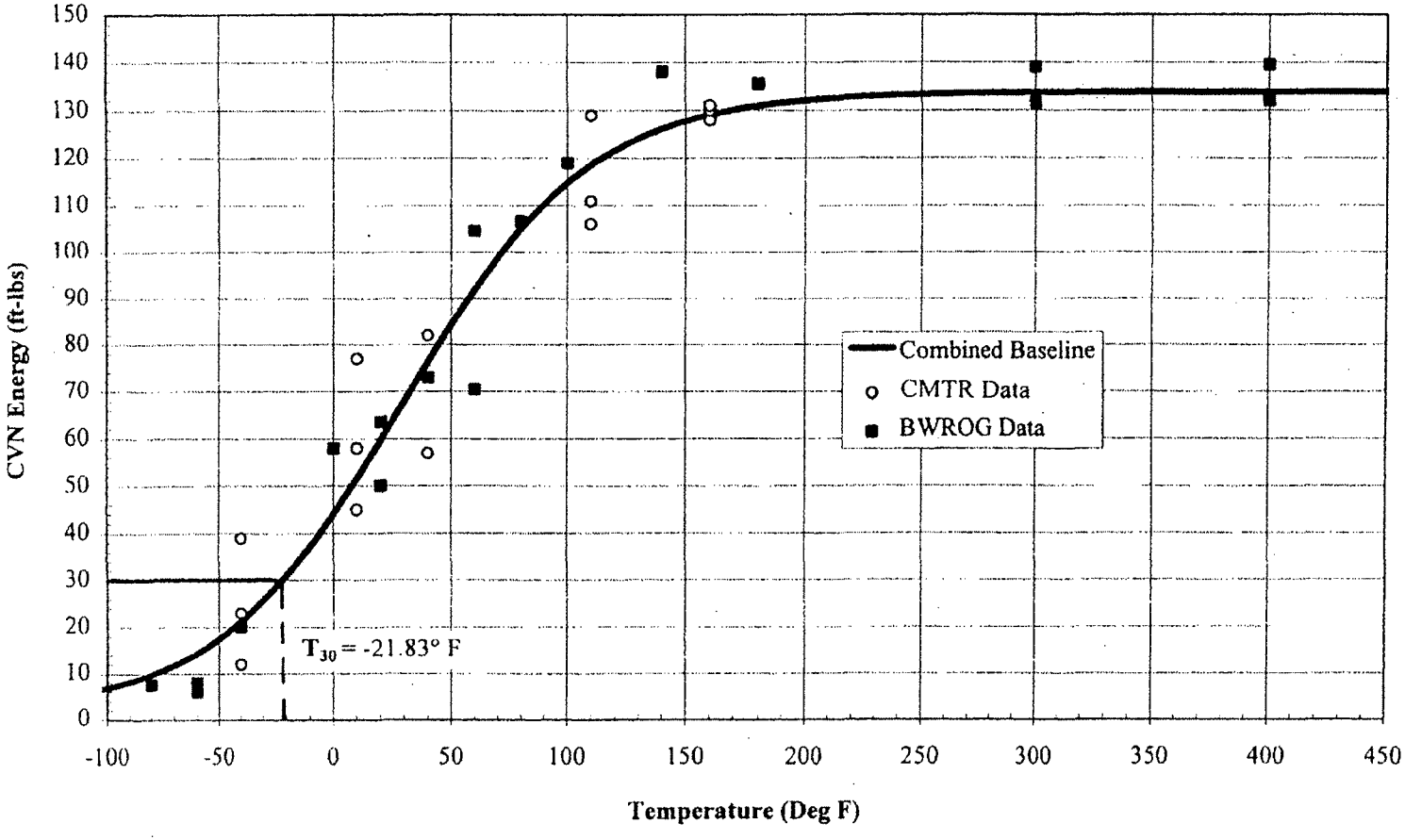

FIGURE 5-13: TANH CURVE-FITTED RESULTS FOR COMBINED BASELINE DATA (PLATE)

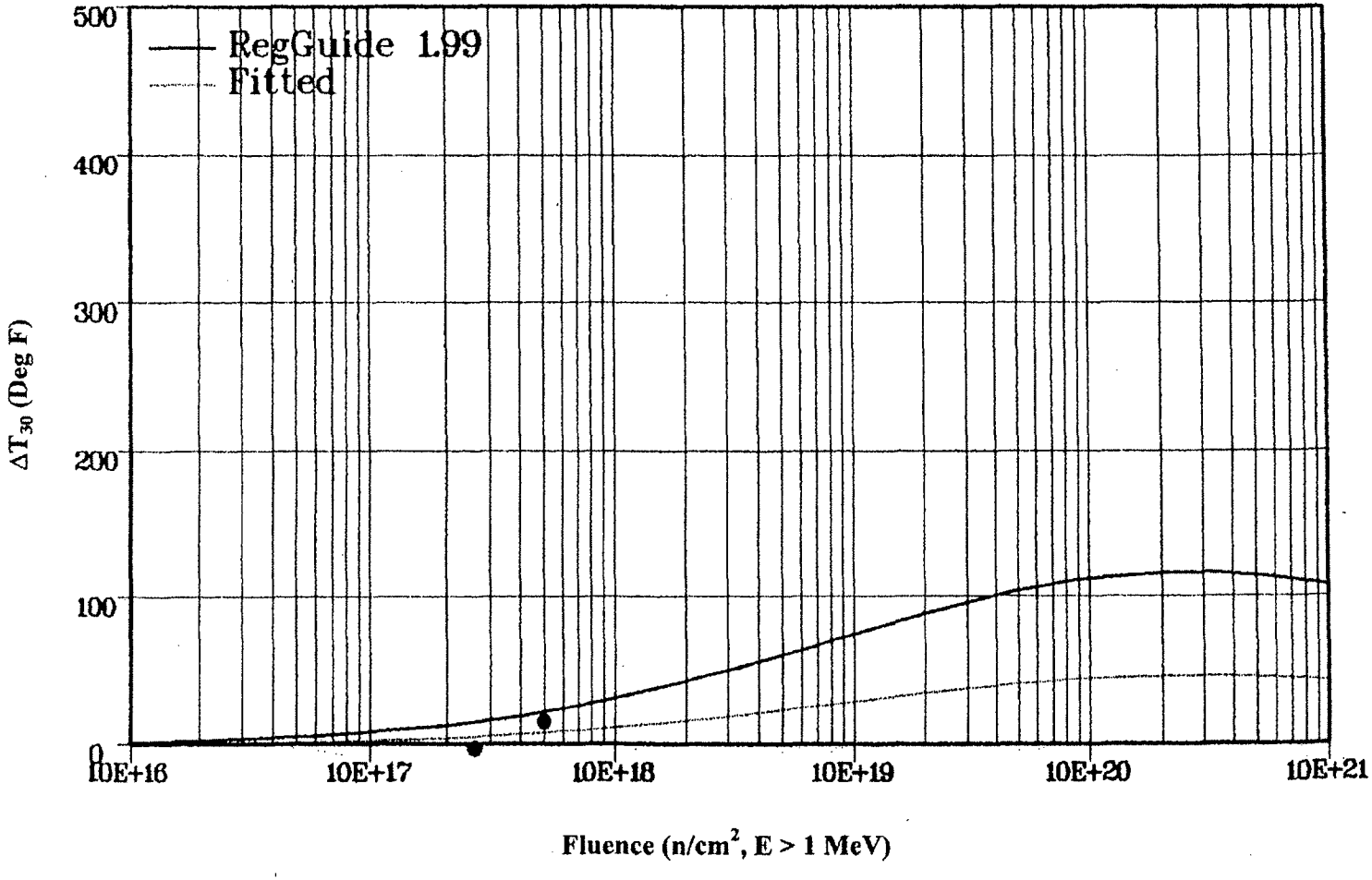

FIGURE 5-14: ΔT_{30} VS. FLUENCE SHOWING PLATE DATA WITH FITTED RESULTS

6. TENSILE TESTING

Eight round bar tensile specimens were recovered from the surveillance capsule. Uniaxial tensile tests were conducted in air at room temperature (70°F) at RPV operating temperature (550°F) for base, weld and HAZ specimens, and at an intermediate temperature of 185°F for an additional base and weld specimen. The tests were conducted in accordance with ASTM E8-89 [14].

6.1 PROCEDURE

All tests were conducted using a screw-driven Instron test frame equipped with a 20-kip load cell and special pull bars and grips. Heating was done with a Satec resistance clamshell furnace centered around the specimen load train. The test temperature was monitored by a chromel-alumel thermocouple spot-welded to an Inconel clip that was friction-clipped to the surface of the specimen at its midline.

All tests were conducted at a calibrated crosshead speed of 0.005 in/min until well past yield, at which time the speed was increased to 0.05 inch/min until fracture. Crosshead displacement was used to monitor specimen extension during the test.

The test specimens were machined with a minimum nominal diameter of 0.250 inch at the center of the gage length. The yield strength (YS) and ultimate tensile strength (UTS) were calculated by dividing the measured area into the 0.2% offset load and into the maximum test load, respectively. The values listed for the uniform and total elongation were obtained from plots that recorded load versus specimen extension and are based on a 1.5 inch nominal gage length. Reduction of area (RA) values were determined from post-test measurements of the necked specimen diameters using a calibrated blade micrometer and employing the following formula:

$$RA = 100\% * (A_O - A_f)/A_O \qquad (6\text{-}1)$$

After testing, each broken specimen was photographed end-on, showing the fracture surface, and lengthwise, showing the fracture location and local necking behavior.

6.2 RESULTS

Irradiated tensile test properties of Yield Strength (YS), Ultimate Tensile Strength (UTS), Reduction of Area (RA), Uniform Elongation (UE), and Total Elongation (TE) are presented in Table 6-1. A stress-strain curve for a 550°F base metal irradiated specimen is shown in Figure 6-1. This curve is typical of the stress-strain characteristics of all the tested specimens. Photographs of the necking behavior and fracture surfaces are given in Figures 6-2 through 6-4, and Figures 6-5 through 6-7, respectively.

6.3 IRRADIATED VERSUS UNIRRADIATED TENSILE PROPERTIES

Only unirradiated room temperature tensile test data for the base metal was available for comparison. The data from the first surveillance capsule is also shown. No trend could be identified from the data (see Tables 6-2 and 6-3). The conclusion is that the material properties, especially ductility, have not been significantly degraded.

TABLE 6-1: TENSILE TEST RESULTS FOR IRRADIATED RPV MATERIALS

	Specimen Number	Test Temp. (°F)	Yield[a] Strength (ksi)	Ultimate Strength (ksi)	Uniform Elongation (%)	Total Elongation (%)	Reduction of Area (%)
Base:	5C1	RT	72.5	94.7	13.4	23.9	71.0
	5C7	185	69.6	89.5	11.6	20.3	71.9
	5CJ	550	66.7	88.1	10.7	18.2	69.3
Weld:	5D3	RT	92.6	107.8	12.9	21.7	65.7
	5D4	185	87.9	104.7	12.2	19.8	62.0
	5DD	550	83.7	100.4	10.9	16.4	51.9
HAZ:	5EA	RT	81.9	104.6	10.2	17.8	67.8
	5EE	550	73.9	94.7	10.7	17.4	63.4

[a] Yield Strength is determined by 0.2% offset.

TABLE 6-2: COMPARISON OF UNIRRADIATED AND IRRADIATED TENSILE PROPERTIES AT ROOM TEMPERATURE

		Yield Strength (ksi)	Ultimate Strength (ksi)	Total Elongation (%)	Reduction of Area (%)
Base:	Unirradiated[b]	67.7	89.3	27.0	69.8
	1st Capsule	71.4	93.6	20.6	68.7
	2nd Capsule	66.7	88.1	18.2	69.3
Weld	1st Capsule	88.6	105.0	18.5	64.5
	2nd Capsule	92.6	107.8	21.7	65.7
HAZ:	1st Capsule	77.2	99.6	17.3	68.2
	2nd Capsule	81.9	104.6	17.8	67.8

[b] Values taken as average of data in the material certification reports.

TABLE 6-3: COMPARISON OF IRRADIATED TENSILE PROPERTIES AT 185°F

		Yield Strength (ksi)	Ultimate Strength (ksi)	Total Elongation (%)	Reduction of Area (%)
Base:	1st Capsule	68.5	88.7	20.7	72.5
	2nd Capsule	69.6	89.5	20.3	71.9
HAZ:	1st Capsule	73.2	94.0	16.3	69.1
Weld:	2nd Capsule	87.9	104.7	19.8	62.0

TABLE 6-4: COMPARISON OF IRRADIATED TENSILE PROPERTIES AT 550°F

		Yield Strength (ksi)	Ultimate Strength (ksi)	Total Elongation (%)	Reduction of Area (%)
Base:	1st Capsule	65.1	89.1	17.4	65.9
	2nd Capsule	66.7	88.1	18.2	69.3
Weld	1st Capsule	76.3	96.2	14.4	44.7
	2nd Capsule	83.7	100.4	16.4	51.9
HAZ:	1st Capsule	74.4	98.0	13.9	54.8
	2nd Capsule	73.9	94.7	17.4	63.4

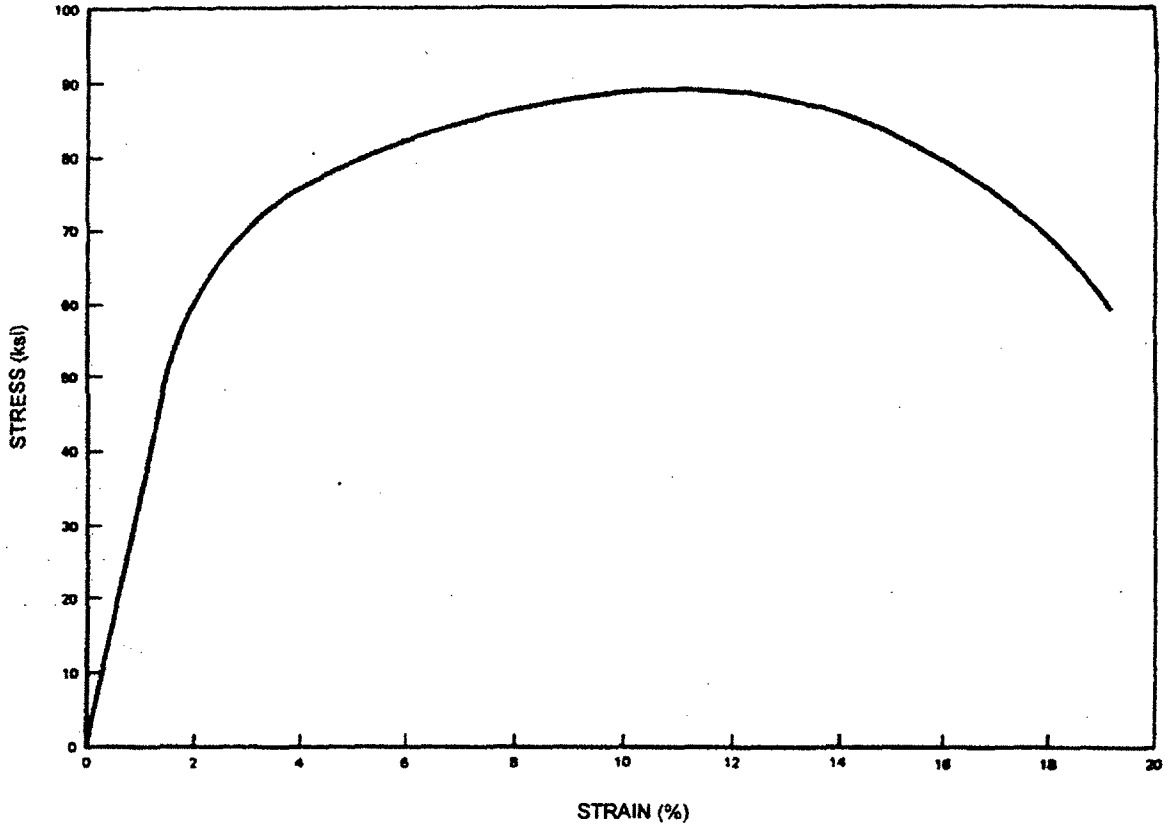

FIGURE 6-1. TYPICAL ENGINEERING STRESS-STRAIN FOR IRRADIATED RPV MATERIALS

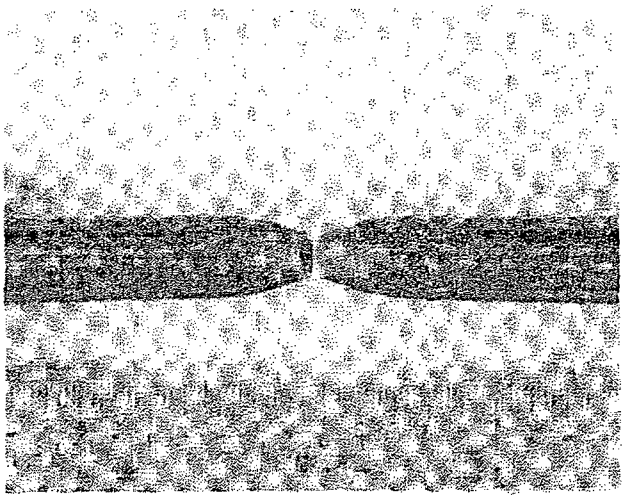

5C1 RT

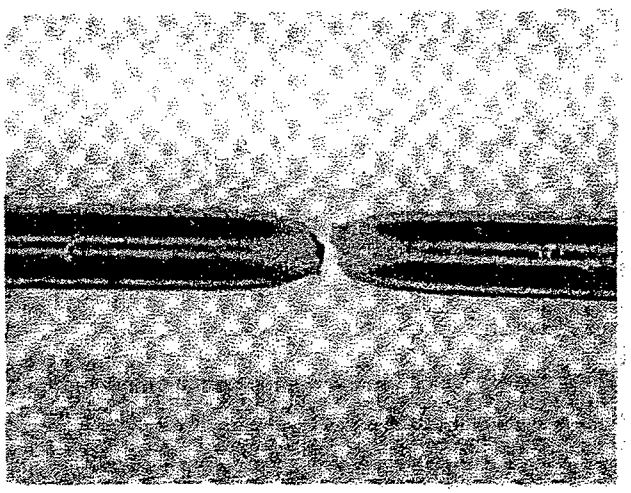

5CJ 550°F

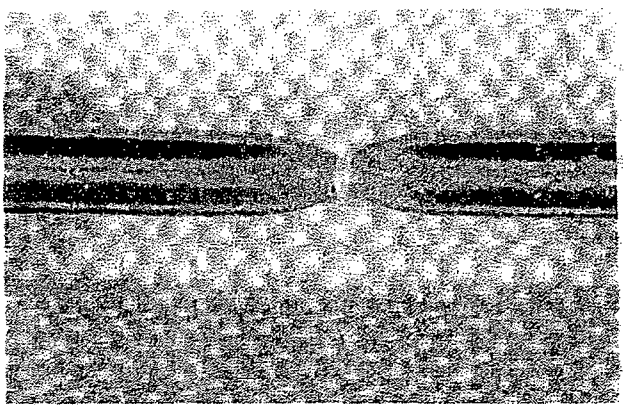

5C7 185°F

FIGURE 6-2: FRACTURE LOCATION AND NECKING BEHAVIOR FOR IRRADIATED BASE METAL TENSILE SPECIMENS

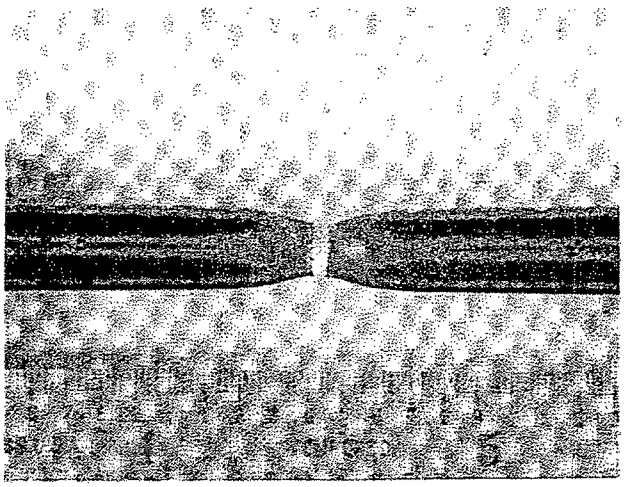

5D3 RT

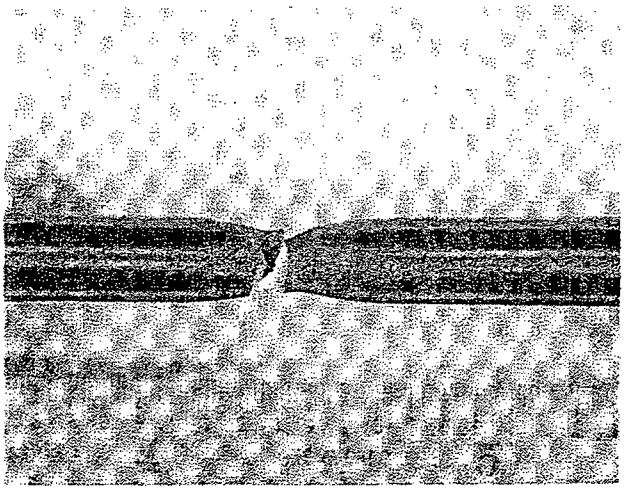

5DD 550°F

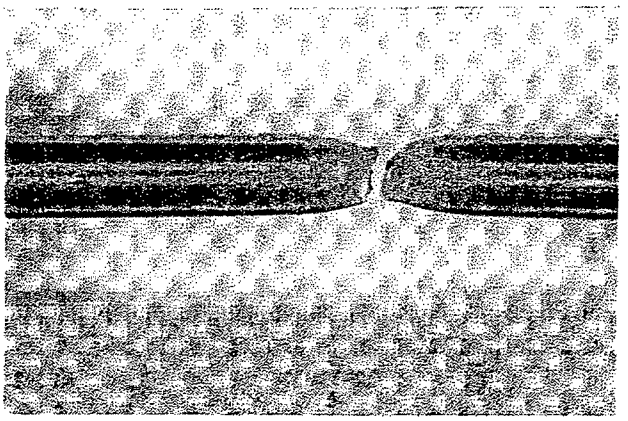

5D4 185°F

FIGURE 6-3: FRACTURE LOCATION AND NECKING BEHAVIOR FOR IRRADIATED WELD METAL TENSILE SPECIMENS

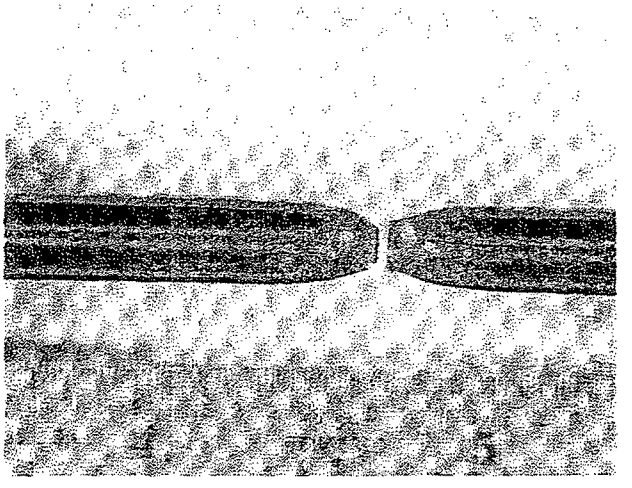

5EA RT°F

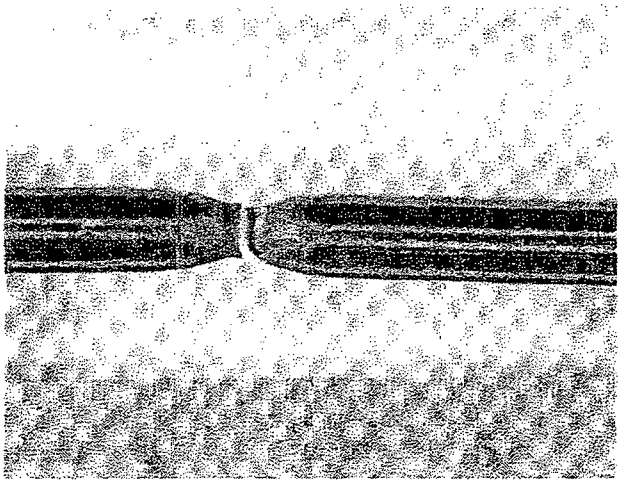

5EE 550°F

FIGURE 6-4: FRACTURE LOCATION AND NECKING BEHAVIOR FOR IRRADIATED HAZ TENSILE SPECIMENS

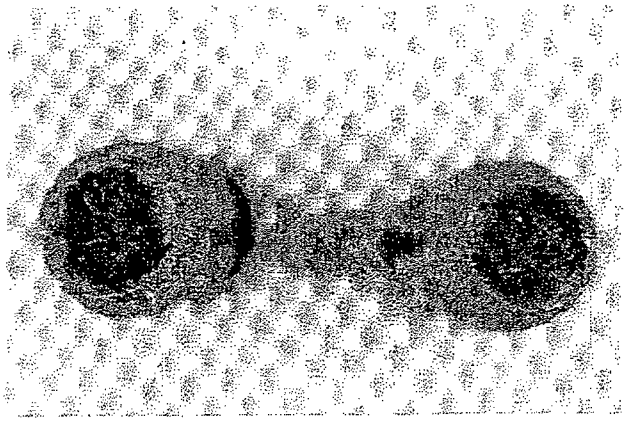

5C1 RT

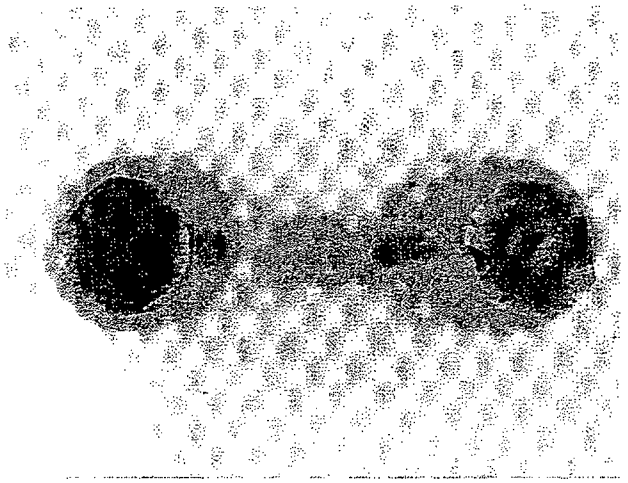

5CJ 550°F

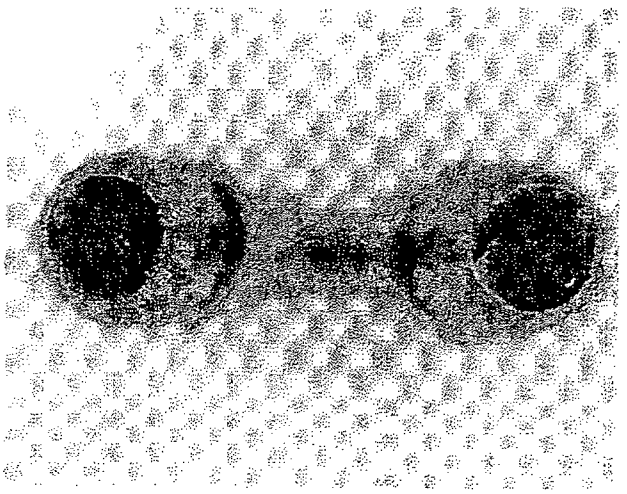

5C7 185°F

FIGURE 6-5: FRACTURE APPEARANCE FOR IRRADIATED BASE METAL TENSILE SPECIMENS

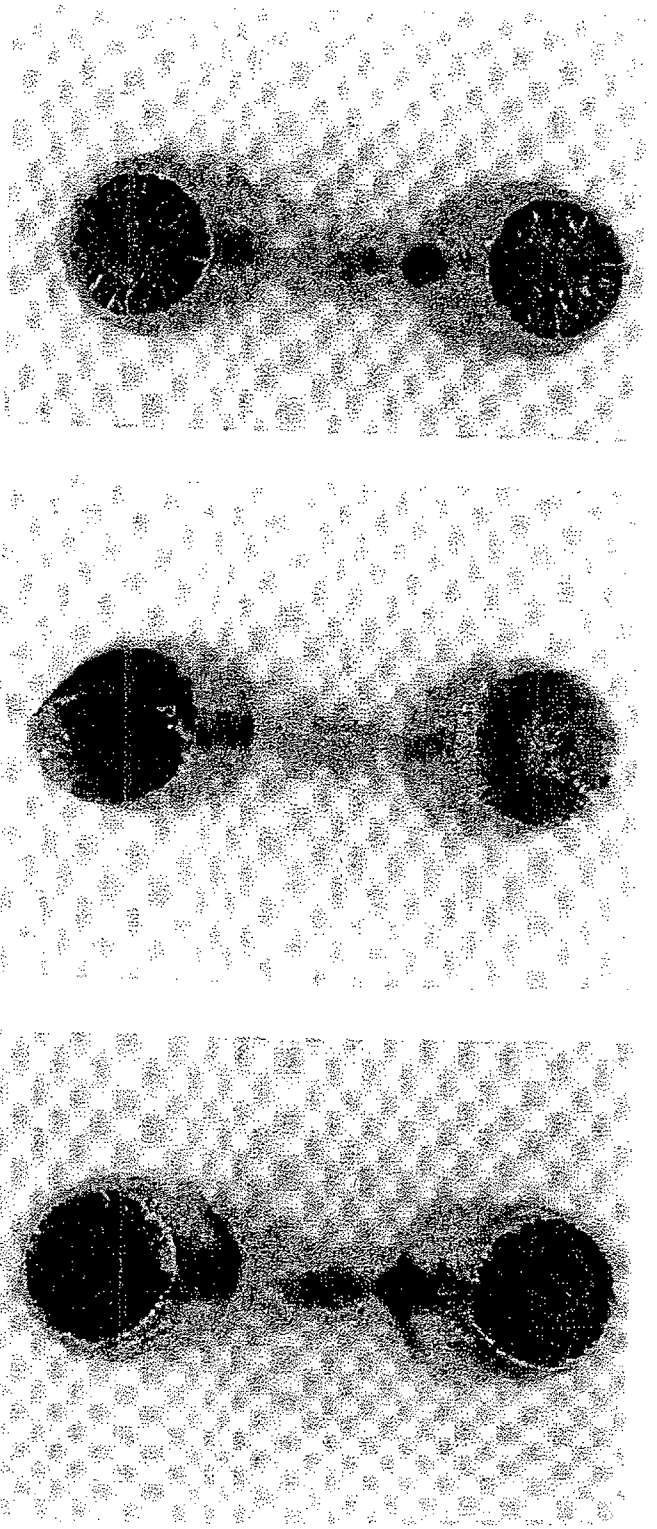

FIGURE 6-6: FRACTURE APPEARANCE FOR IRRADIATED WELD METAL TENSILE SPECIMENS

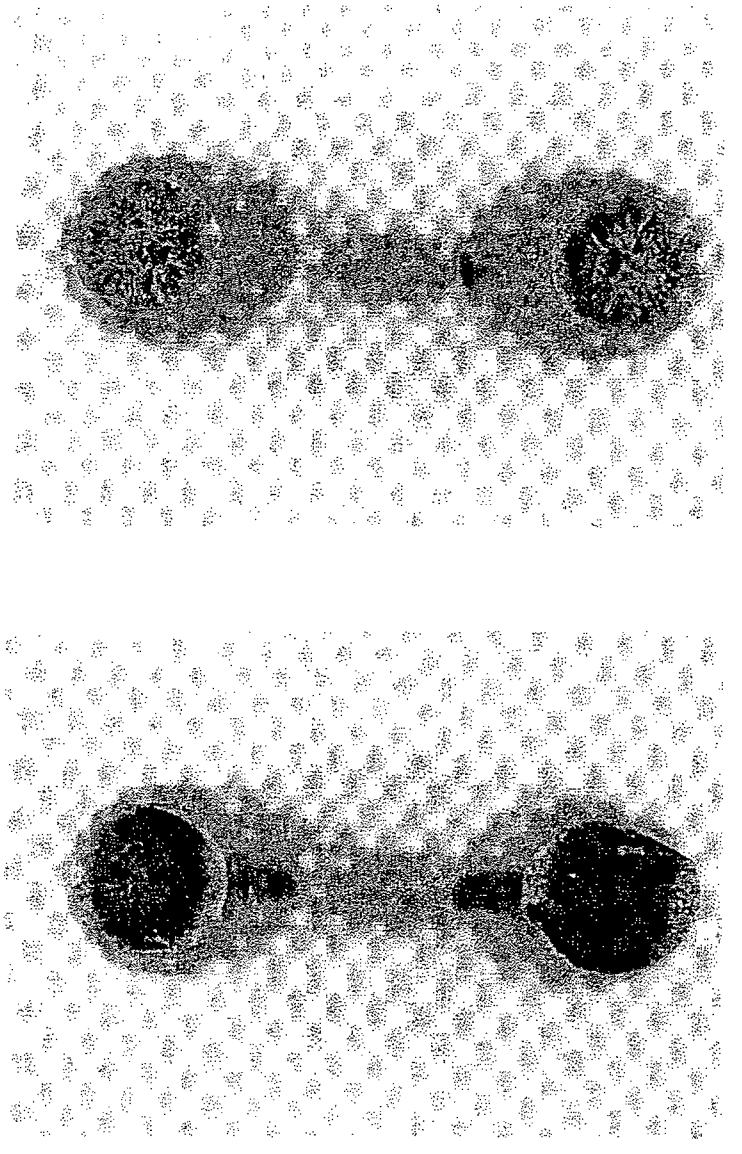

5EA RT°F

5EE 550°F

FIGURE 6-7: FRACTURE APPEARANCE FOR IRRADIATED HAZ TENSILE SPECIMENS

7. ADJUSTED REFERENCE TEMPERATURE AND UPPER SHELF ENERGY

The 32 EFPY peak fluence value of 1.81×10^{18} n/cm^2 defined in Section 4.3 is used to calculate the 32 EFPY 1/4 T peak fluence value of 1.31×10^{18} n/cm^2. The 32 EFPY 1/4 T fluence is used in this section to calculate adjusted reference temperatures (ARTs) and upper shelf energy (USE) decrease for the beltline materials.

7.1 ADJUSTED REFERENCE TEMPERATURE AT 32 EFPY

The effect on adjusted reference temperature (ART) due to irradiation in the beltline materials is determined according to the methods in Rev. 2 [7], as a function of neutron fluence and the element contents of copper (Cu) and nickel (Ni). The specific relationship from Rev. 2 [7] is:

$$ART = \text{Initial } RT_{NDT} + \Delta RT_{NDT} + \text{Margin} \quad (7\text{-}1)$$

where:

$$\Delta RT_{NDT} = CF \bullet f^{(0.28 - 0.1 \bullet \log f)} \quad (7\text{-}2)$$

$$Margin = 2\sqrt{\sigma_I^2 + \sigma_\Delta^2} \quad (7\text{-}3)$$

CF = chemistry factor from Tables 1 or 2 of Rev. 2 [7],
f = 1/4 T fluence (n/cm^2) divided by 10^{19},
σ_I = standard deviation on initial RT_{NDT}, which is taken to be 0°F.
σ_Δ = standard deviation on ΔRT_{NDT}, 28°F for welds and 17°F for base material, except that σ_Δ need not exceed 0.50 times the ΔRT_{NDT} value. If 2 or more sets of credible surveillance data are used, σ_Δ is 1/2 the above values.

The ART values are calculated based upon chemistry data as described in Table 7.1. Once two sets of surveillance capsule data are available, the CF values per Rev. 2 [7] can be adjusted to reflect the results. The method is described in Position 2.1 of Rev. 2 [7], and is summarized below.

7.2 SURVEILLANCE CF ADJUSTMENT

The surveillance CF adjustment is based on a least squares fit of the surveillance data to the ΔRT_{NDT} Equation 7-2, restated as:

$$\Delta RT_{NDT} = CF * FF$$

where FF is the fluence factor shown in (7-2).

The least squares approach uses the actual shifts of the 30° and 120° capsule Charpy specimens, combined with the fluence factors applicable to those capsule fluences.

$$CF = \frac{\left(Shift_{30°} * FF_{30°} + Shift_{120°} * FF_{120°}\right)}{\left(FF_{30°}{}^2 + FF_{120°}{}^2\right)} \qquad (7\text{-}4)$$

The values for Equation 7-4 are in Section 5.4.1 and Table 5-3:

The chemistry for the surveillance plate is 0.11% Cu and 0.60% Ni, which has a Chemistry Factor from Table 2 of Rev. 2 (Rev. 2 CF) of 74.0 (Section 5.4.1).

Location	Fluence	FF	Plate Shift	CF per Rev. 2
30°	2.6×10^{17}	0.205	-3.31	
120°	5.0×10^{17}	0.293	14.97	74.0

(For the weld material, no unirradiated data was available; therefore the CF could not be adjusted. The ART was calculated for the weld in accordance with Position 1 of Rev. 2 [7].)

Substituting these values into Equation 7-4 gives a CF of 29.4 based on the surveillance data. The surveillance CF is compared to the Rev. 2 CF to establish the adjustment of generic Rev. 2 predictions to actual plant conditions:

Plate adjustment = 29.4/74.0 = 0.40

7.3 APPLICATION OF CF ADJUSTMENT TO BELTLINE MATERIALS

The assumption made in applying the CF adjustments to the beltline materials is that the plant-specific conditions that affected the surveillance material shifts also affect the beltline material shifts. This is the same assumption made in Rev. 2, Position 2.1, for the case where the vessel weld chemistry differs significantly from the surveillance weld chemistry. Position 2.1 recommends that, when chemistries differ, the measured surveillance shifts be adjusted by the ratios of the beltline and surveillance material CFs, and then the least squares calculation be done to determine the adjusted beltline CF. The same basic approach is followed below.

In Position 2.1 of Rev. 2, it appears that the CF ratio approach is intended for the case where the beltline and surveillance base material and welds are the same heat, but chemistry results are significantly different. Here, in applying the CF ratio approach it is assumed that the surveillance CF adjustments should be applied to other beltline heats, as well as to the same beltline heats. This assumption and the recommendation in Position 2.1 have the same basis; that is that the CFs for different chemistries in the Rev. 2 tables are correct relative to one another. The result is that Equation 7-2 from Rev. 2 is multiplied by the surveillance adjustment (SA):

$$\Delta RT_{NDT} = CF * FF * SA \qquad (7\text{-}5)$$

Implicit in this approach is the assumption that there is a variable other than chemistry or fluence that is affecting the ΔRT_{NDT}. This assumption is feasible when evaluating a BWR, because nearly all of the data base used to develop Rev. 2 was PWR data, taken at significantly higher fluxes and fluences than are typical for BWRs. Fluxes may vary by a factor of 2 to 100, depending on the specific BWR and PWR compared. Fluence differences are large as well. There is also a temperature difference between PWR and BWR surveillance capsule irradiation conditions; BWR irradiation temperatures are 525°F to 535°F, 15°F to 35°F lower than PWR irradiation temperatures. One, or a combination of these variables may account for the quantity SA.

The ΔRT_{NDT} values for the beltline plate materials are calculated using Equation 7-5. The margin terms are taken as half the normal values, as permitted by Position 2.1 of Rev. 2.

7.4 ART VS. EFPY

Each beltline plate and weld ΔRT_{NDT} value is determined by multiplying the CF from Rev. 2 determined for the Cu-Ni content of the material, by the fluence factor for the EFPY being evaluated and the surveillance adjustment, if appropriate. The Initial RT_{NDT}, ΔRT_{NDT} and Margin are added to obtain the ART of the material. The 32 EFPY ART values for all of the beltline plates and several of the most limiting beltline welds are shown in Table 7-1. The ART for the limiting beltline material, Longitudinal Weld Heat 27204/12008, at 32 EFPY is 109°F. The ART for the limiting beltline plate, heat number C3376-2, at 32 EFPY is 56 °F. The ART vs. EFPY curve for the limiting beltline weld and plate materials is shown in Figure 7-1.

7.5 UPPER SHELF ENERGY AT 32 EFPY

Unirradiated Upper Shelf data were not available for all of the material heats. Due to the lack of specific pre-operational USE data, FitzPatrick has been evaluated to verify that the BWR Owners' Group Equivalent Margin Analyses are applicable. The calculations in Tables 7-2 and 7-3 show that the equivalent margin analyses are applicable. The Equivalent Margin Analyses demonstrate that the 10 CFR 50, Appendix G safety requirements are satisfactorily met for FitzPatrick. The Owners' Group Program Report [16] was submitted to the NRC in December 1993 and approved by SER on December 8, 1993.

TABLE 7-1: 32 EFPY ART VALUES

BELTLINE ART VALUES FOR FITZPATRICK

Lower Intermediate
Thickness = 5.375 inches

Lower Intermediate
32 EFPY Peak I.D. fluence = 1.81E+18 n/cm^2 [a]
32 EFPY Peak 1/4 T fluence = 1.31E+18 n/cm^2 [a]

Lower
Weld Thickness = 5.375 inches (Girth)
Plate Thickness= 6.375 inches

Lower
32 EFPY Peak I.D. fluence = 1.61E+18 n/cm^2 [a]
32 EFPY Peak 1/4 T weld fluence = 1.17E+18 n/cm^2 [a]
32 EFPY Peak 1/4 T plate fluence = 1.10E+18 n/cm^2 [a]

COMPONENT	Weld Type	HEAT OR HEAT/LOT	%Cu	%Ni	CF	Adjusted CF	Initial RTndt °F	32 EFPY Δ RTndt °F	σ_I	σ_Δ	Margin °F	32 EFPY Shift °F	32 EFPY ART °F
PLATES:													
Lower													
G-3415-1R		C3394-1	0.11	0.56	73.6	29.2	-10	12.8	0.0	6.4[b]	12.8	26	16
G-3415-3		C3376-2	0.13	0.60	91	36.2	24	15.8	0.0	7.9[b]	15.8	32	56
G-3415-2		C3103-2	0.14	0.57	99	39.3	-2	17.2	0.0	8.5[b]	17.0	34	32
Lower-Interm.													
G-3413-7		C3368-1	0.12	0.50	81	32.2	-10	15.2	0.0	7.6[b]	15.2	30	20
G-3414-2		C3278-2	0.11	0.60	74	29.4	-10	13.9	0.0	6.95[b]	13.9	28	18
G-3414-1		C3301-1	0.18	0.57	131	52.1	-18	24.7	0.0	8.5[b]	17.0	42	24
WELDS:													
Lower Long.	2-233	27204/12008 Flux 3774	0.219	0.996	231	231	-48	101	0.0	28.0	56	157	109
Lower Intermed. Long.	1-233	13253/12008 Flux 3774	0.210	0.873	208.7	208.7	-50	99	0.0	28.0	56	155	105
Girth	1-240	305414 Flux 3947	0.337	0.609	209.1	209.1	-50	91.4	0.0	28.0	56	150	100

[a] Includes effects of 105% power uprate

[b] Reduced σ_Δ based on use of credible data

TABLE 7-2: PLATE EQUIVALENT MARGIN ANALYSIS

PLANT APPLICABILITY VERIFICATION FORM
FOR FITZPATRICK - BWR 4/MK I - Including Uprated Power Condition

BWR/3-6 PLATE

Surveillance Plate USE:

%Cu = 0.11

1st Capsule Fluence = 2.6×10^{17} n/cm^2
2nd Capsule Fluence = 5.0×10^{17} n/cm^2

Unirradiated to 1st Capsule Measured % Decrease = 0.37 (Charpy Curves)
Unirradiated to 2nd Capsule Measured % Decrease = 9.2 (Charpy Curves)

1st Rev. 2 Predicted % Decrease = 9 (Rev. 2, Figure 2)
2nd Rev. 2 Predicted % Decrease = 10 (Rev. 2, Figure 2)

Limiting Beltline Plate USE:

%Cu = 0.18

32 EFPY 1/4 T Fluence = 1.31×10^{18} n/cm^2

Rev. 2 Predicted % Decrease = 18 (Rev. 2, Figure 2)

Adjusted % Decrease = N/A (Rev. 2, Position 2.2)

18 % ≤ 21%, so vessel plates are bounded by equivalent margin analysis

TABLE 7-3: WELD EQUIVALENT MARGIN ANALYSIS

PLANT APPLICABILITY VERIFICATION FORM
FOR FITZPATRICK - BWR 4/MK I - Including Uprated Power Condition

BWR/2-6 WELD

Surveillance Weld USE:

%Cu = 0.29

1st Capsule Fluence = 2.6×10^{17} n/cm^2
2nd Capsule Fluence = 5.0×10^{17} n/cm^2

Unirradiated to 1st or 2nd Capsule Measured % Decrease = Unknown
1st to 2nd Capsule Measured % Decrease = -12.1 (Charpy Curves)

1st Rev 2 Predicted % Decrease = 19 (Rev. 2, Figure 2)
2nd Rev 2 Predicted % Decrease = 22 (Rev. 2, Figure 2)

Limiting Beltline Weld USE:

%Cu = 0.33

32 EFPY 1/4 T Fluence = 1.31×10^{18} n/cm^2

Rev 2 Predicted % Decrease = 29 (Rev. 2, Figure 2)

Adjusted % Decrease = N/A (Rev. 2, Position 2.2)

29 % $\leq$ 34%, so vessel welds are bounded by equivalent margin analysis

Note: the limiting beltline weld case (0.33 wt% Cu @ 1.31×10^{18} n/cm^2) is not physically possible. However, it represents a worst case condition

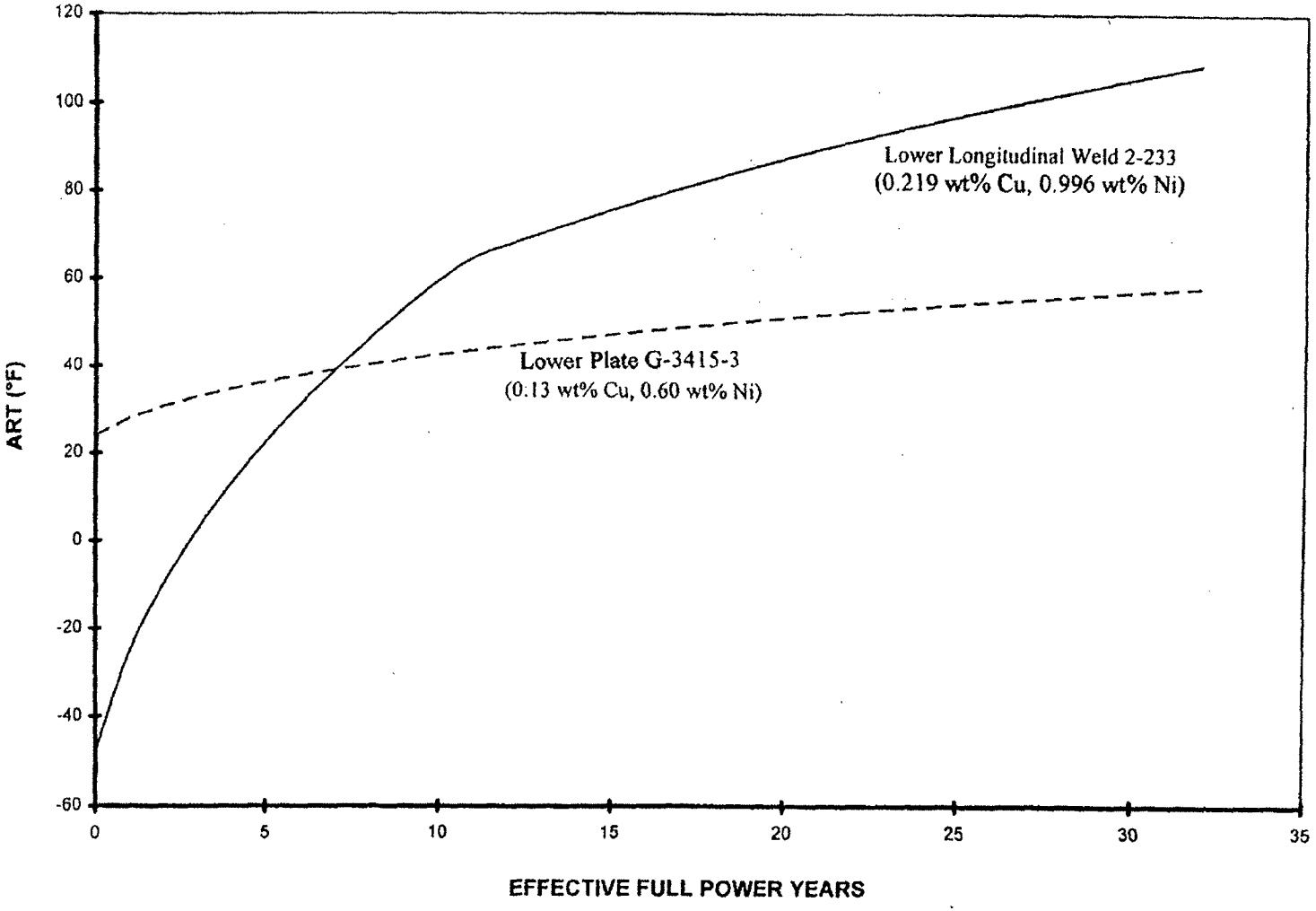

FIGURE 7-1. ADJUSTED REFERENCE TEMPERATURE VS. EFPY FOR LIMITING BELTLINE PLATE AND WELD

8. PRESSURE-TEMPERATURE CURVES

8.1 BACKGROUND

Nuclear Regulatory Commission (NRC) 10CFR50 Appendix G [1] specifies fracture toughness requirements to provide adequate margins of safety during operation to which the pressure-retaining component pressure boundary may be subjected over its service lifetime. The ASME Code (Appendix G of Section XI of the ASME Code) forms the basis for the requirements of 10CFR50 Appendix G. The limits for pressure and temperature are required by 10CFR50 Appendix G for three categories of operation: (a) hydrostatic pressure tests and leak tests, (b) core not critical heatup/cooldown, and (c) core critical operation. The condition that results in the highest temperature for the limiting material determines the minimum temperature requirement for the vessel.

In all cases, the applicable temperature is the greater of the 10CRF50 minimum temperature requirement and the ASME Appendix G limits. A summary of the requirements is as follows:

Operating Condition and Pressure	Minimum Temperature Requirement, °F
I. Hydrostatic Pressure Test & Leak Test (Core is Not Critical) - Curve A	
1. At ≤ 20% of preservice hydrotest pressure	Larger of ASME Limits or highest of closure flange region initial RT_{NDT} + 60°F*
2. At > 20% of preservice hydrotest pressure	Larger of ASME Limits or highest of closure flange region initial RT_{NDT} + 90°F

* 60°F adder is included by GE as an additional conservatism as described in Section 8.3

Operating Condition and Pressure	Minimum Temperature Requirement, °F
II. Normal operation (heat-up and cool-down), including anticipated operational occurrences	
A. Core not critical - Curve B	
1. At ≤ 20% of preservice hydrotest pressure	Larger of ASME Limits or highest of closure flange region initial RT_{NDT} + 60°F*
2. At > 20% of preservice hydrotest pressure	Larger of ASME Limits or highest of closure flange region initial RT_{NDT} + 120°F
B. Core critical - Curve C	
1. At ≤ 20% of preservice hydrotest pressure with the water level within the normal range for power operation.	Larger of ASME Limits + 40°F or A.1
2. At > 20% of preservice hydrotest pressure	Larger of ASME Limits + 40°F or A.2 + 40°F or the minimum permissible temperature for the inservice system hydrostatic pressure test

* 60°F adder is included by GE as an additional conservatism as described in Section 8.3

Note: The core critical operation curve is identical to the core not critical heatup/cooldown curve but shifted by 40°F, as required in 10CFR50, Appendix G [1]. Hence, the methods used for determining the core not critical heatup/cooldown curves apply to the core critical curves, as well.

There are three vessel regions that affect the operating limits: the closure flange region, the core beltline region, and the remainder of the vessel, or non-beltline regions. The closure flange region limits are controlling at lower pressures primarily because of 10CFR50, Appendix G requirements. The non-beltline and beltline region operating limits are evaluated according to procedures in 10CFR50, Appendix G [1], ASME Boiler and Pressure Vessel Code, Section XI, Appendix G [2], and Welding Research Council (WRC) Bulletin 175 [10]. The beltline region minimum temperature limits are adjusted to account for vessel irradiation.

The P-T curves for the non-beltline region were conservatively developed for a large BWR/6 (nominal inside diameter of 251 inches). The analysis is considered appropriate for FitzPatrick as the FitzPatrick specific values are bounded by this generic analysis. The generic

value was adapted to the conditions at FitzPatrick by using the specific RT_{NDT} values for the FitzPatrick reactor pressure vessel (RPV). The presence of nozzles and control rod (CRD) penetration holes of the upper vessel and bottom head, respectively, has made the analysis different from a shell analysis such as the beltline. This was the result of the stress concentrations and higher thermal stresses for certain transient conditions, experienced by the upper vessel and the bottom head.

P-T curves are provided for 32 EFPY. The 32 EFPY curves are effective through the end-of-life (EOL). The 32 EFPY curves are provided in Figures 8-1, 8-2 and 8-3. The corresponding numerical values for the curves are given in Table 8-1. The P-T curves for 24 EFPY are shown in Appendix B, Figures B-1 through B-3.

Under certain conditions, the minimum bottom head temperature can be significantly cooler than the beltline or closure flange region. These conditions can occur when the recirculation pumps are operating at low speed (or off), and during water injection through the control rod drives. To account for these circumstances, individual temperature limits for the bottom head were established.

8.2 P-T CURVE METHODOLOGY

8.2.1 Non-Beltline Regions

Non-beltline regions are defined as the vessel locations that are remote from the active fuel such that the neutron fluence is not sufficient to cause any shift of RT_{NDT}. Non-beltline components include the nozzles, the closure flanges, some shell plates, the top and bottom head plates and the control rod drive (CRD) penetrations. Detailed stress analyses of the non-beltline components were performed for the BWR/6 specifically for the purpose of fracture toughness analysis. The analyses took into account all mechanical loading and anticipated thermal transients. Transients considered included 100°F/hr startup and shutdown, SCRAM, loss of feedwater heaters or flow, loss of recirculation pump flow, and all transients involving emergency core cooling injections. Primary membrane and bending stresses and secondary membrane and bending stresses due to the most severe of these transients were used according to the ASME Code [2] to develop plots of allowable pressure (P) versus temperature relative to the reference temperature ($T - RT_{NDT}$). Plots were developed for the two most limiting BWR/6 components; the feedwater nozzle and the CRD penetration (bottom head). All other components in the non-beltline regions are categorized under one of these two components.

The non-beltline curves are based on the most limiting (conservative) properties of either the upper vessel region or the bottom head. The non-beltline curves are shifted based on the most limiting initial RT_{NDT} values for the appropriate non-beltline components; the initial RT_{NDT} values are listed in Table 3-2. For the case of Curve A, pressure test for the non-beltline region, the recirculation inlet nozzle (#N2) is the limiting case. Curve B, for core not critical heatup/cooldown of the non-beltline region is also based on the recirculation inlet nozzle being the limiting case.

For pressures below 20% of preservice hydrostatic test pressure (312 psig) and with full bolt preload, the closure flange region metal temperature is required to be at RT_{NDT} or greater as described in Section 8.3. At low pressure, the ASME Code [2] allows the beltline and bottom head regions to experience even lower metal temperatures than the flange region RT_{NDT}. However, temperatures should not be permitted to be lower than 68°F for the reason discussed below.

The shutdown margin is calculated for a water temperature of 68°F. Shutdown margin is the quantity of reactivity needed for a reactor core to reach criticality with the strongest-worth control rod frilly withdrawn and all other control rods fully inserted. Although it may be possible to safely allow the water temperature to fall below this 68°F limit, further extensive calculations would be required to justify a lower temperature. However, the boltup temperature as described in Section 8.3 is at 90°F. Because the water temperature is currently limited to a minimum of 90°F, the metal temperature should not fall below this limit while fuel is in the vessel. The 90°F limit applies when the head is on and tensioned, and also, when the head is off. (When fuel has been removed from the vessel, the head is tensioned, and the pressure is below 20 psig, the limiting vessel temperature is equal to the limiting RT_{NDT} of the vessel materials. This limiting RT_{NDT} is 30°F. When the head is not tensioned and fuel is not in the vessel, the requirements of 10CFR50 Appendix G [1] do not apply, and there are no limits on the vessel temperatures.

8.2.2 Pressure Test - Non-Beltline, Curve A (Using Bottom Head)

In the finite element analysis, the BWR/6 CRD penetration region was modeled to compute the local stresses for determination of the stress intensity factor, K_I. The results of that computation were K_I = 154.3 ksi-in$^{1/2}$ for an applied pressure of 1593 psig (1563 psig preservice hydrotest pressure plus 30 psig hydrostatic pressure at the bottom of the vessel). The computed value of ($T - RT_{NDT}$) was 161°F.

The method to solve for $(T - RT_{NDT})$ for a specific K_I is based on the curve in Figure G-2210-1 in ASME Appendix G [2]:

$$(T - RT_{NDT}) = \ln [K_I - 26.78)/1.223] / 0.0145 - 160$$

$$(T - RT_{NDT}) = \ln [(154.3 - 26.78) / 1.223] / 0.0145 - 160$$

$$(T - RT_{NDT}) = 161°F$$

The generic curve was generated by scaling 154.3 ksi-in$^{1/2}$ by the nominal pressures and calculating the associated $(T - RT_{NDT})$:

CRD Penetration K_I and $(T - RT_{NDT})$ as a Function of Pressure

Nominal Pressure (psig)	K_I (ksi-in$^{1/2}$)	$T - RT_{NDT}$ (°F)
1563	154.3	161
1400	138.2	151
1200	118.5	138
1000	98.7	121
800	79.0	99
600	59.2	66
400	39.5	1

The highest RT_{NDT} for the bottom head plates and welds is 10°F, as shown in Table 3-2. The generic curve is applied to the FitzPatrick bottom head by shifting the P vs. $(T - RT_{NDT})$ values above to reflect the RT_{NDT} value of 10°F.

The P-T curve is dependent on the K_I value calculated, which is proportional to the stress and the crack depth according to the relationship:

$$K_I \propto \sigma \bullet (\pi a)^{1/2} \qquad (8\text{-}1)$$

The stress is proportional to R/t and, for the P-T curves, crack depth, a, is t/4. Thus, K_I is proportional to $R/t^{1/2}$. The generic curve value of $R/t^{1/2}$, based on the generic BWR/6 bottom head dimensions, is:

$$\text{Generic } R/t^{1/2} = 138.2/8^{1/2} = 48.9 \text{ inch}^{1/2} \quad (8\text{-}2)$$

The FitzPatrick specific bottom head dimensions are R = 110.50 inches and t = 6.813 inches, resulting in:

$$\text{FitzPatrick specific } R/t^{1/2} = 110.50/6.813^{1/2} = 42.3 \text{ inch}^{1/2} \quad (8\text{-}3)$$

Since the generic value of $R/t^{1/2}$ is larger than that for FitzPatrick, the generic P-T curve is conservative when applied to the FitzPatrick bottom head.

8.2.3 Core Not Critical Heatup/Cooldown - Non-Beltline Curve B (Using Feedwater Nozzle/Upper Vessel Region)

The feedwater nozzle was selected to represent non-beltline components for fracture toughness analysis because the thermal conditions are the most severe experienced in the vessel. In addition to the more severe pressure and piping load stresses resulting from the nozzle discontinuity, the feedwater nozzle region experiences relatively cold feedwater flow in hotter vessel coolant.

Stresses are taken from finite element analysis done specifically for fracture toughness analysis purposes. Analyses were performed for all feedwater nozzle transients that involve rapid temperature changes. The most severe of these was normal operation with cold 40°F feedwater injection.

The non-beltline curves based on feedwater nozzle limits were calculated according to the methods for nozzles in Appendix 5 of the Welding Research Council (WRC) Bulletin 175 [10].

The stress intensity factor for a nozzle flaw under primary stress conditions is given in WRC Bulletin 175 Appendix 5 by the expression for a flaw at a hole in a flat plate:

$$K_{IP} = SF \bullet \sigma \bullet (\pi a)^{1/2} \bullet F(a/r_n) \quad (8\text{-}4)$$

where: SF is the safety factor applied per WRC Bulletin 175 recommended ranges, and $F(a/r_n)$ is the shape correction factor.

Finite element analysis of a nozzle corner flaw was performed to determine appropriate values of $F(a/r_n)$ for Equation 8-4. These values are shown in Figure A5-1 of WRC Bulletin 175 [10].

The stresses used in Equation 8-4 were taken from BWR/6 design stress reports for the feedwater nozzle. The stresses considered are primary membrane, σ_{pm} and primary bending, σ_{pb}. Secondary membrane, σ_{sm} and secondary bending, σ_{sb} stresses are included in the total K_I by using ASME Appendix G [2] methods for secondary portion, K_{Is}:

$$K_{Is} = M_m \bullet (\sigma_{sm} + 2/3 \bullet \sigma_{sb}) \quad (8\text{-}5)$$

In the case where the total stress exceeded yield stress, a plasticity correction factor was applied based on the recommendations of WRC Bulletin 175 Section 5.C.3 [10). However, the correction was not applied to primary membrane stresses. K_{Ip} and K_{Is} are added to obtain the total value of stress intensity factor, K_I.

The safety factors applied to primary stresses were 1.3 for pressure test conditions and 1.6 for core not critical heatup/cooldown conditions.

Once K_I was calculated, the following relationship was used to determine $(T - RT_{NDT})$. The highest RT_{NDT} for the appropriate non-beltline components was then used to establish the P-T curves.

$$(T - RT_{NDT}) = \ln [K_I - 26.78) / 1.223) / 0.0145 - 160 \quad (8\text{-}6)$$

8.2.4 Example Core Not Critical Heatup/Cooldown Calculation for Feedwater Nozzle/Upper Vessel Region

The non-beltline core not critical heatup/cooldown curve was based on the feedwater nozzle generic analysis, where feedwater injection of 40°F into the vessel while at operating conditions (551.4°F and 1050 psig) was the limiting normal or upset condition from a brittle fracture perspective. The feedwater nozzle corner stresses were obtained from finite element analysis. These stresses, and other inputs used in the generic calculations, are shown below:

σ_{pm} = 20.49 ksi	σ_{sm} = 16.19 ksi	σ_{ys} = 45.0 ksi	t = 7.5 inch
σ_{pb} = 0.22 ksi	σ_{sb} = 19.04 ksi	a = 1.88 inch	r_n = 6.94 inch

In this case, the total stress, 55.94 ksi, exceeds the yield stress σ_{ys}, so the correction factor, R, is calculated according to the following equation:

$$R = [\sigma_{ys} - \sigma_{pm} + ((\sigma_{total} - \sigma_{ys}) / 30))/ (\sigma_{total} - \sigma_{pm}) \quad (8\text{-}7)$$

For the stresses given, the Ratio, R = 0.70. Therefore, all the stresses are adjusted by the factor 0.70, except for σ_{pm}. The resulting stresses are:

σ_{pm} = 20.49 ksi σ_{sm} = 11.33 ksi

σ_{pb} = 0.15 ksi σ_{sb} = 13.33 ksi

The value of M_m from Figure G-2214-1 [2], was based on a thickness of 7.5 inches, hence, $t^{1/2}$ = 2.74. The stress to yield ratio, σ/σ_{ys}, was conservatively assumed to be 1.0. The resulting value obtained was:

M =2.84

The value $F(a/r_n)$ is taken from Figure A5-1 of WRC Bulletin 175 for an a/r_n of 0.27.

$F(a/r_n)$ =1.6

K_{Ip} is calculated from Equation 8-4:

$$K_{Ip} = 1.6 \bullet (20.49 + 0.15) \bullet (\pi \bullet 1.88)^{1/2} \bullet 1.6$$

$$K_{Ip} = 128.4 \text{ ksi-in}^{1/2}$$

K_{Is} is calculated from Equation 8-5:

$$K_{Is} = 2.84 \bullet (11.33+2/3 \bullet 13.33)$$

$$K_{Is} = 57.4 \text{ ksi-in}^{1/2}$$

The total K_I is therefore 186 ksi-$in^{1/2}$.

The total K_I is substituted into Equation 8-6 to solve for $(T - RT_{NDT})$:

$$(T - RT_{NDT}) = \ln[(186 - 26.78) / 1.223) / 0.0145 - 160$$

$$(T - RT_{NDT}) = 176°F$$

The generic curve was generated by scaling the stresses used to determine the K_I. The primary stresses were scaled by the nominal pressures, while the secondary stresses were scaled by temperature difference of the 40°F water injected into the hot reactor vessel nozzle. In the base case that yielded a K_I value of 186 ksi-in$^{1/2}$, the pressure is 1050 psig and the hot reactor vessel temperature is 551.4°F. Since the reactor vessel temperature follows the saturation temperature curve, the secondary stresses are scaled by ($T_{saturation}$ - 40) / (551.4 - 40). From the K_I the associated (T - RT_{NDT}) can be calculated:

Feedwater Nozzle K_I and (T - RT_{NDT}) as a Function of Pressure

Nominal Pressure (psig)	**Saturation Temp. (°F)**	**K_I (ksi-in$^{1/2}$)**	**(T-RT_{NDT}) (°F)**
1563	604	226	191
1400	588	213	187
1200	557	198	181
1050	551	186	176
1000	546	182	174
800	520	166	167
600	489	146	156
400	448	115	135

The highest non-beltline RT_{NDT} for the feedwater region component (nozzle #N2) at FitzPatrick is 30°F as shown in Table 3-2. The generic curve is applied to the FitzPatrick upper vessel by shifting the P vs. (T-RT_{NDT}) values above to reflect the RT_{NDT} value of 30°F.

8.2.5 Core Beltline Region

The pressure-temperature (P-T) operating limits for the beltline region are determined according to the ASME Code. As the beltline fluence increases with the increase in operating life, the P-T curves shift to a higher temperature.

The stress intensity factors (K_I), calculated for the beltline region according to ASME Code Appendix G procedures [2], were based on a combination of pressure and thermal stresses for a 1/4 T flaw in a flat plate. The pressure stresses were calculated using thin-walled cylinder equations. Thermal stresses were calculated assuming the through-wall temperature distribution of

a flat plate; values were calculated for 100°F/hr thermal gradient. The shift value of the most limiting ART material was used to adjust the RT_{NDT} values for the P-T limits.

8.2.6 Beltline Region - Pressure Test

The methods of ASME Code Section III, Appendix G [2] are used to calculate the pressure test beltline limits. The vessel shell, with an inside radius (R) to minimum thickness (t_{min}) ratio of 15, is treated as a thin-walled cylinder. The maximum stress is the hoop stress, given as:

$$\sigma_m = PR/t_{min} \quad (8\text{-}8)$$

The stress intensity factor, K_{Im}, is calculated using Figure G-2214-1 of the ASME Code, Appendix G [2], accounting for the proper ratio of stress to yield strength. Figure G-2214-1 was taken from Welding Research Council (WRC) Bulletin 175 [10], based on a 1/4 T radial flaw with a six-to-one aspect ratio (length of 1.5T). The flaw is oriented normal to the maximum stress direction, in this case a vertically oriented flaw. This orientation is used even in the case where the circumferential weld is the limiting beltline material, as traditionally required by the NRC in the past.

The calculated value of K_{Im} for pressure test is multiplied by a safety factor (SF) of 1.5, per ASME Appendix G [2] for comparison with K_{IR}, the material fracture toughness. A safety factor of 2.0 is used for the core not critical and core critical conditions.

The relationship between K_{Ir} and temperature relative to reference temperature ($T - RT_{NDT}$) is shown in Figure G-2210-1 of ASME Appendix G [2], represented by the relationship:

$$K_{Im} \bullet SF = K_{Ir} = 1.223 \exp[0.0145 (T - RT_{NDT} + 160)] + 26.78 \quad (8\text{-}9)$$

This relationship is derived in the Welding Research Council (WRC) Bulletin 175 [10] as the lower bound of all dynamic fracture toughness and crack arrest toughness data. This relationship provides values of pressure versus temperature (from K_{Ir} and ($T - RT_{NDT}$), respectively).

For the pressure test curve, a stress intensity factor, K_{It}, is added for a heatup/cooldown rate of 20°F/hr to consider operating conditions. For the core not critical and core critical condition curves, a stress intensity factor is added for a heatup/cool down rate of 100°F/hr. The K_{It} calculation for a heatup/cooldown rate of 100°F/hr is described in Sections 8.2.8 and 8.2.9.

8.2.7 Calculations for the Beltline Region - Pressure Test

This sample calculation is for a pressure test pressure of 1128 psig for 32 EFPY. The following inputs were used in the beltline limit calculation:

Adjusted RT_{NDT}	A = 109 °F
(Based on ART values in Table 7-1)	
Vessel Height,	H = 825.2 inches
Bottom of Active Fuel Height,	B = 208.6 inches
Vessel Radius (to inside of clad),	R = 110.375 inches
Vessel Thickness (without clad),	t = 5.375 inches
Beltline Material Yield Strength,	σ_y = 50 ksi
Operating temperature at P,	T = (calculated) °F

Pressure is calculated to include hydrostatic pressure for a full vessel:

$$P = 1128 \text{ psi} + (H - B) \bullet 0.0361 \text{ psi/inch} = P \text{ psig} \quad (8\text{-}10)$$

$$= 1128 + (825.2 - 208.6) \bullet 0.0361 = 1150 \text{ psig}$$

Pressure stress:

$$\sigma = PR/t \quad (8\text{-}11)$$

$$= 1.150 \bullet 110.375 / 5.375 = 23.62 \text{ ksi}$$

The factor M_m (=2.23) depends on (σ/σ_y) and $t^{1/2}$ and is determined from Figure G-2214-1 of the ASME Code, Appendix G [2]. The stress intensity factor for the pressure stress is $K_{IM} = M_m \bullet \sigma$. The stress intensity factor for the thermal stress, K_{It}, is calculated as described in Section 8.3.8 below except that the value of "G" is 20°F/hr instead of 100°F/hr.

Equation 8-9 can be rearranged, and $1.5 \bullet K_{Im}$ substituted for K_{Ir}, to solve for $(T - RT_{NDT})$. Using ASME Appendix G, Fig. G-2210-1 [2], K_{Im} = 52.67, and K_{It} = 1.76 for a 20°F/hr heatup/cooldown rate:

$$(T - RT_{NDT}) = \ln[(1.5 \bullet K_{Im} + K_{It} - 26.78) / 1.223] / 0.0145 - 160 \quad (8\text{-}12)$$

$$= \ln[(1.5 \bullet 52.67 + 1.76 - 26.78) / 1.223] / 0.0145 - 160$$

$$= 101°F$$

T can be calculated by adding the adjusted RT_{NDT}:

$T = 101 + 109 = 210°F$ $P = 1128$ psig

8.2.8 Beltline Region - Core Not Critical Heatup/Cooldown

The beltline curves for core not critical heatup/cooldown conditions are influenced by pressure stresses and thermal stresses, according to the relationship in ASME Appendix G [2]:

$$K_{Ir} = 2.0 \bullet K_{Im} + K_{It} \quad (8\text{-}13)$$

where K_{Im} is primary membrane K due to pressure and K_{It} is radial thermal gradient K due to heatup/cooldown.

The pressure stress intensity factor K_{Im} is calculated by the method described above, the only difference being the larger safety factor applied. The thermal gradient stress intensity factor calculation is described below.

The thermal stresses in the vessel wall are caused by a radial thermal gradient that is created by changes in the adjacent reactor coolant temperature in heatup or cooldown conditions. The stress intensity factor is computed by multiplying the coefficient M_t from Figure G-2214-2 of ASME Appendix G [2] by the through-wall temperature gradient ΔT_w, given that the temperature gradient has a through-wall shape similar to that shown in Figure G-2214-3 of ASME Appendix G [2].

The relationship used to compute the through-wall ΔT_w is based on one-dimensional heat conduction through an insulated flat plate:

$$\partial^2 T(x,t) / \partial x^2 = 1/\beta \, (\partial T(x,t)/ \partial t) \quad (8\text{-}14)$$

where T(x,t) is temperature of the plate at depth x and time t, and β is the thermal diffusivity.

The maximum stress will occur when the radial thermal gradient reaches a quasi-steady state distribution, so that $\partial T(x,t)/ \partial t = dT(t)/dt = G$, where G is the heatup/cooldown rate, normally 100°F/hr. The differential equation is integrated over x for the following boundary conditions:

1. Vessel inside surface (x = 0) temperature is the same as coolant temperature, T_0.
2. Vessel outside surface (x = C) is perfectly insulated; the thermal gradient dT/dx = 0.

The integrated solution results in the following relationship for wall temperature:

$$T = Gx^2/2\beta - GCx/\beta + T_0 \quad (8\text{-}15)$$

This equation is normalized to plot $(T - T_0)/\Delta T_w$ versus x/C. The resulting through-wall gradient compares very closely with Figure G-2214-3 of ASME Appendix G [2]. Therefore, ΔT_w calculated from Equation 8-14 is used with the appropriate Mt of Figure G-2214-2 of ASME Appendix G [2] to compute K_{It} for heatup and cooldown.

The M_t relationships were derived in the Welding Research Council (WRC) Bulletin 175 [10] for infinitely long cracks of 1/4 T and 1/8 T. For the flat plate geometry and radial thermal gradient, orientation of the crack is not important.

The stress generated by the thermal gradient is a bending stress that changes sign from one side of the plate to the other. In combining pressure and thermal stresses, it is usually necessary to evaluate stresses at the 1/4 T location (inside surface flaw) and the 3/4 T location (outside surface flaw). This is because the thermal gradient tensile stress of interest is in the inner wall during cooldown and is in the outer wall during heatup. However, as a conservative simplification, the thermal gradient stress at the 1/4 T is assumed to be tensile for both heatup and cooldown. This results in the conservative approach of applying the maximum tensile stress at the 1/4 T location. This approach is conservative because irradiation effects cause the allowable toughness, K_{Ir} , at 1/4 T to be less than that at 3/4 T for a given metal temperature. This conservatism of the approach causes no operational difficulties, since the BWR is at steam saturation conditions during normal operation, well above the heatup/cooldown curve limits.

8.2.9 Calculations for the Beltline Region Core Not Critical Heatup/Cooldown

This sample calculation is for a pressure of 1128 psi for 32 EFPY.

The core not critical heatup/cooldown curve at 1128 psig uses the same K_{Im} as the pressure test curve, but with a safety factor of 2.0 instead of 1.5. The increased safety factor is used because the heatup/cooldown cycle represents an operational rather than test condition (which includes nuclear boiling) that necessitates a higher safety factor. In addition, there is a K_{It} term for the thermal stress. The additional inputs used to calculate K_{It} are:

Heatup/cool down rate, normally 100°F/hr, G = 100 °F/hr

Vessel thickness, including clad thickness, C = 0.474 ft (5.688 inches)

Thermal diffusivity at 550°F (most conservative value), $\beta = 0.354$ ft^2/ hr [16]

Equation 8-15 can be solved for the through-wall temperature (x=C), resulting in the absolute value of ΔT for heatup or cooldown of:

$$\Delta T = GC^2 / 2\beta \qquad (8\text{–}16)$$

$$= 100 \bullet (0.474)^2 / (2 \bullet 0.354) = 31.7$$

The analyzed case for thermal stress is a 1/4 T flaw depth with wall thickness of C. The corresponding value of M_t (0.280) can be found from ASME Appendix G, Figure G-2214-2 [2]. Thus the thermal stress intensity factor, $K_{It} = M_t \bullet \Delta T$, can be calculated.

The pressure and thermal stress terms are substituted into Equation 8-9 to solve for $(T\text{-}RT_{NDT})$:

$$(T - RT_{NDT}) = \ln[(2 \bullet K_{Im} + K_{It}) - 26.78) / 1.223] / 0.0145 - 160 \qquad (8\text{-}17)$$
$$= \ln[(2 \bullet 52.67 + 8.9 - 26.78) / 1.223] / 0.0145 - 160$$
$$= 134\ °F$$

T can be calculated by adding the adjusted RT_{NDT}:

$T = 134 + 109 = 243$ °F P = 1128 psig

8.3 CLOSURE FLANGE REGION

10CFR50 Appendix G [1] sets several minimum requirements for pressure and temperature in addition to those outlined in the ASME Code, based on the closure flange region RT_{NDT}. In some cases, the results of analysis for other regions exceed these requirements and closure flange limits do not affect the shape of the P-T curves. However, some closure flange requirements do impact the curves.

The ASME Code [2] requirement for boltup was at qualification temperature (T_{30L}) plus 60°F. Current ASME Code requirements state in Paragraph G-2222(c), that for application of full bolt preload and reactor pressure up to 20% of hydrostatic test pressure, the RPV metal temperature must be at RT_{NDT} or greater. The approach used for FitzPatrick for the boltup

temperature must be at RT_{NDT} or greater. The approach used for FitzPatrick for the boltup temperature was based on a more conservative value of (RT_{NDT} + 60), or the LST of the bolting materials, whichever is greater. The 60°F adder is included by GE for two resaons: 1) The pre-1971 requirements of ASME Code Section III, Subsection NA, Appendix G included the 60°F adder, and 2) Inclusion of the additional 60°F requirement above the RT_{NDT} provides an additional assurance that a flaw size between 0.1 and 0.24 inches is acceptable. As shown in Table 3-2, the limiting initial RT_{NDT} for the closure flange region was the upper shell plate material at 30°F and the LST of the closure studs was 70°F, however, an RT_{NDT} + 60°F will conservatively be used; therefore the boltup temperature value used was 90°F. This conservatism is appropriate because boltup is one of the more limiting operating conditions (high stress and low temperature) for brittle fracture.

10CFR50 Appendix G, paragraph IV.A.2 [1] including Table 1, sets minimum temperature requirements for pressure above 20% hydrotest pressure based on the RT_{NDT} of the closure region. Curve A temperature must be no less than (RT_{NDT} + 90°F) and Curve B temperature no less than (RT_{NDT} + 120°F). The Curve A requirement causes a 30°F shift at 20% hydrotest pressure of 312 psig. The Curve B shift at 312 psig is not visible in Figure 8-2, as the discontinuity curves are limiting.

8.4 CORE CRITICAL OPERATION REQUIREMENTS OF 10CFR50, APPENDIX G

Curve C, the core critical operation curve, is generated from the requirements of 10CFR50 Appendix G [1, Table 1]. Table 1 of [1] requires that core critical P-T limits be 40°F above any Curve A or B limits when pressure exceeds 20% of the pre-service system hydrotest pressure. Curve B is more limiting than Curve A, so limiting Curve C values must be at least Curve B plus 40°F for pressures above 312 psig.

Table 1 of 10CFR50 Appendix G [1] indicates that for BWRs with water level within normal range for power operation, the allowed initial criticality at the closure flange region is (RT_{NDT} + 60°F) at pressures below 312 psig. This requirement makes the minimum criticality temperature 90°F, based on an RT_{NDT} of 30°F. In addition, above 312 psig the Curve C temperature must be at least the greater of RT_{NDT} of the closure region + 160°F or the temperature required for the hydrostatic pressure test (Curve A at 1128 psig). Therefore, this requirement causes Curve C to shift at 20% hydrostatic test pressure or 312 psig. This shift is visible in Figure 8-3.

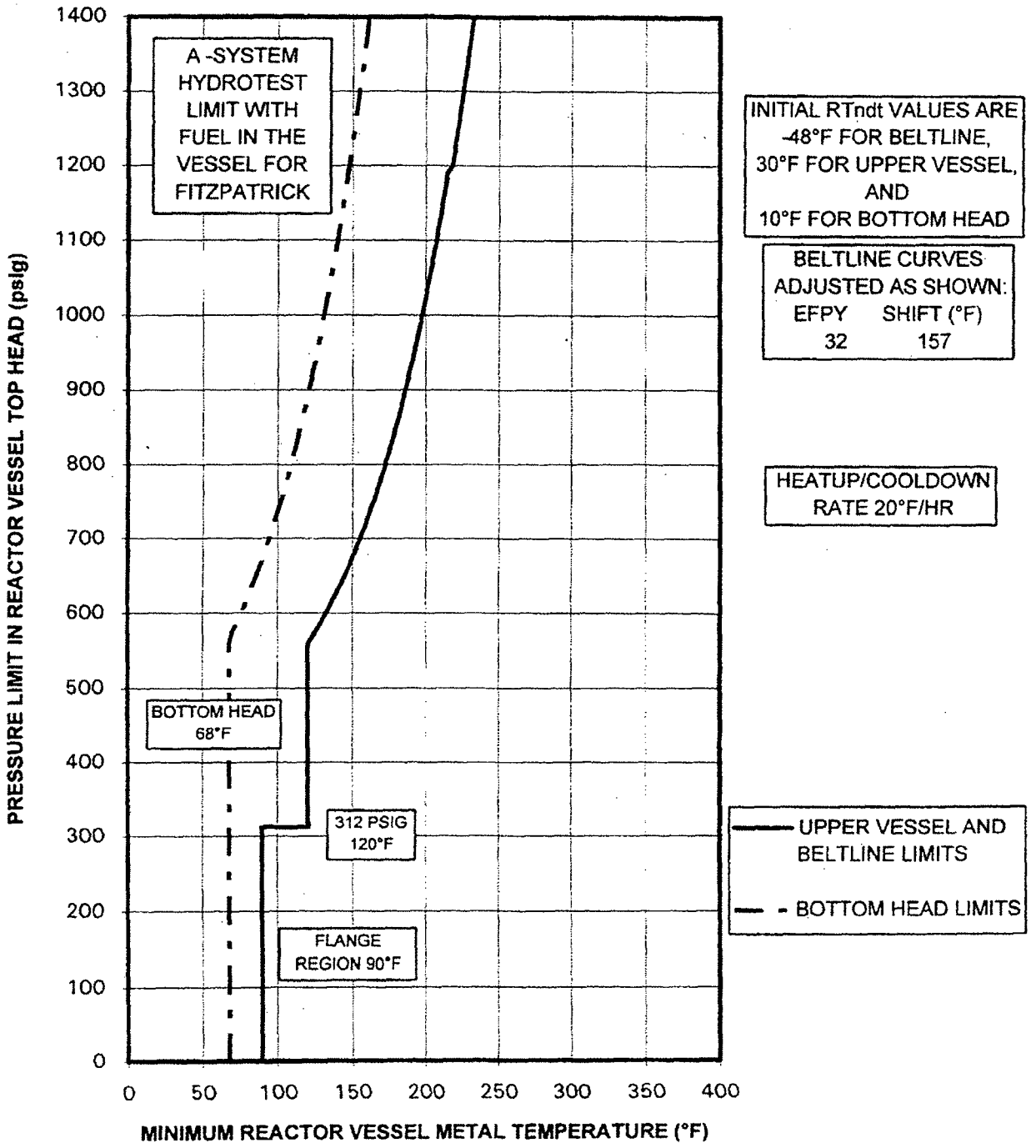

FIGURE 8-1: PRESSURE TEST CURVE (CURVE A)

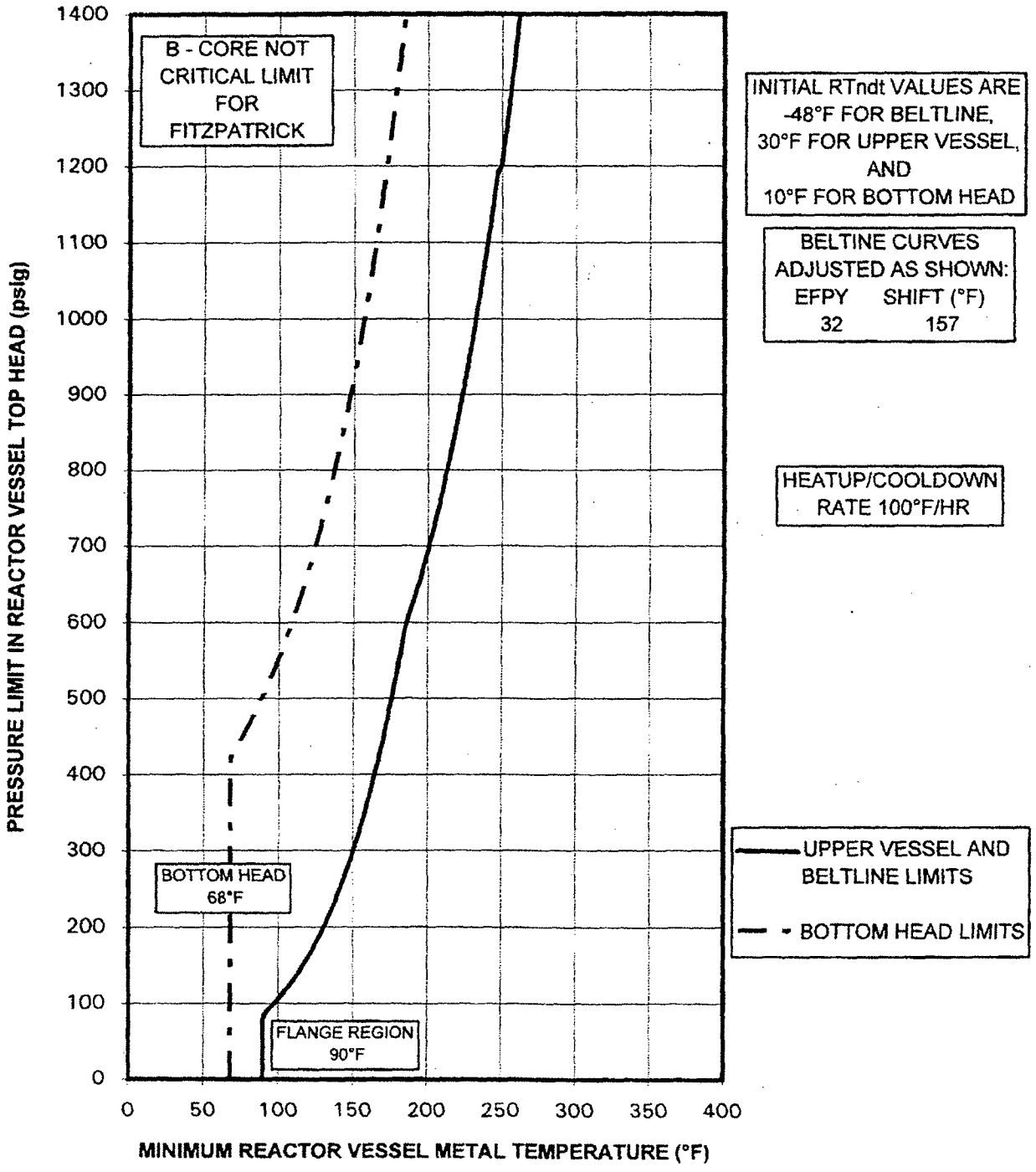

FIGURE 8-2: NON-NUCLEAR HEATUP/COOLDOWN (CURVE B)

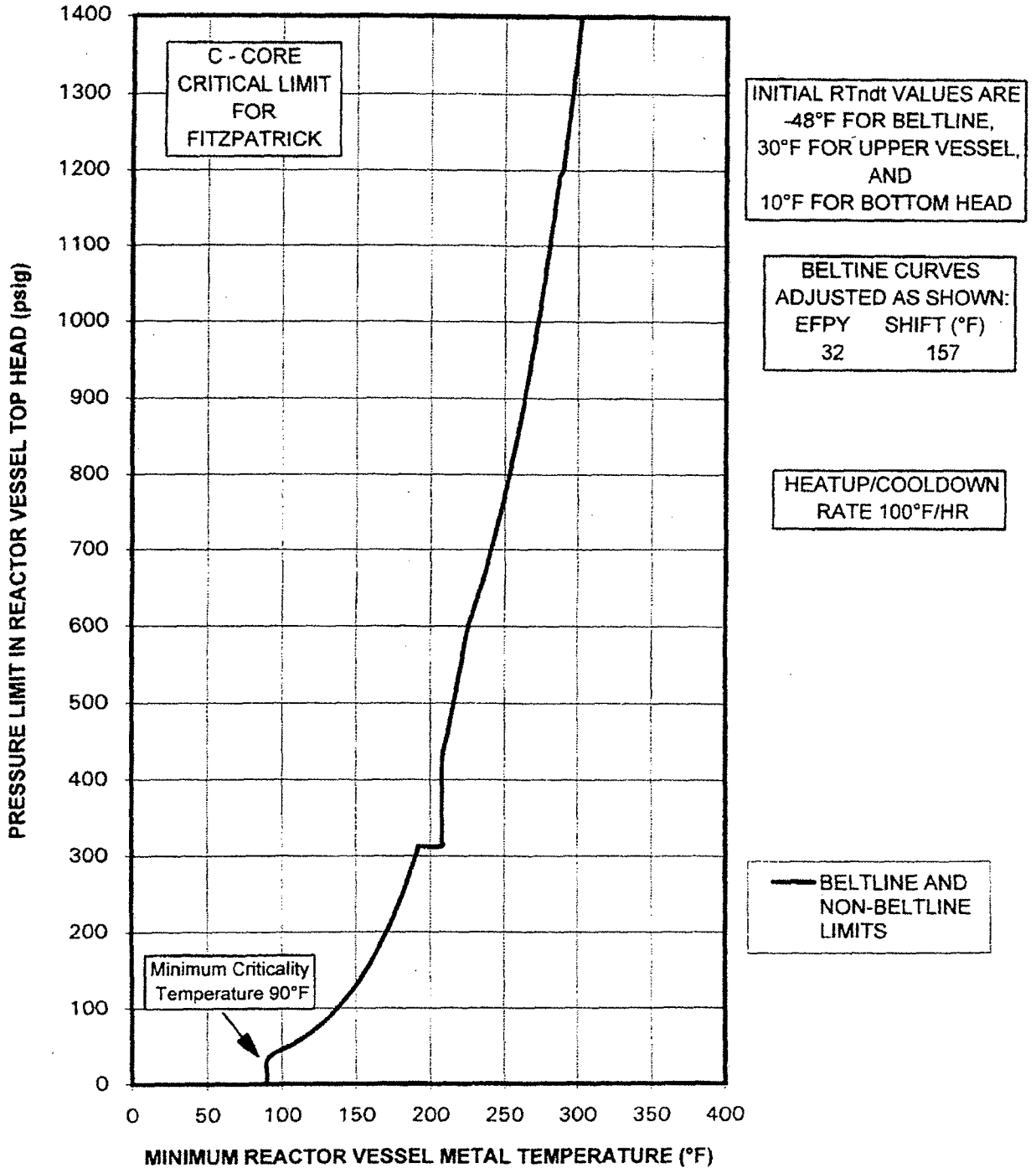

FIGURE 8-3: CORE CRITICAL OPERATION (CURVE C)

TABLE 8-1. FitzPatrick P-T Curve Values for 32 EFPY

Required Temperatures at 100 °F/hr for Curves B & C and 20 °F/hr for Curve A

FOR FIGURES 8-1 THROUGH 8-3

PRESSURE	BOTTOM HEAD CURVE A	RPV & 32 EFPY BELTLINE CURVE A	BOTTOM HEAD CURVE B	RPV & 32 EFPY BELTLINE CURVE B	RPV & 32 EFPY BELTLINE CURVE C
(PSIG)	(°F)	(°F)	(°F)	(°F)	(°F)
0	68.0	90.0	68.0	90.0	90.0
10	68.0	90.0	68.0	90.0	90.0
20	68.0	90.0	68.0	90.0	90.0
30	68.0	90.0	68.0	90.0	90.0
40	68.0	90.0	68.0	90.0	94.5
50	68.0	90.0	68.0	90.0	105.2
60	68.0	90.0	68.0	90.0	113.9
70	68.0	90.0	68.0	90.0	121.1
80	68.0	90.0	68.0	90.0	127.4
90	68.0	90.0	68.0	92.7	132.7
100	68.0	90.0	68.0	97.5	137.5
110	68.0	90.0	68.0	101.9	141.9
120	68.0	90.0	68.0	106.1	146.1
130	68.0	90.0	68.0	110.1	150.1
140	68.0	90.0	68.0	113.6	153.6
150	68.0	90.0	68.0	116.8	156.8
160	68.0	90.0	68.0	119.8	159.8
170	68.0	90.0	68.0	122.8	162.8
180	68.0	90.0	68.0	125.6	165.6
190	68.0	90.0	68.0	128.2	168.2
200	68.0	90.0	68.0	130.6	170.6
210	68.0	90.0	68.0	132.9	172.9
220	68.0	90.0	68.0	135.2	175.2
230	68.0	90.0	68.0	137.4	177.4
240	68.0	90.0	68.0	139.4	179.4
250	68.0	90.0	68.0	141.4	181.4
260	68.0	90.0	68.0	143.3	183.3
270	68.0	90.0	68.0	145.1	185.1
280	68.0	90.0	68.0	147.0	187.0
290	68.0	90.0	68.0	148.7	188.7
300	68.0	90.0	68.0	150.3	190.3
310	68.0	90.0	68.0	152.0	192.0
312.5	68.0	90.0	68.0	152.3	192.3
312.5	68.0	120.0	68.0	152.3	208.7
320	68.0	120.0	68.0	153.5	208.7
330	68.0	120.0	68.0	155.1	208.7

TABLE 8-1. FitzPatrick P-T Curve Values for 32 EFPY

Required Temperatures at 100 °F/hr for Curves B & C and 20 °F/hr for Curve A

FOR FIGURES 8-1 THROUGH 8-3

PRESSURE	BOTTOM HEAD CURVE A	RPV & 32 EFPY BELTLINE CURVE A	BOTTOM HEAD CURVE B	RPV & 32 EFPY BELTLINE CURVE B	RPV & 32 EFPY BELTLINE CURVE C
(PSIG)	(°F)	(°F)	(°F)	(°F)	(°F)
340	68.0	120.0	68.0	156.6	208.7
350	68.0	120.0	68.0	158.0	208.7
360	68.0	120.0	68.0	159.4	208.7
370	68.0	120.0	68.0	160.8	208.7
380	68.0	120.0	68.0	162.1	208.7
390	68.0	120.0	68.0	163.4	208.7
400	68.0	120.0	68.0	164.7	208.7
410	68.0	120.0	68.0	166.0	208.7
420	68.0	120.0	68.0	167.2	208.7
430	68.0	120.0	70.3	168.4	208.7
440	68.0	120.0	73.2	169.6	209.6
450	68.0	120.0	76.1	170.7	210.7
460	68.0	120.0	78.8	171.8	211.8
470	68.0	120.0	81.5	172.9	212.9
480	68.0	120.0	84.0	174.0	214.0
490	68.0	120.0	86.5	175.1	215.1
500	68.0	120.0	88.8	176.1	216.1
510	68.0	120.0	91.1	177.1	217.1
520	68.0	120.0	93.3	178.1	218.1
530	68.0	120.0	95.5	179.1	219.1
540	68.0	120.0	97.6	180.1	220.1
550	68.0	120.0	99.6	181.1	221.1
560	68.0	122.0	101.5	182.0	222.0
570	69.5	125.1	103.5	182.9	222.9
580	71.8	128.0	105.3	184.6	224.6
590	74.0	130.8	107.1	186.3	226.3
600	76.1	133.6	108.9	187.9	227.9
610	78.2	136.2	110.6	189.5	229.5
620	80.2	138.7	112.3	191.1	231.1
630	82.1	141.1	113.9	192.6	232.6
640	84.0	143.5	115.5	194.1	234.1
650	85.9	145.8	117.1	195.6	235.6
660	87.7	148.0	118.6	197.0	237.0
670	89.4	150.1	120.1	198.4	238.4
680	91.1	152.2	121.6	199.8	239.8
690	92.8	154.2	123.0	201.1	241.1

TABLE 8-1. FitzPatrick P-T Curve Values for 32 EFPY

Required Temperatures at 100 °F/hr for Curves B & C and 20 °F/hr for Curve A

FOR FIGURES 8-1 THROUGH 8-3

PRESSURE	BOTTOM HEAD CURVE A	RPV & 32 EFPY BELTLINE CURVE A	BOTTOM HEAD CURVE B	RPV & 32 EFPY BELTLINE CURVE B	RPV & 32 EFPY BELTLINE CURVE C
(PSIG)	(°F)	(°F)	(°F)	(°F)	(°F)
700	94.4	156.1	124.4	202.4	242.4
710	96.0	158.0	125.8	203.7	243.7
720	97.6	159.9	127.1	205.0	245.0
730	99.1	161.7	128.4	206.3	246.3
740	100.6	163.4	129.7	207.5	247.5
750	102.0	165.1	131.0	208.7	248.7
760	103.5	166.8	132.3	209.9	249.9
770	104.8	168.4	133.5	211.1	251.1
780	106.2	170.0	134.7	212.2	252.2
790	107.6	171.6	135.9	213.3	253.3
800	108.9	173.1	137.0	214.4	254.4
810	110.2	174.6	138.2	215.5	255.5
820	111.4	176.0	139.3	216.6	256.6
830	112.7	177.5	140.4	217.7	257.7
840	113.9	178.9	141.5	218.7	258.7
850	115.1	180.2	142.6	219.7	259.7
860	116.3	181.6	143.6	220.8	260.8
870	117.5	182.9	144.7	221.8	261.8
880	118.6	184.2	145.7	222.7	262.7
890	119.7	185.5	146.7	223.7	263.7
900	120.8	186.7	147.7	224.7	264.7
910	121.9	187.9	148.7	225.6	265.6
920	123.0	189.1	149.7	226.5	266.5
930	124.0	190.3	150.6	227.5	267.5
940	125.1	191.5	151.6	228.4	268.4
950	126.1	192.6	152.5	229.3	269.3
960	127.1	193.7	153.4	230.1	270.1
970	128.1	194.9	154.3	231.0	271.0
980	129.1	195.9	155.2	231.9	271.9
990	130.0	197.0	156.1	232.7	272.7
1000	131.0	198.1	157.0	233.6	273.6
1010	131.9	199.1	157.8	234.4	274.4
1020	132.9	200.1	158.7	235.2	275.2
1030	133.8	201.1	159.5	236.0	276.0
1040	134.7	202.1	160.4	236.8	276.8
1050	135.6	203.1	161.2	237.6	277.6

TABLE 8-1. FitzPatrick P-T Curve Values for 32 EFPY

Required Temperatures at 100 °F/hr for Curves B & C and 20 °F/hr for Curve A

FOR FIGURES 8-1 THROUGH 8-3

PRESSURE	BOTTOM HEAD CURVE A	RPV & 32 EFPY BELTLINE CURVE A	BOTTOM HEAD CURVE B	RPV & 32 EFPY BELTLINE CURVE B	RPV & 32 EFPY BELTLINE CURVE C
(PSIG)	(°F)	(°F)	(°F)	(°F)	(°F)
1060	136.5	204.1	162.0	238.4	278.4
1070	137.3	205.0	162.8	239.2	279.2
1080	138.2	206.0	163.6	239.9	279.9
1090	139.0	206.9	164.4	240.7	280.7
1100	139.9	207.8	165.1	241.4	281.4
1110	140.7	208.7	165.9	242.2	282.2
1120	141.5	209.6	166.7	242.9	282.9
1130	142.3	210.5	167.4	243.6	283.6
1140	143.1	211.4	168.1	244.4	284.4
1150	143.9	212.2	168.9	245.1	285.1
1160	144.7	213.1	169.6	245.8	285.8
1170	145.5	213.9	170.3	246.5	286.5
1180	146.2	214.7	171.0	247.2	287.2
1190	147.0	215.6	171.7	247.8	287.8
1200	147.7	218.8	172.4	250.6	290.6
1210	148.5	219.6	173.1	251.2	291.2
1220	149.2	220.4	173.8	251.9	291.9
1230	149.9	221.1	174.5	252.5	292.5
1240	150.6	221.9	175.1	253.2	293.2
1250	151.3	222.7	175.8	253.8	293.8
1260	152.0	223.4	176.5	254.5	294.5
1270	152.7	224.2	177.1	255.1	295.1
1280	153.4	224.9	177.8	255.7	295.7
1290	154.1	225.6	178.4	256.3	296.3
1300	154.8	226.3	179.0	256.9	296.9
1310	155.4	227.0	179.6	257.5	297.5
1320	156.1	227.7	180.3	258.2	298.2
1330	156.8	228.4	180.9	258.7	298.7
1340	157.4	229.1	181.5	259.3	299.3
1350	158.1	229.8	182.1	259.9	299.9
1360	158.7	230.5	182.7	260.5	300.5
1370	159.3	231.1	183.3	261.1	301.1
1380	159.9	231.8	183.9	261.7	301.7
1390	160.6	232.5	184.5	262.2	302.2
1400	161.2	233.1	185.0	262.8	302.8

9. REFERENCES

[1] "Fracture Toughness Requirements," Appendix G to Part 50 of Title 10 of the Code of Federal Regulations, December 1995.

[2] " Protection Against Non-Ductile Failure," Appendix G to Section XI of the 1989 ASME Boiler & Pressure Vessel Code.

[3] "Reactor Vessel Material Surveillance Program Requirements," Appendix H to Part 50 of Title 10 of the Code of Federal Regulations, December 1995.

[4] "Surveillance Test for Nuclear Reactor Vessels," Annual Book of ASTM Standards, E185-70.

[5] T. A. Caine, "Implementation of Regulatory Guide 1.99, Revision 2 for the James A. FitzPatrick Nuclear Power plant, GENE, San Jose, CA, June 1989, (GE Report SASR 89-50).

[6] "Conducting Surveillance Tests for Light Water Cooled Nuclear Power Reactor Vessels," Annual Book of ASTM Standards, E185-82, July 1982.

[7] "Radiation Embrittlement of Reactor Vessel Materials," USNRC Regulatory Guide 1.99, Revision 2, May 1988.

[8] T. A. Caine, "James A. FitzPatrick Nuclear Power Plant, Reactor Pressure Vessel Surveillance Materials Testing and Fracture Toughness Analysis", GENE, San Jose, CA, April 1986, GE Report MDE-49-0386.

[9] James A. FitzPatrick Nuclear Power Updated Safety Analysis Report, Section 4.2.

[10] "PVRC Recommendations on Toughness Requirements for Ferritic Materials", Welding Research Council Bulletin 175, August 1972.

[11] Martin, G.C., "Fast Neutron Cross-Section Determination for BWR's Using Neutron Dosimeters," November 11, 1993 (FMT Transmittal 93-212-0045).

[12] "Standard Methods for Notched Bar Impact Testing of Metallic Materials," Annual Book of ASTM Standards, E23-94b.

[13] "Nuclear Plant Irradiated Steel Handbook," EPRI Report NP-4797, September 1986.

[14] "Standard Test Methods for Tension Testing of Metallic Materials," Annual Book of ASTM Standards, E8-89.

[15] B.J. Branlund, "Reactor Vessel Fracture Toughness Engineering Evaluation for the James A. FitzPatrick 104% Power Uprate," March 1996, GE-NE-B1301805-05R1.

[16] H. S. Mehta, T. A. Caine, and S. E. Plaxton, "10 CFR 50 Appendix G Equivalent Margin Analysis for Low Upper Shelf Energy in BWR/2 through BWR/6 Vessels, Rev. 1," GENE, San Jose, CA, February, 1994, (NEDO-32205-A).

[17] T. A. Caine, "Progress Report on Phase 2 of the BWR Owners' Group Supplemental Surveillance Program," January 1992, GE-NE-523-101-1290.

[18] "Best Estimate Copper and Nickel Values in CE Fabricated Reactor Vessel Welds," CEOG Task 902, June 1997, CE NPSD-1039.

[19] Letter from Jeffrey L. Beck (Lukens Steel, Coatesville, PA)) to Richard Chau (NYPA, White Plains, NY) dated October 14, 1985 on "FitzPatrick Vessel Plate Copper Chemistries."

[20] R. M. Kruger and R. D. Reager, "Determination of Fast Neutron Fluence in Flux Wires at the FitzPatrick Nuclear Power Station (Cycle 1-12 Irradiations), August 1997, GE-NE Report B11-00732-RMK1.

[21] "Response to Genric Letter 92-01, James A. FitzPatrick Nuclear Power Plant," Submitted to U.S. NRC by New York Power Authority, July 9, 1992.

APPENDIX A
IRRADIATED CHARPY SPECIMEN FRACTURE SURFACE PHOTOGRAPHS

Photographs of each Charpy specimen fracture surface were taken per the requirements of ASTM E185-82. The pages following show the fracture surface photographs along with a summary of the Charpy test results for each irradiated specimen. The pictures are arranged in the order of base, weld, and HAZ materials.

BASE: 53P
Temp: 24 °F
Energy: 44.2 ft-lb
MLE: 39 mils
Shear: 31 %

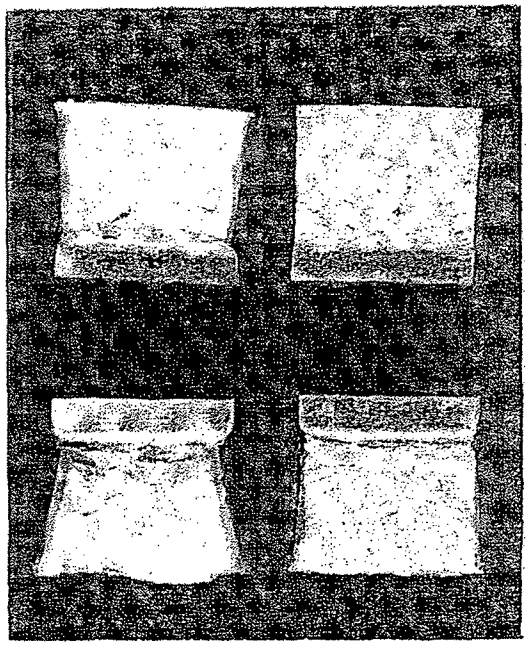

BASE: 53U
Temp: -50 °F
Energy: 10 ft-lb
MLE: 8 mils
Shear: 1 %

BASE: 53Y
Temp: 49 °F
Energy: 81.0 ft-lb
MLE: 65 mils
Shear: 46 %

BASE: 53M
Temp: 0 °F
Energy: 35.4 ft-lb
MLE: 31 mils
Shear: 29 %

BASE: 53L
Temp: 250°F
Energy: 120.4 ft-lb
MLE: 91 mils
Shear: 100 %

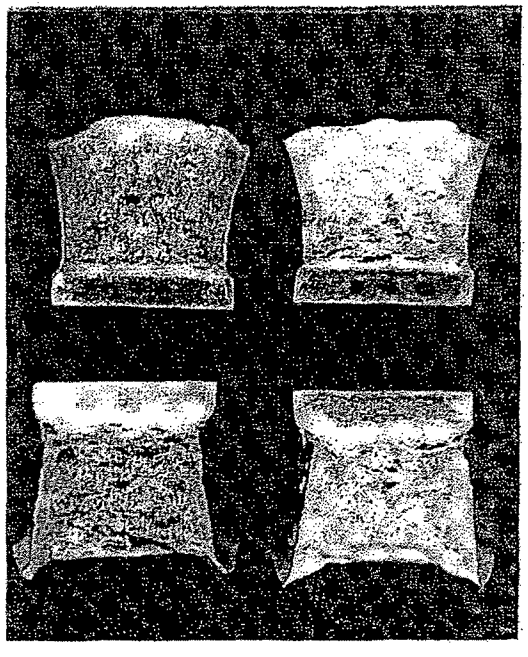

BASE: 53B
Temp: 103°F
Energy: 96.5 ft-lb
MLE: 77 mils
Shear: 78 %

BASE: 527
Temp: 400°F
Energy: 126.7 ft-lb
MLE: 93 mils
Shear: 100 %

BASE: 52D
Temp: 150°F
Energy: 117.4 ft-lb
MLE: 89 mils
Shear: 100 %

WELD: 563
Temp: 103°F
Energy: 29.4 ft-lb
MLE: 27 mils
Shear: 34 %

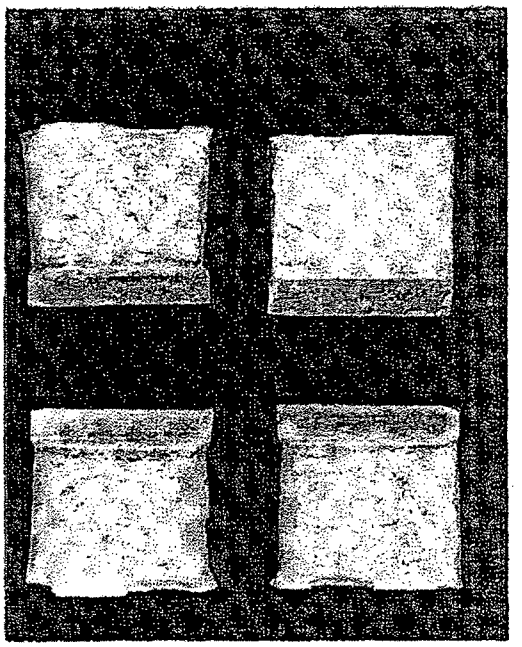

WELD: 56A
Temp: 0 °F
Energy: 3.2 ft-lb
MLE: 3 mils
Shear: 1 %

WELD: 56L
Temp: 120 °F
Energy: 33.7 ft-lb
MLE: 32 mils
Shear: 55 %

WELD: 565
Temp: 80 °F
Energy: 18.9 ft-lb
MLE: 18 mils
Shear: 30 %

WELD: 54M
Temp: 250 °F
Energy: 72.5 ft-lb
MLE: 66 mils
Shear: 100 %

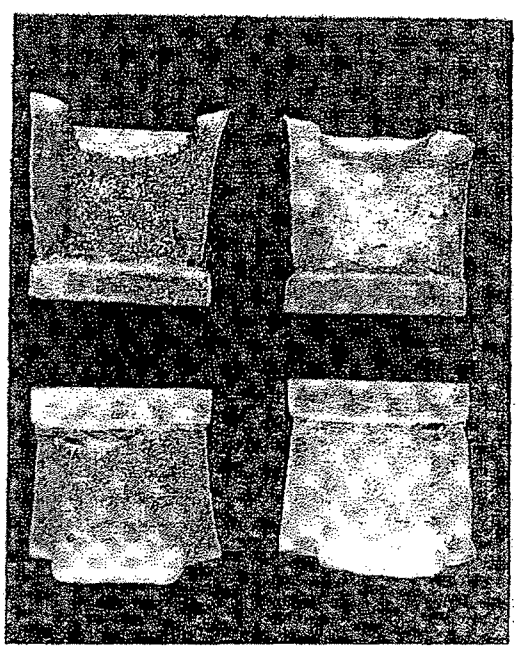

WELD: 55Y
Temp: 163°F
Energy: 56.8 ft-lb
MLE: 43 mils
Shear: 75 %

WELD: 54T
Temp: 400 °F
Energy: 75.0 ft-lb
MLE: 73 mils
Shear: 100 %

WELD: 55B
Temp: 202 °F
Energy: 68.1 ft-lb
MLE: 61 mils
Shear: 88 %

HAZ: 5AK
Temp: 0 °F
Energy: 44.0 ft-lb
MLE: 41 mils
Shear: 22 %

HAZ: 5AU
Temp: 48°F
Energy: 98.3 ft-lb
MLE: 78 mils
Shear: 30 %

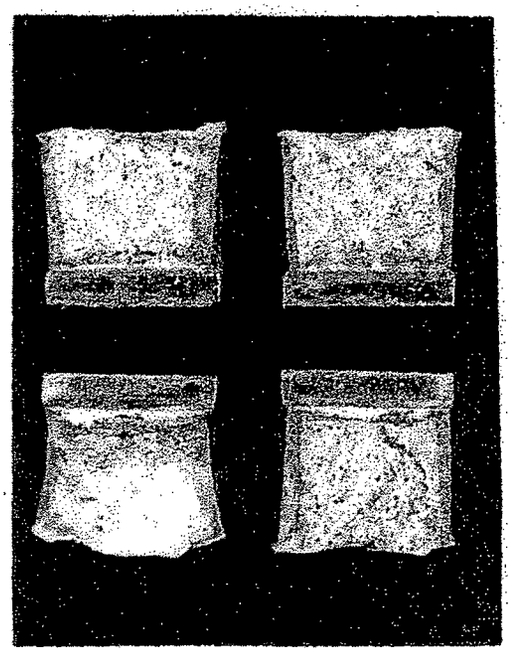

HAZ: 5AT
Temp: -80 °F
Energy: 36.0 ft-lb
MLE: 29 mils
Shear: 38 %

HAZ: 5AY
Temp: -50 °F
Energy: 36.6 ft-lb
MLE: 30 mils
Shear: 41 %

HAZ: 5AB
Temp: 202 °F
Energy: 102.2 ft-lb
MLE: 82 mils
Shear: 100 %

HAZ: 5A6
Temp: 400 °F
Energy: 112.6 ft-lb
MLE: 95 mils
Shear: 100 %

HAZ: 57P
Temp: 80 °F
Energy: 77.6 ft-lb
MLE: 67 mils
Shear: 82 %

HAZ: 575
Temp: 120 °F
Energy: 74.1 ft-lb
MLE: 69 mils
Shear: 100 %

APPENDIX B

PRESSURE TEMPERATURE CURVES

VALID TO 24 EFPY

APPENDIX B

PRESSURE TEMPERATURE CURVES

VALID TO 24 EFPY

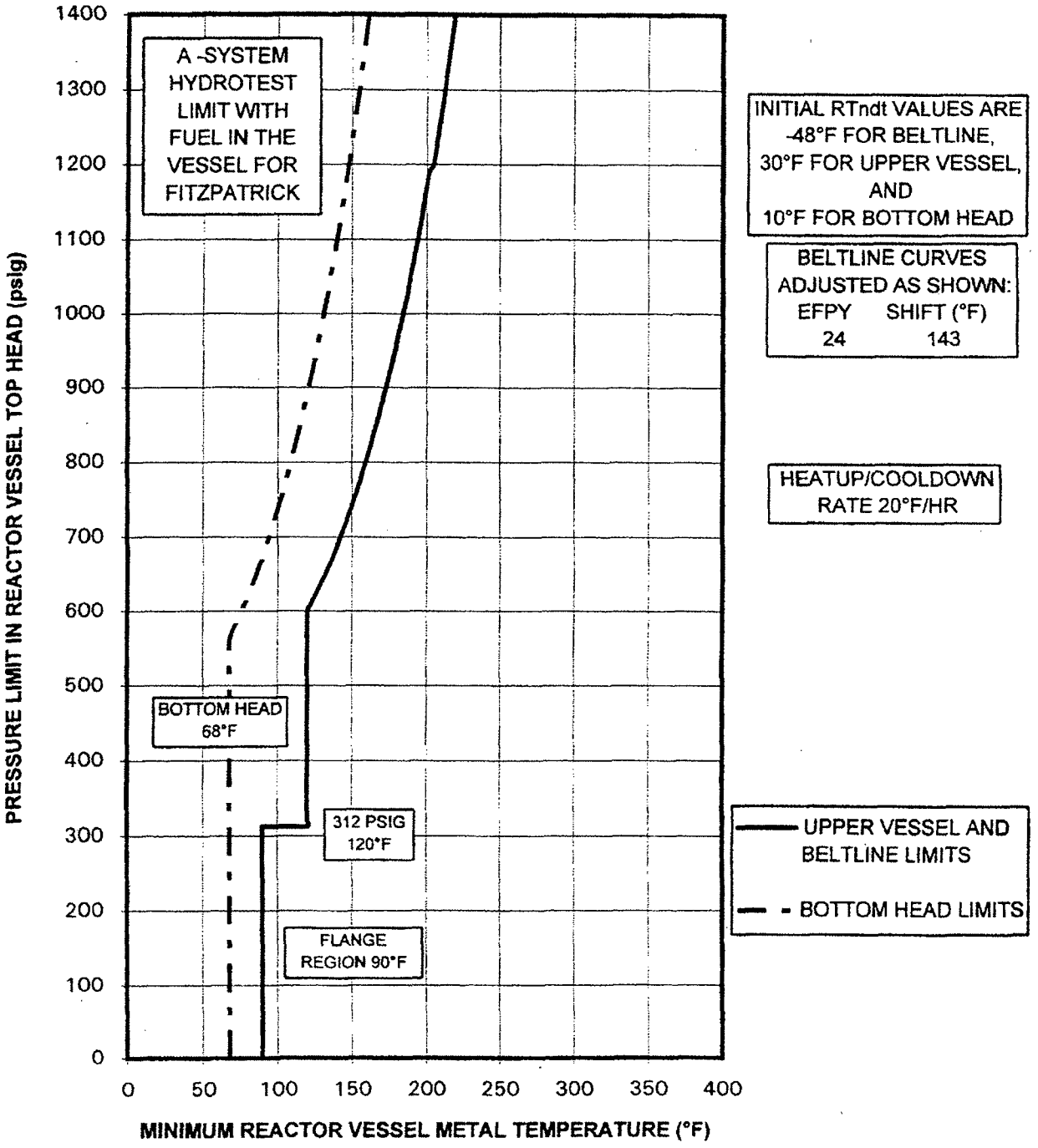

FIGURE B-1: PRESSURE TEST CURVE (CURVE A)

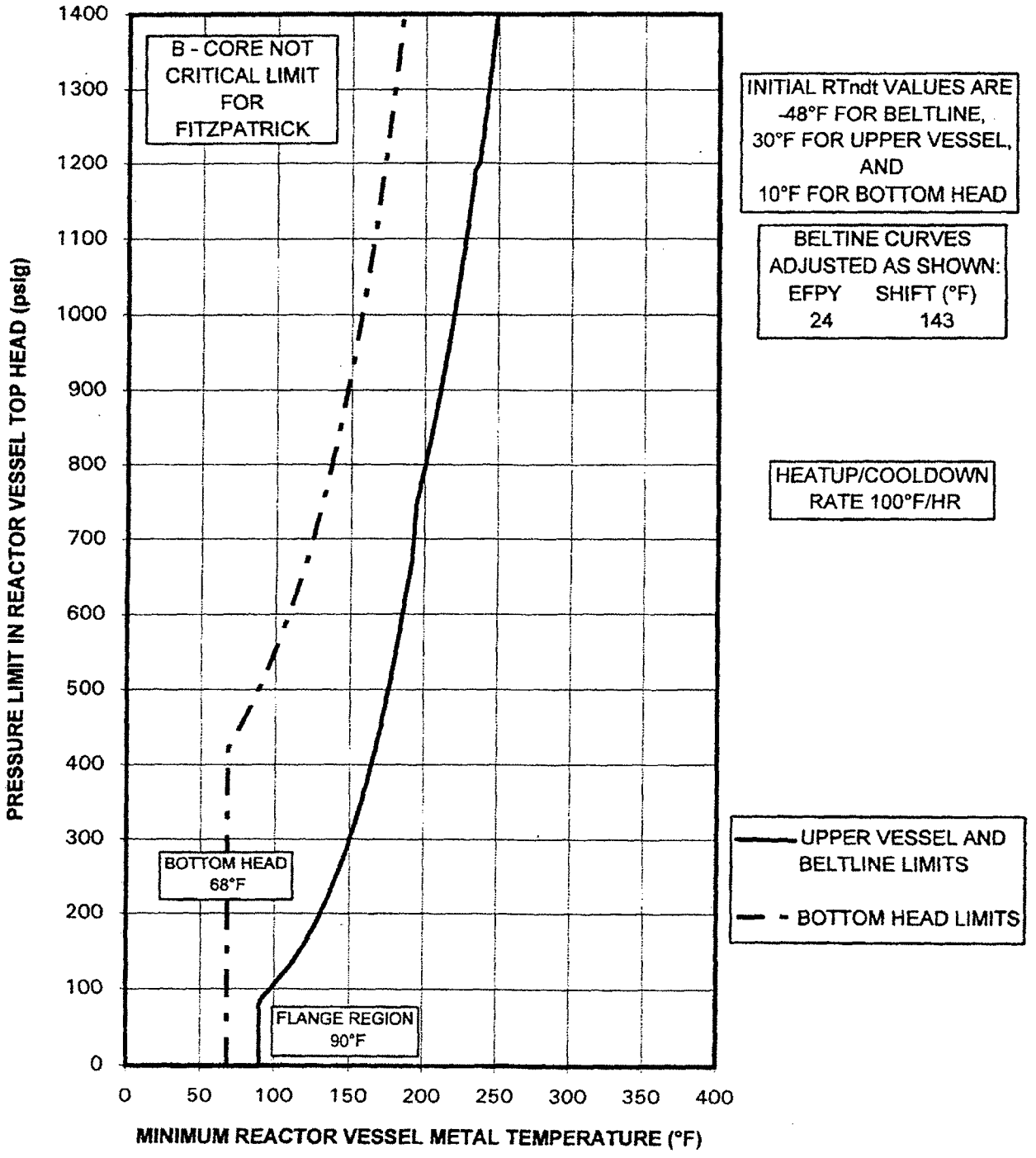

FIGURE B-2: NON-NUCLEAR HEATUP/COOLDOWN (CURVE B)

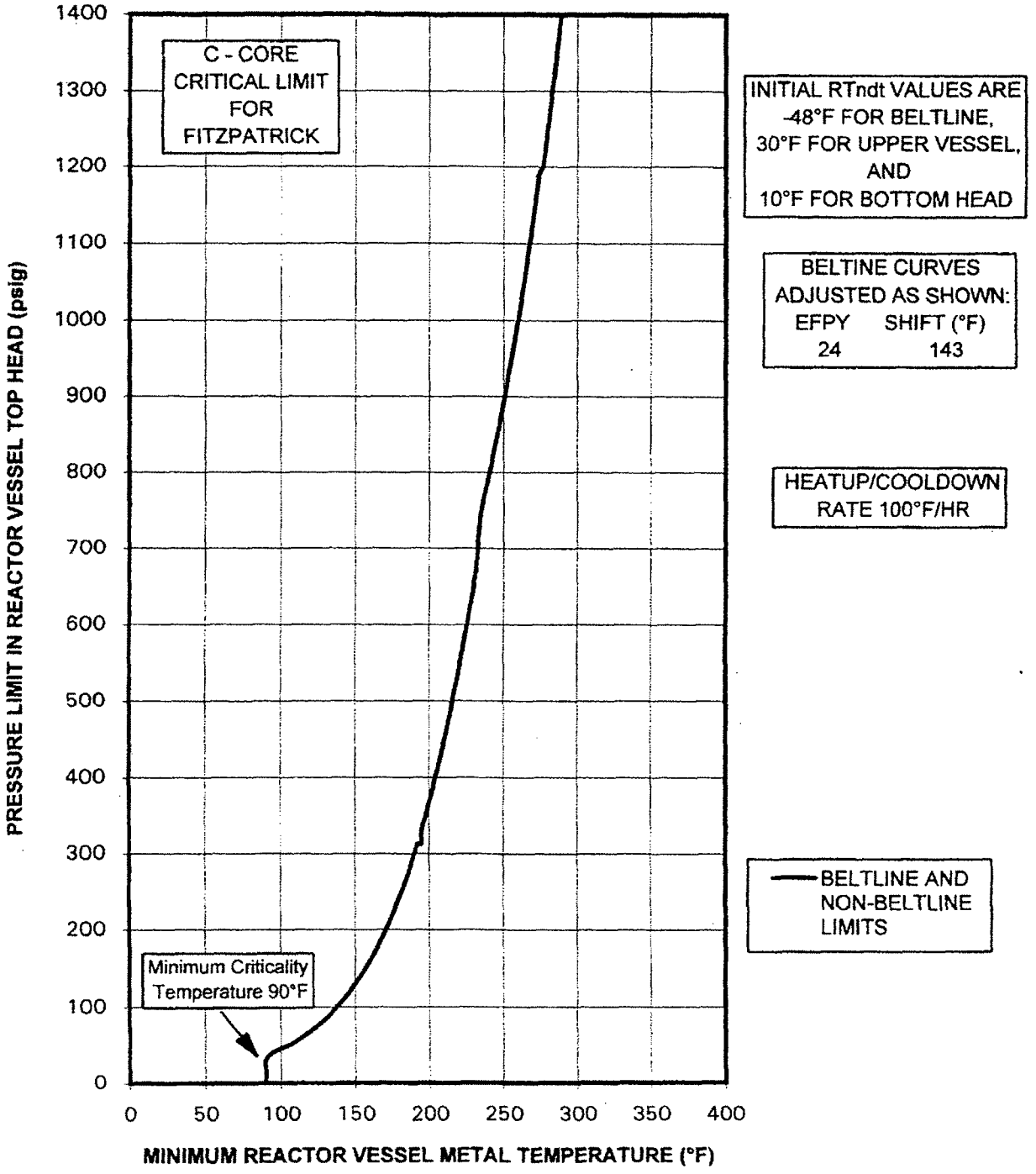

FIGURE B-3: CORE CRITICAL OPERATION (CURVE C)

TABLE B-1. FitzPatrick P-T Curve Values for 24 EFPY

Required Temperatures at 100 °F/hr for Curves B & C and 20 °F/hr for Curve A

FOR FIGURES B-1 THROUGH B-3

PRESSURE	BOTTOM HEAD CURVE A	RPV & 24 EFPY BELTLINE CURVE A	BOTTOM HEAD CURVE B	RPV & 24 EFPY BELTLINE CURVE B	RPV & 24 EFPY BELTLINE CURVE C
(PSIG)	(°F)	(°F)	(°F)	(°F)	(°F)
0	68.0	90.0	68.0	90.0	90.0
10	68.0	90.0	68.0	90.0	90.0
20	68.0	90.0	68.0	90.0	90.0
30	68.0	90.0	68.0	90.0	90.0
40	68.0	90.0	68.0	90.0	94.5
50	68.0	90.0	68.0	90.0	105.2
60	68.0	90.0	68.0	90.0	113.9
70	68.0	90.0	68.0	90.0	121.1
80	68.0	90.0	68.0	90.0	127.4
90	68.0	90.0	68.0	92.7	132.7
100	68.0	90.0	68.0	97.5	137.5
110	68.0	90.0	68.0	101.9	141.9
120	68.0	90.0	68.0	106.1	146.1
130	68.0	90.0	68.0	110.1	150.1
140	68.0	90.0	68.0	113.6	153.6
150	68.0	90.0	68.0	116.8	156.8
160	68.0	90.0	68.0	119.8	159.8
170	68.0	90.0	68.0	122.8	162.8
180	68.0	90.0	68.0	125.6	165.6
190	68.0	90.0	68.0	128.2	168.2
200	68.0	90.0	68.0	130.6	170.6
210	68.0	90.0	68.0	132.9	172.9
220	68.0	90.0	68.0	135.2	175.2
230	68.0	90.0	68.0	137.4	177.4
240	68.0	90.0	68.0	139.4	179.4
250	68.0	90.0	68.0	141.4	181.4
260	68.0	90.0	68.0	143.3	183.3
270	68.0	90.0	68.0	145.1	185.1
280	68.0	90.0	68.0	147.0	187.0
290	68.0	90.0	68.0	148.7	188.7
300	68.0	90.0	68.0	150.3	190.3
310	68.0	90.0	68.0	152.0	192.0
312.5	68.0	90.0	68.0	152.3	192.3
312.5	68.0	120.0	68.0	152.3	195.0
320	68.0	120.0	68.0	153.5	195.0
330	68.0	120.0	68.0	155.1	195.1

TABLE B-1. FitzPatrick P-T Curve Values for 24 EFPY

Required Temperatures at 100 °F/hr for Curves B & C and 20 °F/hr for Curve A

FOR FIGURES B-1 THROUGH B-3

PRESSURE	BOTTOM HEAD CURVE A	RPV & 24 EFPY BELTLINE CURVE A	BOTTOM HEAD CURVE B	RPV & 24 EFPY BELTLINE CURVE B	RPV & 24 EFPY BELTLINE CURVE C
(PSIG)	(°F)	(°F)	(°F)	(°F)	(°F)
340	68.0	120.0	68.0	156.6	196.6
350	68.0	120.0	68.0	158.0	198.0
360	68.0	120.0	68.0	159.4	199.4
370	68.0	120.0	68.0	160.8	200.8
380	68.0	120.0	68.0	162.1	202.1
390	68.0	120.0	68.0	163.4	203.4
400	68.0	120.0	68.0	164.7	204.7
410	68.0	120.0	68.0	166.0	206.0
420	68.0	120.0	68.0	167.2	207.2
430	68.0	120.0	70.3	168.4	208.4
440	68.0	120.0	73.2	169.6	209.6
450	68.0	120.0	76.1	170.7	210.7
460	68.0	120.0	78.8	171.8	211.8
470	68.0	120.0	81.5	172.9	212.9
480	68.0	120.0	84.0	174.0	214.0
490	68.0	120.0	86.5	175.1	215.1
500	68.0	120.0	88.8	176.1	216.1
510	68.0	120.0	91.1	177.1	217.1
520	68.0	120.0	93.3	178.1	218.1
530	68.0	120.0	95.5	179.1	219.1
540	68.0	120.0	97.6	180.1	220.1
550	68.0	120.0	99.6	181.1	221.1
560	68.0	120.0	101.5	182.0	222.0
570	69.5	120.0	103.5	182.9	222.9
580	71.8	120.0	105.3	183.8	223.8
590	74.0	120.0	107.1	184.7	224.7
600	76.1	120.0	108.9	185.6	225.6
610	78.2	122.4	110.6	186.5	226.5
620	80.2	125.0	112.3	187.3	227.3
630	82.1	127.4	113.9	188.2	228.2
640	84.0	129.7	115.5	189.0	229.0
650	85.9	132.0	117.1	189.8	229.8
660	87.7	134.2	118.6	190.6	230.6
670	89.4	136.3	120.1	191.4	231.4
680	91.1	138.4	121.6	191.9	231.9
690	92.8	140.4	123.0	192.3	232.3

TABLE B-1. FitzPatrick P-T Curve Values for 24 EFPY

Required Temperatures at 100 °F/hr for Curves B & C and 20 °F/hr for Curve A

FOR FIGURES B-1 THROUGH B-3

PRESSURE	BOTTOM HEAD CURVE A	RPV & 24 EFPY BELTLINE CURVE A	BOTTOM HEAD CURVE B	RPV & 24 EFPY BELTLINE CURVE B	RPV & 24 EFPY BELTLINE CURVE C
(PSIG)	(°F)	(°F)	(°F)	(°F)	(°F)
700	94.4	142.1	124.4	192.8	232.8
710	96.0	144.0	125.8	193.2	233.2
720	97.6	145.9	127.1	193.6	233.6
730	99.1	147.7	128.4	194.0	234.0
740	100.6	149.4	129.7	194.4	234.4
750	102.0	151.1	131.0	194.8	234.8
760	103.5	152.8	132.3	195.9	235.9
770	104.8	154.4	133.5	197.1	237.1
780	106.2	156.0	134.7	198.2	238.2
790	107.6	157.6	135.9	199.3	239.3
800	108.9	159.1	137.0	200.4	240.4
810	110.2	160.6	138.2	201.5	241.5
820	111.4	162.0	139.3	202.6	242.6
830	112.7	163.5	140.4	203.7	243.7
840	113.9	164.9	141.5	204.7	244.7
850	115.1	166.2	142.6	205.7	245.7
860	116.3	167.6	143.6	206.8	246.8
870	117.5	168.9	144.7	207.8	247.8
880	118.6	170.2	145.7	208.7	248.7
890	119.7	171.5	146.7	209.7	249.7
900	120.8	172.7	147.7	210.7	250.7
910	121.9	173.9	148.7	211.6	251.6
920	123.0	175.1	149.7	212.5	252.5
930	124.0	176.3	150.6	213.5	253.5
940	125.1	177.5	151.6	214.4	254.4
950	126.1	178.6	152.5	215.3	255.3
960	127.1	179.7	153.4	216.1	256.1
970	128.1	180.9	154.3	217.0	257.0
980	129.1	181.9	155.2	217.9	257.9
990	130.0	183.0	156.1	218.7	258.7
1000	131.0	184.1	157.0	219.6	259.6
1010	131.9	185.1	157.8	220.4	260.4
1020	132.9	186.1	158.7	221.2	261.2
1030	133.8	187.1	159.5	222.0	262.0
1040	134.7	188.1	160.4	222.8	262.8
1050	135.6	189.1	161.2	223.6	263.6

TABLE B-1. FitzPatrick P-T Curve Values for 24 EFPY

Required Temperatures at 100 °F/hr for Curves B & C and 20 °F/hr for Curve A

FOR FIGURES B-1 THROUGH B-3

PRESSURE	BOTTOM HEAD CURVE A	RPV & 24 EFPY BELTLINE CURVE A	BOTTOM HEAD CURVE B	RPV & 24 EFPY BELTLINE CURVE B	RPV & 24 EFPY BELTLINE CURVE C
(PSIG)	(°F)	(°F)	(°F)	(°F)	(°F)
1060	136.5	190.1	162.0	224.4	264.4
1070	137.3	191.0	162.8	225.2	265.2
1080	138.2	192.0	163.6	225.9	265.9
1090	139.0	192.9	164.4	226.7	266.7
1100	139.9	193.8	165.1	227.4	267.4
1110	140.7	194.7	165.9	228.2	268.2
1120	141.5	195.6	166.7	228.9	268.9
1130	142.3	196.5	167.4	229.6	269.6
1140	143.1	197.4	168.1	230.4	270.4
1150	143.9	198.2	168.9	231.1	271.1
1160	144.7	199.1	169.6	231.8	271.8
1170	145.5	199.9	170.3	232.5	272.5
1180	146.2	200.7	171.0	233.2	273.2
1190	147.0	201.6	171.7	233.8	273.8
1200	147.7	204.8	172.4	236.6	276.6
1210	148.5	205.6	173.1	237.2	277.2
1220	149.2	206.4	173.8	237.9	277.9
1230	149.9	207.1	174.5	238.5	278.5
1240	150.6	207.9	175.1	239.2	279.2
1250	151.3	208.7	175.8	239.8	279.8
1260	152.0	209.4	176.5	240.5	280.5
1270	152.7	210.2	177.1	241.1	281.1
1280	153.4	210.9	177.8	241.7	281.7
1290	154.1	211.6	178.4	242.3	282.3
1300	154.8	212.3	179.0	242.9	282.9
1310	155.4	213.0	179.6	243.5	283.5
1320	156.1	213.7	180.3	244.2	284.2
1330	156.8	214.4	180.9	244.7	284.7
1340	157.4	215.1	181.5	245.3	285.3
1350	158.1	215.8	182.1	245.9	285.9
1360	158.7	216.5	182.7	246.5	286.5
1370	159.3	217.1	183.3	247.1	287.1
1380	159.9	217.8	183.9	247.7	287.7
1390	160.6	218.5	184.5	248.2	288.2
1400	161.2	219.1	185.0	248.8	288.8

123 Main Street
White Plains, New York 10601
914 681.6840
914 287.3309 (FAX)

New York Power Authority

James Knubel
Senior Vice President and
Chief Nuclear Officer

March 9, 1998
JPN-98-008

U.S. Nuclear Regulatory Commission
Attn: Document Control Desk
Mail Station P1-137
Washington, D.C. 20555

SUBJECT: JAMES A. FITZPATRICK NUCLEAR POWER PLANT
DOCKET NO. 50-333
REVISED REACTOR PRESSURE VESSEL MATERIAL SURVEILLANCE PROGRAM SUMMARY REPORT AND IMPLEMENTATION SCHEDULE

REFERENCES: 1. NYPA Letter, R. J. Deasy to NRC, "Reactor Pressure Vessel Material Surveillance Program Summary Report and Implementation Schedule," (JPN-97-035), dated November 10, 1997

Dear Sir:

The lotter provides a copy of the revised FitzPatrick Reactor Pressure Vessel (RPV) Material Testing and Analysis Report. The changes do not affect the conclusion or technical basis of the report and the requirements of 10 CFR 50 Appendix G continue to be satisfied. A schedule and technical justification for the next capsule withdrawal is submitted for NRC review and approval. In addition, the Authority is providing the results of the ongoing Owner's Group RPV integrity program relative to FitzPatrick. The Authority committed to provide this information in Reference 1.

Attachment 1 describes the Authority's resolution to the Reference 1 Commitments. Attachment 2 is the revised FitzPatrick RPV Surveillance Materials Testing and Analysis report. Attachment 3 is a summary of the commitments made in this letter.

If you have any questions, please contact Ms. C. Faison.

Very Truly Yours,

J. Knubel
Chief Nuclear Officer and
Senior Vice President

cc: Regional Administrator
U.S. Nuclear Regulatory Commission
475 Allendale Road
King of Prussia, PA 19406

Office of the Resident Inspector
U.S. Nuclear Regulatory Commission
P.O. Box 136
Lycoming, New York 13093

Mr. J. Williams, Project Manager
Project Directorate I-1
Division of Reactor Projects I/II
U.S. Nuclear Regulatory Commission
Mail Stop 14 B2
Washington, DC 20555

Attachment 1 to JPN-98-008

RESOLUTION OF COMMITMENT NUMBERS JPN-97-035-001 AND JPN-97-035-002

New York Power Authority

JAMES A. FITZPATRICK NUCLEAR POWER PLANT
Docket No. 50-333
DPR-59

Introduction and Background

The Authority committed (JPN-97-035, Reference 1) to provide the NRC with a copy of the test result report, revised to reflect the resolution of comments and concerns within 120 days. Included in this response is a description of the Quality Assurance (QA) finding regarding specimen test procedures, and its resolution. A schedule and technical justification for the next capsule withdrawal is also submitted at this time for NRC review and approval. In addition, the Authority is providing the results of the ongoing Owner's Group Reactor Pressure Vessel (RPV) integrity program relative to FitzPatrick.

Resolution of QA Concerns

The Authority had a concern regarding how the capsule testing was performed based on the results of an audit conducted on the General Electric (GE) Company by the Authority's QA Department in November 1997. The subject of the audit was reactor vessel surveillance specimen testing for FitzPatrick. As a result of this audit, one finding was identified concerning the availability and use of procedures for conducting charpy impact tests. Specifically, the finding stated the following:

> "The test engineer responsible for the testing of NYPA's (JAF) surveillance capsules charpy specimen stated that testing was performed without a procedure."

The Authority performed an audit in February 1998 to address this finding. During this audit, the GE personnel that actually performed the FitzPatrick specimen testing were interviewed. The Authority was informed during these interviews that the 1993 version of the charpy test procedure, valid at the time of testing, was available in a file cabinet in the hot lab test room where the tests were performed. However, the GE personnel did not refer to this procedure during testing. The Authority determined during this audit that the GE personnel performing the testing were familiar with the requirements of the 1993 charpy test procedure and followed these requirements to perform the various tasks necessary to conduct the tests. Each engineer has the requisite education and experience required to qualify them to perform these tests.

At the time the FitzPatrick tests were performed, a draft revision to the charpy test procedure existed. This draft test procedure included a newly purchased 300 ft-lb charpy test machine in the list of applicable apparatus. This machine was used to test the FitzPatrick surveillance capsule specimens. However, at the time of the test, the 1993 test procedure had neither been amended nor revised to include this test machine in the list of applicable apparatus. Other than the omission of the new test machine, there was no substantive difference between the two procedures. The draft revision to the procedure was approved in October 1997. This version of the charpy test procedure contains the requirements that GE followed during the conduct of the FitzPatrick surveillance capsule charpy specimen test.

Based on the above, the Authority is satisfied that the tests were performed properly and in accordance with the newly revised charpy test procedure. The test results are therefore valid for use in GE Report No. GE-NE-B1100732-01, Revision 1, "Plant FitzPatrick RPV Surveillance Material Testing and Analysis of 120° Capsule at 13.4 EFPY" (Reference 2).

Editorial Comments

The following two changes were made to GE Report No. GE-NE-B1100732-01 (Reference 3) and are incorporated in Revision 1 (Reference 2) to this report:

1. Page 12, Table 3-3

   Weld 1-233 charpy energy values of 74ft-lb, 63ft-lb, and 82ft-lb have been corrected and replaced with charpy energy values of 60ft-lb, 64ft-lb, and 56ft-lb, respectively. The original values were incorrectly taken from a previous report. Since this weld continued not to be the limiting weld/plate, this correction does not change the results of the original GE report.

2. Page 17, Section 4.1.1, Third Paragraph, Third Sentence

   Delete:

   "The calculated fluence results for the Fe, Ni, and Cu wires differed by less than 10%, thus, an average fluence value was used."

   Replace with:

   "The calculated fluence result from the iron flux wire was used. The Ni and Cu flux wires confirmed the fluence result from the iron specimen, with all three results differing by less than 10%."

   This change has no effect on the results of the original GE report.

Based on the above, the editorial comments and QA concerns did not alter the overall conclusion of the report. The revised report continues to demonstrate that the requirements of 10 CFR 50, Appendix G are satisfied.

Schedule and Technical Justification for Next Capsule Removal

Based on ASTM E185-82 (Reference 4), the third capsule does not need to be withdrawn until end of license (i.e., 2014). The curves contained in the GE report are valid for up to 32 Effective Full Power Years (EFPY) of operation which corresponds to at least the end of license. Vessel fluence is expected to be less than 32 EFPY at that time. The third capsule will be withdrawn at approximately 30 EFPY. This will support operation beyond 32 EFPY, should the operating license be extended. In accordance with 10 CFR 50, Appendix H, Section III.B.3, the Authority requests NRC approval of this proposed withdrawal schedule.

Status of ongoing BWR Owner's Group RPV Integrity Program Relative to FitzPatrick

A revised report, "BWR Vessel and Internals Project Update of Bounding Assessment of BWR/2-6 Reactor Pressure Vessel Integrity Issues (BWRVIP-46)," EPRI, Palo Alto, Ca., December 1997, (EPRI TR-109727) was submitted by EPRI to the NRC. This revised report included data not previously reported and concluded that there is no effect on the Pressure-Temperature (P-T) curves due to chemistry variability for the BWR vessels.

References

1. NYPA Letter, R. J. Deasy to NRC, "Reactor Pressure Vessel Material Surveillance Program Summary Report and Implementation Schedule," (JPN-97-035), dated November 10, 1997

2. General Electric Company Final Report, "Plant FitzPatrick RPV Surveillance Materials Testing and Analysis of 120° Capsule at 13.4 EFPY," GE-NE-B1100732-01, Revision 1, Class II, dated February 1998

3. General Electric Company Final Report, "Plant FitzPatrick RPV Surveillance Materials Testing and Analysis of 120° Capsule at 13.4 EFPY," GE-NE-B1100732-01, Class II, dated October 1997

4. American Society for Testing and Materials, Standard Practice Regarding Conducting Surveillance Tests for Light-Water Cooled Nuclear Power Reactor Vessels, ASTM E185-82, approved July 1, 1982

Attachment 2 to JPN-98-008

GENERAL ELECTRIC REPORT NO. GE-NE-B1100732-01, REVISION 1

FITZPATRICK REACTOR PRESSURE VESSEL SURVEILLANCE MATERIALS TESTING AND ANALYSIS REPORT OF 120 DEGREE CAPSULE AT 13.4 EFPY

New York Power Authority

JAMES A. FITZPATRICK NUCLEAR POWER PLANT
Docket No. 50-333
DPR-59

Attachment 3 to JPN-98-008

Summary of Commitments

Commitment Number	Description	Due Date
JPN-98-008-01	Withdraw the third capsule.	Approximately 30 EFPY